INTERMITTENCY MEASURING TECHNIQUES USING A PROBABILITY DENSITY ANALYZER

A thesis submitted to the Faculty of
the Graduate School of the University
of Manitoba

by

R. H. Hummel

In partial fulfillment of the requirement
for the degree of Master of Science in
Engineering.

March 1970

ACKNOWLEDGEMENTS

The author would like to express his thanks to Dr. R. S. Azad, who intitated the project and guided its progress throughout. The assistance of Helmut Krueger in making the special two-wire probe was very much appreciated. The author would also like to thank Valdis Kibens for the enlightening tour and discussion of his research project at the Johns Hopkins University.

The author holds a Post Industrial Experience Research (PIER) Fellowship in Engineering from the National Research Council of Canada and wishes to acknowledge the financial support of the National Research Council during the period of the work.

ABSTRACT

A set of preliminary experiments has been conducted in a conical diffuser, to determine the intermittent nature of the flow structure. An interface detector, based on the work of Townsend (1949) was constructed. The detector produces an output signal I(t) equal to 1 when the flow is turbulent and 0 when the flow is non-turbulent. A technique, based on probability density plots taken with a multi-channel analyzer, was developed to measure the intermittency factor, γ, and hence calibrate the interface detector. Instrumentation was also designed to measure "zone" averages and "zone" probability densities of the velocity.

Preliminary results, based on a single traverse, indicate that the line of demarcation between turbulent and non-turbulent fluid is not sharp and, in fact, where the intermittency is a maximum more than 50% of the fluid is in a state of transition from one type of flow to the other. In view of these developments the intermittency factor was redefined, based on the need to specify what percentage of transition flow was turbulent. An intermittency intensity factor, β, was also defined on the amount of transition flow existing at maximum intermittency (γ=.5).

On traversing radially outward from the axis of the diffuser, the flow was seen to divide itself into four distinct regions; the core region, the core intermittent region, the fully turbulent region and the wall intermittent region. Two intermittent regions exist separated by a thin layer of highly turbulent fluid. The flow model thus proposed serves as a basis for further investigation.

TABLE OF CONTENTS

LIST OF FIGURES

1.0 INTRODUCTION

The diverging flow has been investigated by Jeffrey (1915), Hamel (1917), Rosenhead (1940), Millsaps and Pohlhausen (1953), and Fraenkel (1962), using potential flow theory and similarity solutions. Classical theory of a purely divergent flow {see Batchelor (1967)} predicts unstable flow even for a moderately low Reynolds number, and a similarity solution at high velocity gives many identical regions of outflow and of inflow. Furthermore, the boundary layer theory cannot be used since the flow in a diffuser violates the basic assumption that the thickness of the boundary layer is very small in comparison to the streamwise length dimension. Hence it was decided to study the flow experimentally since step by step experimental work will throw light on the physical picture of the flow and thus enable a theory to be developed to explain the diverging flow. To this end, Lipka (1968), Van der Spiegel (1969), Slusar (1969), and Krueger (1970) have experimentally investigated main flow, pressure rise, turbulent intensities, and Reynolds stresses in a conical diffuser. Bearing in mind the same object it was decided to investigate whether the flow alternates irregularly between relatively quiescent and turbulent flow, and whether, within each pack of turbulent flow, local isotropy exists. Flow with these properties is regarded as being intermittent.

While explaining the intermittent nature of the turbulent motion, Townsend (1948) says, "whatever the detailed explanation, the mechanism is

likely to be common to all examples of free turbulence when there is a mixing of undisturbed fluid with the turbulent flow." The flow in diffusers is not a true example of free turbulence such as free jet and wake flow, but the process, which controls the mechanism of the intermittent flow, i.e., a mixing of undisturbed fluid with the turbulent flow, exists in diffuser flow. Corrsin and Kistler (1955) say "In reality, however, every turbulent flow is bounded by fluid, not in a turbulent state." They also define the distinction between turbulent and non-turbulent zones by the presence or absence, respectively, of random vorticity fluctuations. The undisturbed fluid may be interpreted as the degree of quiescence of the fluid relative to the turbulent flow. Since the difference of velocity between the completely quiescent flow and the turbulent flow in the case of a free jet at low velocity, can be almost equal to the difference of velocity between the partially quiescent flow at the wall and the high velocity core flow of the diffuser, it is not unreasonable to assume the existence of intermittent flow in a conical diffuser.

One of the conditions {Townsend (1949)} required for the existence of an intermittent turbulent flow is that the Reynolds number of the flow must be large. This requirement is satisfied in the range of velocities to be investigated since the velocity varies from 15 meters/sec. to 80 meters/sec. It is noted that the maximum velocity in Townsend's experiments was 12.8 meters/sec.

Patel and Head (1969) give the criteria of developing flow in pipes. One of their criteria is the presence of intermittency as the flow

develops. The value of the intermittency factor, γ, is very small in the beginning of the developing flow while the value of γ tends to 1 for fully developed flow. This criterion may be used for developing flow in diffusers.

Preceeding discussions give a strong indication of the presence of intermittent flow in a conical diffuser. An intermittent flow is characterized by intervals of nearly laminar flow separating "bursts" of fully developed turbulence. The intermittency factor, γ, is defined as the fractional time spent by a fixed probe in turbulent fluid. Two methods of measuring intermittency factor were introduced by Townsend (1948,1949). The first method is based on the measurement of the "flattening factor" of the probability density of the intermittent signal and on the hypothesis of local isotrophy, due to Kolmogorov (1941). The second method is the construction of an electrical signal, I(t), which is zero except when the hot wire is in a region of turbulent motion, where it takes the value unity.

For the present exploratory work it was first necessary to design and construct the necessary equipment and subsequently organize an experiment suitable for measuring the intermittency factor γ, and associated parameters. The instruments were subsequently tested using signals derived from real flow in a conical diffuser.

2.0 THE INTERMITTENCY CONCEPT

2.1 Description and Occurrence of Intermittency.

Intermittency is the name given to the alternation between turbulent and non-turbulent motion that characterizes certain types of flows. The intermittency factor γ is defined as the ratio of time turbulent to total time. It is therefore a measure of the probability of finding turbulent flow at any instant at a point considered.

Intermittency is observed in two quite different flow situations. Firstly, in the breakdown of a laminar shear flow to a turbulent flow, a process which normally occurs over a considerable streamwise distance and is characterized by the growth of initially small and randomly distributed patches of turbulence which finally coallesce. This type of intermittent flow exists, for example, in the transition region of a turbulent boundary layer.

Secondly, at the free boundary of a fully developed turbulent shear flow where the outer edge of the turbulence fluctuates with time so that over an appreciable distance in the cross stream direction the flow alternates between turbulence and non-turbulence. An example of this is the flow in the wake of a cylinder.

It has been found {Fiedler and Head (1966)} that with adverse pressure gradients (diffuser flow) the intermittent flow moves outward from the surface, while the width of the intermittent zone decreases. The converse is true of favourable pressure gradients (developing pipe flow); in some cases the intermittent zone may exist all the way to the wall.

Turbulence occurring in jets, wakes and boundary layers is instantaneously confined within a more or less clearly defined boundary, commonly termed the turbulence front which is highly irregular in shape and constantly varying with time.

According to Corrsin and Kistler (1955) -

a) the turbulence front takes on the form of a continuous laminar superlayer.

b) there is a sharp division between the turbulent and non-turbulent zones.

c) advances of the turbulent front and entrainment of non-turbulent fluid take place through the action of viscosity.

2.2 The Averaging Problem in Intermittent Flow

All conventional measurements taken in the intermittent zone of a turbulent shear flow average any particular quantity alternately over regions of intense turbulent fluctuations followed by relatively quiet flow. Thus any distribution of mean intensity taken across the intermittent zone will show great inhomogeneity which is mostly due to probability of occurrence of turbulent fluid and little to variation in properties of the turbulent fluid itself.

It is therefore desirable to devise methods for the measurement of mean values which consider only that portion of the total time of observation for which the point of observation is immersed in fully turbulent or non-turbulent fluid.

To this end Townsend (1949) has defined a quantity I(t) which is zero in non-turbulent fluid and unity in fully turbulent fluid. Its mean value equals γ, the intermittency factor.

Thus:

$$\gamma \equiv \overline{I(t)}.$$

In the past, intermittency has generally been measured in two ways, both due to Townsend. They are:

a) The "flatness factor" method

b) Townsend's second method (or Townsend's direct method).

In the next section both methods will be described and compared.

2.3 Measurement of the Intermittency Factor,

2.3.1 Townsend's First Method - the "Flatness Factor" Method.

One important characteristic of isotropic fluid flow is that if a probability density plot of velocity is made, the plot will be normally distributed independent of the direction in which the velocity is measured. Kolmogorov (1941) has postulated and proved the theory of local isotropy. If a probability density plot is made from a flow system which is sometimes turbulent and sometimes not, and the measurements are restricted to the time intervals when the flow is turbulent, then a similar normally distributed plot will be obtained. The basic concepts of the method will be derived for the simplest possible case. For present purposes the signal may be considered to be S(t) which in practice is usually some time derivative of the velocity, u.

The ideal intermittent signal has the following properties.

1) It is either turbulent or non-turbulent (Fig. 1a).

2) The probability density plot corresponding to turbulence is normally distributed with deviation, σ .(Fig. 1b)

3) The non-turbulent signal is free of fluctuations ($\sigma_N=0$).

4) The probability of turbulence is γ, i.e. the signal is turbulent γ percent of full time. Let the probability density plot of the total signal (Fig. 1b) have an area of 1. Then the area of the bell shaped peak is γ. The infinitely narrow peak superimposed on it is an impulse with area $1-\gamma$.

Let I(t) be a signal previously defined. Also, let B(t) denote the full time turbulent signal; N(t) denote the full time non-turbulent

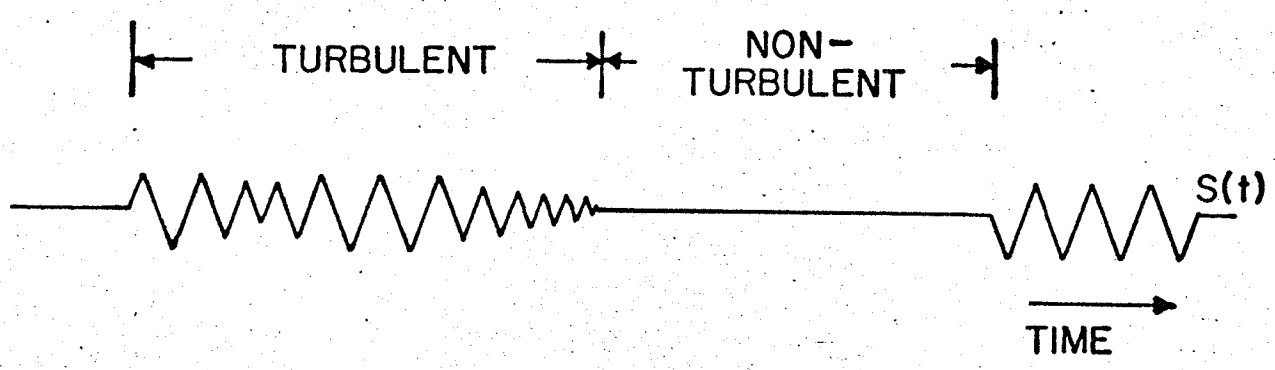

(a)

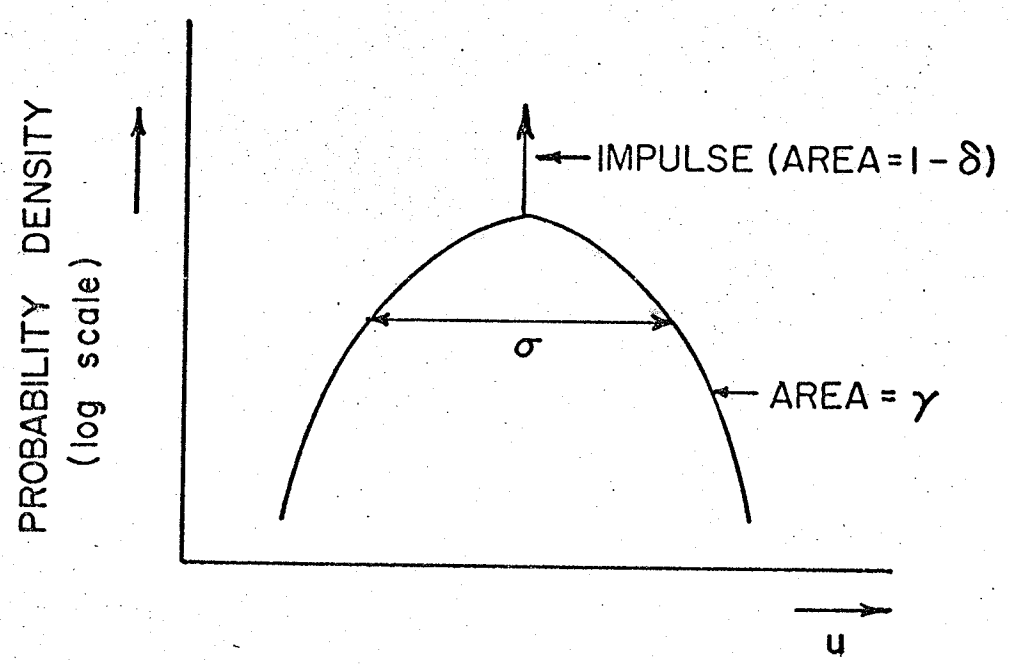

(b)

FIGURE 1 - WAVEFORM AND PROBABILITY DENSITY OF AN IDEAL INTERMITTENT SIGNAL

signal; and S(t) denote the intermittent signal(Fig. 1a)

Then:

$$S(t) = I(t)\,B(t) + (1-I(t))\,N(t)$$

$$= I(t)\,B(t), \qquad (1)$$

since N(t) is assumed to be zero.

Squaring and taking the mean value

$$\overline{S^2} = \overline{I^2 B^2} = \overline{I^2}\ \overline{B^2}$$

$$= \gamma\ \overline{B^2}$$

since $\overline{I^2} = \overline{I} = \gamma$

Squaring again gives,

$$(\overline{S^2})^2 = \gamma^2\ (\overline{B^2})^2 \qquad (2)$$

From (1) it follows that,

$$\overline{S^4} = \overline{A^4 B^4} = \overline{A^4}\ \overline{B^4}. = \gamma\ \overline{B^4} \qquad (3)$$

Combining (2) and (3),gives the "flatness factor" defined by

$$\text{flatness factor} = \frac{\overline{S^4}}{(\overline{S^2})^2} = \frac{\gamma\ \overline{B^4}}{\gamma^2 (\overline{S^2})^2}$$

$$= \frac{1}{\gamma}\left(\frac{\overline{B^4}}{(\overline{B^2})^2}\right)$$

The bracketed term may be written as,

$$F = \frac{\overline{B^4}}{(\overline{B^2})^2} = \frac{\int_{-\infty}^{\infty} B^4 \, P(B) \, dB}{\left[\int_{-\infty}^{\infty} B^2 \, P(B) \, dB\right]^2}$$

where P(B) is the probability of a fluctuation of magnitude B.

Since B is normally distributed,

$$P(B) = \frac{e^{-B^2/2\sigma^2}}{\sqrt{2\pi\sigma^2}}$$

Therefore

$$F = \frac{\int_{-\infty}^{\infty} \frac{B^4 e^{-B^2/2\sigma^2} dB}{\sqrt{2\pi\sigma^2}}}{\left[\int_{-\infty}^{\infty} \frac{B^2 e^{-B^2/2\sigma^2} \, dB}{\sqrt{2\pi\sigma^2}}\right]^2}$$

The integrals are easily evaluated by changing the variables.

Let $y = \frac{B}{\sqrt{2}\sigma}$

Thus F = 3

Therefore:

γ = the intermittency factor

= 3/(flatness factor)

Townsend (1948) describes a circuit for measuring the flatness factor. The circuit uses the parabolic grid characteristics of triodes, suitably biased, as a means of squaring. Such circuits have a tendency to drift with age, temperature,etc. A more modern approach would be to patch up a "flatness factor" detector on an analogue computer equipped with three squaring circuits, a ratio circuit and 2 integrators. Fig. 2 shows a block diagram of the proposed detector.

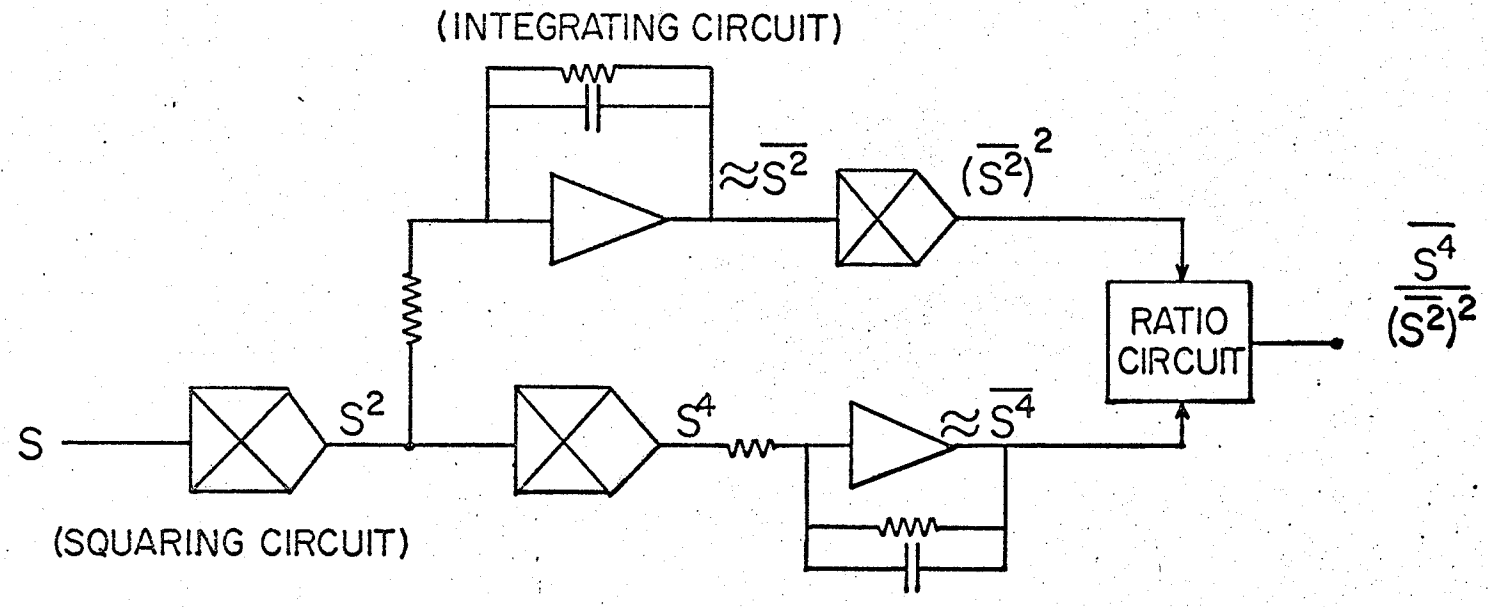

FIG. 2 A PROPOSED FLATNESS FACTOR DETECTOR

2.3.2 Townsend's Direct Method

Townsend (1949) realized the limitations (See Sec. 2.4) of the "flatness factor" method and subsequently devised an alternative method which is used (with variations) almost exclusively in contemporary work. This method derives the electrical intermittency signal, I(t) defined in Sec. 2.2. Briefly the circuit works as follows.

The input signal is taken from a single hot wire. Two time derivatives are taken thus emphasizing the high frequency components. The resulting signal is full-wave rectified followed by a small amount of integration provided by a shunt variable capacitor. Thus a "memory time" or delay is introduced. The alternative of not having the delay results in the output going to zero as each oscillation passes through zero. Such an output would be essentially unusable. Thus to use this technique successfully one must assume that a large number of complete oscillations occur during each period of turbulent motion, i.e. that the Reynolds number of the turbulent fluid be large.

The output from the memory capacitor is fed to a discriminator and limiter. When the input to the discriminator is above a preset level, the output of the limiter is a constant level with magnitude arbitrarily assigned 1. Otherwise the output is 0. This is the desired output I(t).

2.4 Discussion and Comparison of the Two Methods.

The basic limitation of the "flatness factor" method is illustrated by the following argument.

Let M be any quantity such as a velocity derivative. Let $\tilde{\tilde{M}}$, the quantity to be measured, be a mean value with measurements restricted to time intervals when the fluid is turbulent. Such a mean value is called a zone average.

For any intermittent flow system one can write the identity -

$$\overline{IM} = \overline{I}\ \tilde{\tilde{M}}$$

$$\text{or}\quad \tilde{\tilde{M}} = \frac{\overline{IM}}{\overline{I}} \quad .$$

It is possible to measure $\overline{I}$ with the flatness factor detector and the mean value of M can also be found, (for example with a true rms meter). However, in general it is not possible to calculate $\overline{IM}$ given $\overline{M}$ and $\overline{I}$. Thus in general $\tilde{\tilde{M}}$ cannot be found.

If, however, the assumption is made that M is zero everywhere in the non-turbulent zone, then

$$\overline{IM} = \overline{M} \qquad \text{and}$$

$$\tilde{\tilde{M}} = \frac{\overline{M}}{\overline{I}} \quad .$$

Since both quantities on the R.H.S. of the preceeding equation can be measured, $\tilde{\tilde{M}}$ can be found. Thus whenever the zone average coincides with the usually average then the method due to flatness factor can be used. e.g. grid turbulence.

The main advantage of this method is that it gives a unique value for γ, provided one is willing to accept the basic assumptions given in section 2.3.1.

Townsend overcame the basic limitation imposed by the flatness factor method. His second method produced an on-off signal and it was therefore possible to find $\widetilde{M}$ since M could now be averaged only when the flow was turbulent. However, in practice almost any value of γ can be obtained depending on where one sets the discriminator or equivalently where one sets the gain of the amplifiers ahead of the discriminator. As shown later intermittency is not an ideal on-off type of process (in diffuser flow at least) and the question of the value of γ at a point becomes one of definition of γ.

3.0 MODERN INTERMITTENCY MEASURING TECHNIQUES

To the author's knowledge, most modern techniques for measuring the intermittency factor are a modification of Townsend's Direct Method. Many experiments require only a knowledge of the existence of intermittent flow. This is easily done by observing velocity derivatives on an oscilloscope or similar recording device.

An analog circuit with an input-output relationship described by Townsend's Direct Method will be referred to as an "interface detector". The practical difficulty in using such a detector, i.e. setting the discriminator level, can be attributed to the following:

1) the signal to noise ratio, S/N, is finite

where $\frac{S}{N} = \frac{\text{rms value of fulltime turbulent signal}}{\text{rms value of fulltime non-turbulent signal}}$

Ideally this ratio would be very large but in practice it is found to vary from four to ten. Also, for diffuser flow, it has been found that the transitions from bursts of turbulence to non-turbulence and vice versa are not instantaneous.

2) The delay constant, associated with the "memory" capacitor is finite. Thus the time location of each transition of I(t) corresponding to the end of a turbulence burst depends on the discriminator setting.

3.1 Recent Advances in Detector Design

Corrsin and Kistler (1955) attempted to maximize the signal to noise ratio by using a signal proportional to the vorticity fluctuations as the input to the discriminator. They have shown that the vorticity fluctuation level is low in the non-turbulent zones and rises rapidly across the interface.

Fiedler and Head (1966) have proposed a scheme for minimizing the undesirable effect of the "memory time" capacitor. They introduce an effective "memory time" by phase shifting (i.e. differentiating) the signal at a certain stage of processing and then adding the original and shifted signals. Kibens (1968 p. 98,104) gives a detailed account of the effectiveness of this technique.

3.2 A Modern Interface Detector

The two modifications of the previous chapter have been implemented in a detector described by Kibens (1968). For the present work it was decided at the outset to use a similar circuit. Fig. 3 shows a block diagram of the detector. Electronic details are given in Appendix A.3.

The inputs u_1 and u_2 are the linearized outputs of the two parallel hot-wire probes as described in Sec. 4.3. Since the two hot wires are spaced a small (1mm.) distance apart in the y direction the resulting signal is approximately proportional to $\frac{\partial u}{\partial y}$. The signal is then fed to a high pass filter, (or time differentiator) with a variable cut-off frequency, f_1. This is followed by a low-pass filter with variable cut-off frequency, f_2. The cut-off frequency of both is set just above the highest frequency of interest, i.e. the highest frequencies transmitted from the anemometers. The combined action of the two circuits is therefore to provide differentiation over the desired frequency range while removing the higher frequencies. The resulting signal is proportional to $\partial^2 u/\partial y \partial t$ which is also referred to as the probe signal S(t). Kibens (1968) suggests that S(t) is a good approximation to the rate of change of vorticity, i.e., $\partial w/\partial t$, which may be true in a boundary layer where $\partial^2 v/\partial x \partial t$ is small. The extent to which it is true in diffuser flow where no thin boundary layer exists has not been investigated. For intermittent flow, S(t) has the strongly intermittent, burst-like characteristic suitable for detection.

The phase shift, or delay, suggested by Fiedler and Head is provided by the true differentiator. This circuit differentiates S(t)

from just above zero frequency up to approximately 20 KHz. This upper frequency was chosen somewhat arbitrarily but is well above the highest frequency of interest. Upper frequency limiting is necessary in order to maintain an adequate margin of electronic stability. The resulting signal, $\dot{S}(t)$ is proportional to $\partial^3 u/\partial y \partial t^2$. Considered in the time domain with sinusoidal test inputs, $\dot{S}(t)$ crosses zero when $S(t)$ is a maximum and vice versa. For random signals, however, there is a finite probability of both $S(t)$ and $\dot{S}(t)$ being zero simultaneously.

The frequency response of the circuit, for both $S(t)$ and $\dot{S}(t)$ is shown in Fig. 4. The vertical position of the two graphs is arbitrary and may be adjusted by the GAIN control. The $\dot{S}$ curve may be moved vertically with respect to the S curve by adjustment of the $\dot{S}$ GAIN control.

The signals $S(t)$ and $\dot{S}(t)$ are then fed into a gate circuit with output $Y(t)$ such that,

$$Y(t)= \begin{cases} 1 \text{ if } |S| > C \text{ or } |\dot{S}| > C \\ 0 \text{ if } |S| \leq C \text{ and } |\dot{S}| \geq C. \end{cases}$$

The detector threshold is C. Refer to Fig. 5 for a typical sequence of pulses. The signal $Y(t)$ has many lapses such as illustrated at A, B, and D. The one at A is due to both $S(t)$ and $\dot{S}(t)$ being simultaneously zero. This can occur with finite probability since $S(t)$ and $\dot{S}(t)$ are statistically independent. At B both $S(t)$ and $\dot{S}(t)$ are below the threshold C. Both cases produce false indications of non-turbulence. Similarly short bursts, of amplitude larger than C, produce false indications of turbulence. Such a situation is shown at D. For this reason a circuit, with "hold time" τ_H is introduced so that the previous (turbulent or non-turbulent) state

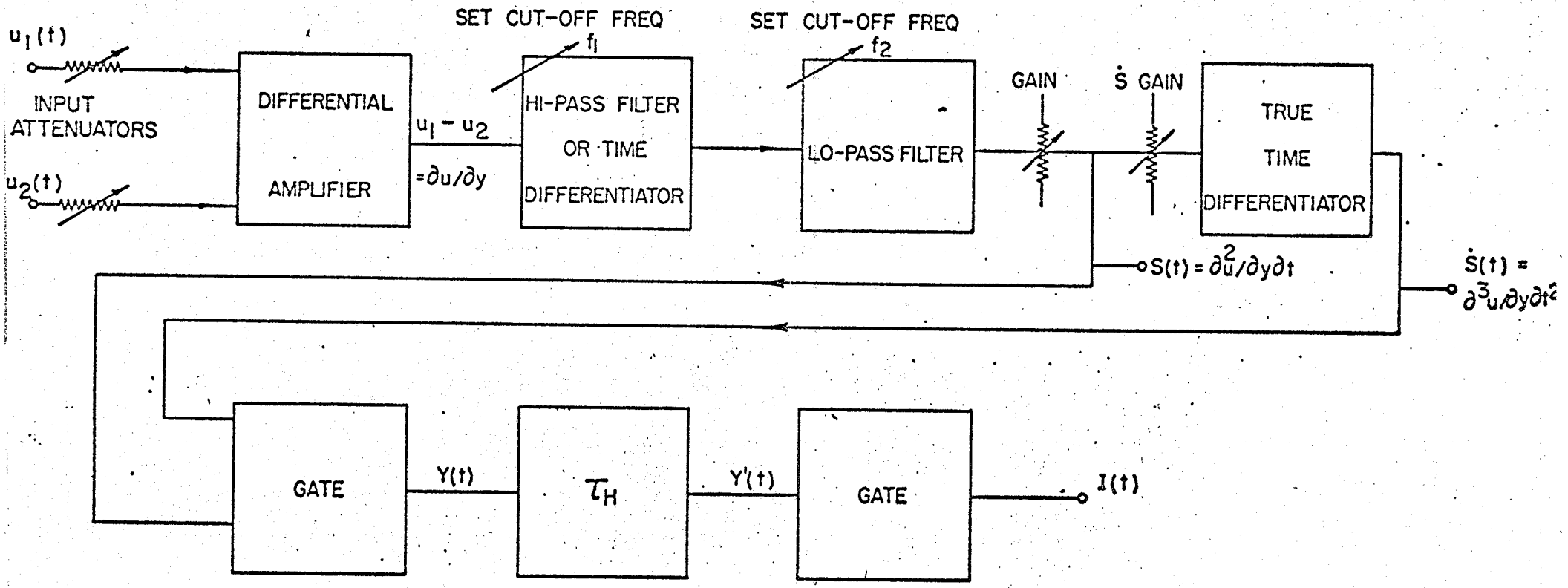

FIG.3 A BLOCK DIAGRAM OF THE INTERFACE DETECTOR

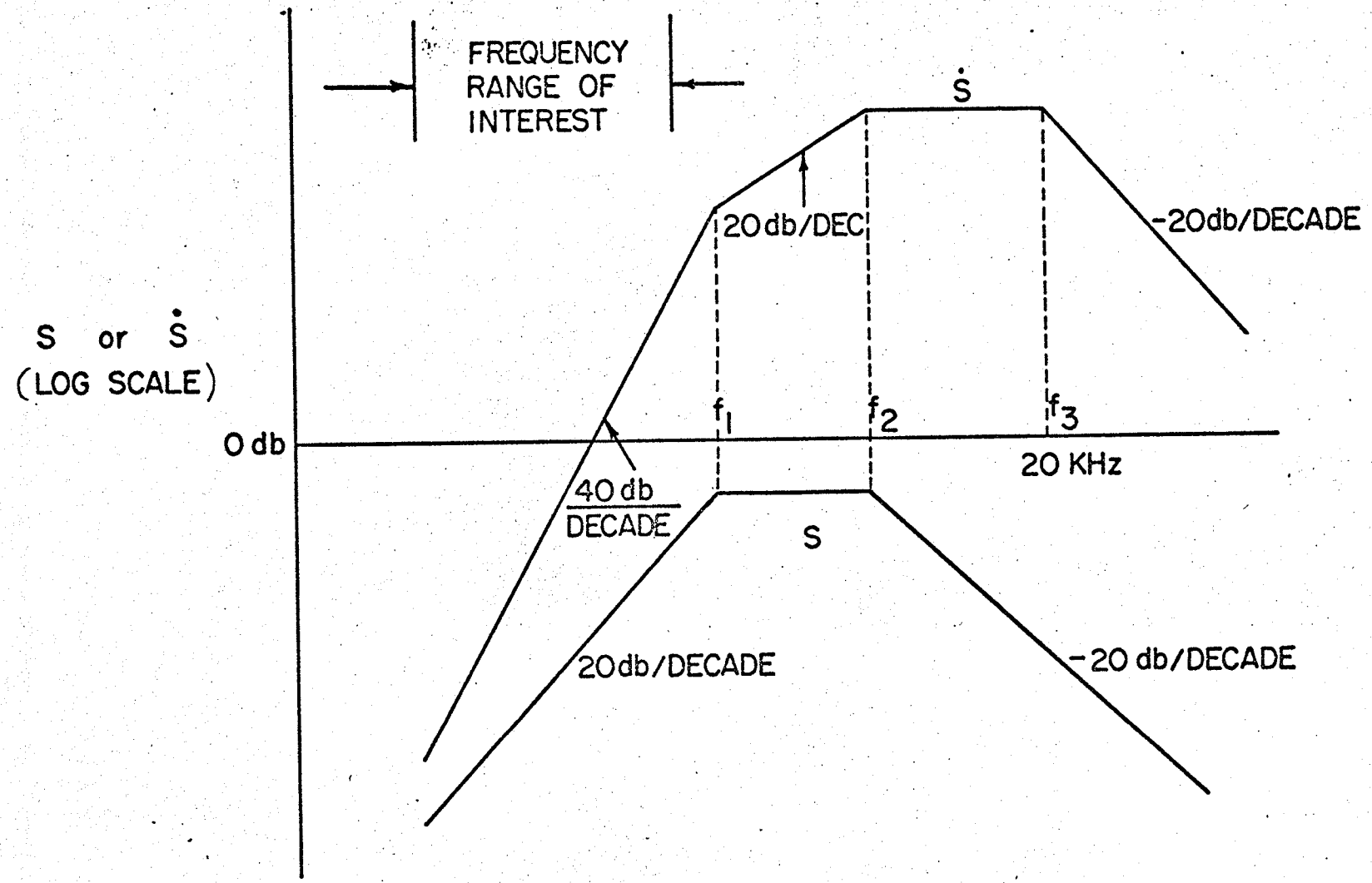

FIG.4 FREQUENCY RESPONSE CHARACTERISTICS FOR THE INTERFACE DETECTOR

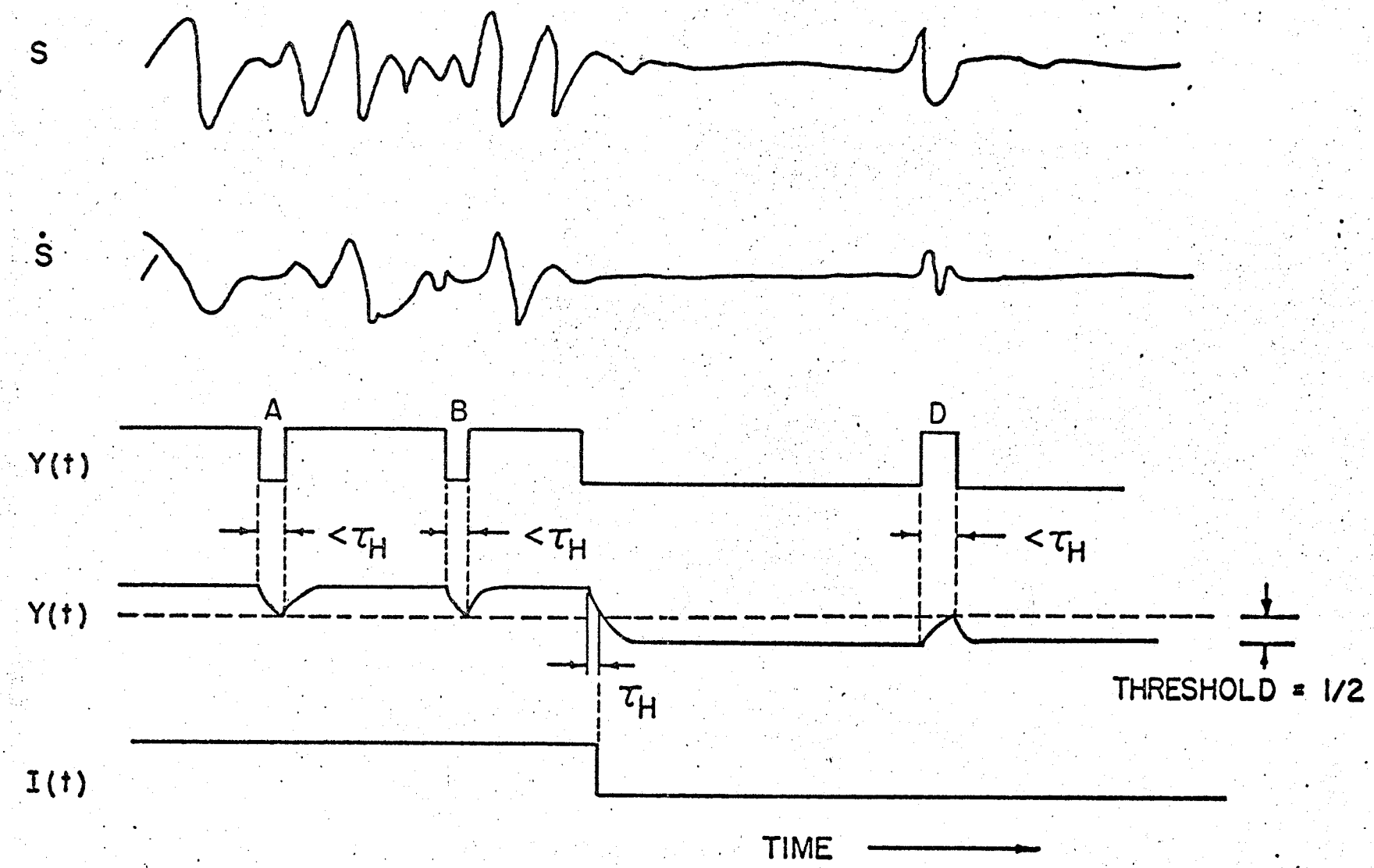

FIG.5 TYPICAL WAVESHAPES IN THE INTERFACE DETECTOR

holds for a time τ_H before a change in the output state takes place.

The output of this circuit, Y'(t) is fed into a gate circuit with output I(t) such that,

$$I(t) = \begin{cases} 1 \text{ if } Y'(t) > 1/2 \\ 0 \text{ if } Y'(t) < 1/2. \end{cases}$$

The final detector output I(t) is a random square wave with a value of 1 or 0 corresponding to turbulence or non-turbulence respectively at the probe location. The hold time represents a delay of detection, thus I(t) lags behind the actual interface crossing by τ_H. Apparently the innovation of Fiedler and Head has not succeeded in removing completely the need of a memory circuit as originally used by Townsend.

3.3 Detector Adjustments

The detection of the state of intermittent flow must be based on a number of threshold criteria. The minimum numbers of adjustable parameters is two. One is a constant level, above which the fluctuation are considered turbulent. This is referred to as the amplitude threshold criterion. The other is a time interval over which the amplitude threshold criterion is applied, i.e. the hold time criterion. The first of these cannot be zero due to a finite signal to noise ratio. The hold time cannot be zero since all signals fluctuate about zero and hence must periodically pass through zero.

The parameters must therefore be set to give the "best" value of γ at any one probe location.

The interface detector has five adjustments, of which the last two are the most basic as already mentioned. They are:

1) adjustment of the input attenuators.
2) adjustment of the cut-off frequencies f_1 and f_2.
3) adjustment of $\dot{S}(t)$ GAIN.
4) adjustment of hold time τ_H.
5) adjustment of GAIN.

The first four are uniquely adjustable. The GAIN can only be set after γ is known, a technique discussed in Chapter 6.

1) Adjustment of Input Attenuators.

These are set so that velocity components, common to both probes precisely cancel in the differential amplifier. They are also set such that

no clipping occurs in the differential amplifier.

2) Adjustment of the Cut-Off Frequencies, f_1 and f_2.

Associated with the energy spectrum of the signal S(t) is the characteristic frequency f_{ch} which is found as follows.

i) set f_1 to a low frequency (say 10Hz) and f_2 to a high frequency (say 20KHz). Measure S(t) with a true rms voltmeter. The probes are positioned in fully turbulent fluid.

ii) Adjust $\dot{S}(t)$ GAIN such that $\dot{S}(t)$ has the same rms value as S(t).

iii) Remove the anemometer signals and replace one input with a sine wave. Adjust the frequency of the sine wave such that rms voltages of S(t) and $\dot{S}(t)$ are equal. The frequency of the sine wave is f_{ch}. Set f_1 and f_2 to approximately twice f_{ch}.

3) Adjustment of the Hold Time, τ_H.

The hold time must be of the order of a characteristic time associated with the fine structure of the turbulence, within the turbulence bursts. Thus a characteristic time of $2/f_{ch}$, is used.

4) Adjustment of $\dot{S}(t)$ GAIN.

With the probes in the fully turbulent zone this gain is adjusted so that S(t) and $\dot{S}(t)$ have equal rms values.

3.4 Conclusion.

It should not be concluded that the detector just described in any way represents an optimum in either design or adjustment. Such refinements as designing a filter that maximizes the signal to noise ratio could well be a topic of further investigation.

Further discussion of the detector is deferred to chapter 6. The following two chapters describe the flow facility and other necessary instrumentation.

4.0 DESCRIPTION OF THE FLOW FACILITY.

This chapter describes briefly the wind tunnel, the diffuser, the traversing mechanism, and hot wire probe assembly. Except for the probe assembly, details for each of the above are given in the following references.

1) Wind tunnel - Friesen(1970).

2) Diffuser - Lipka(1968).

3) Traversing mechanism - Krueger(1970).

4.1 The Wind Tunnel

A layout diagram for the low turbulence wind tunnel is shown in Fig. 6. The fan, driven by a 25 horsepower d.c. motor, blows air into the circular tunnel with diameter .918 meters. The other end of the tunnel is fitted with a contraction cone which has a contraction ratio of 89 to 1. Coupling of the output of the contraction cone to the input of the diffuser was provided by a duct, 1.47 meters long with a nominal diameter of 10 cm.

4.2 The Conical Diffuser

A detailed drawing of the straight conical diffuser is given in Fig. 7. The diffuser had the following dimensions.

inlet - 10.14 cm. internal diameter.

outlet - 20.22 cm. internal diameter.

length - 70.90 cm.

The opening angle was 8.01°.

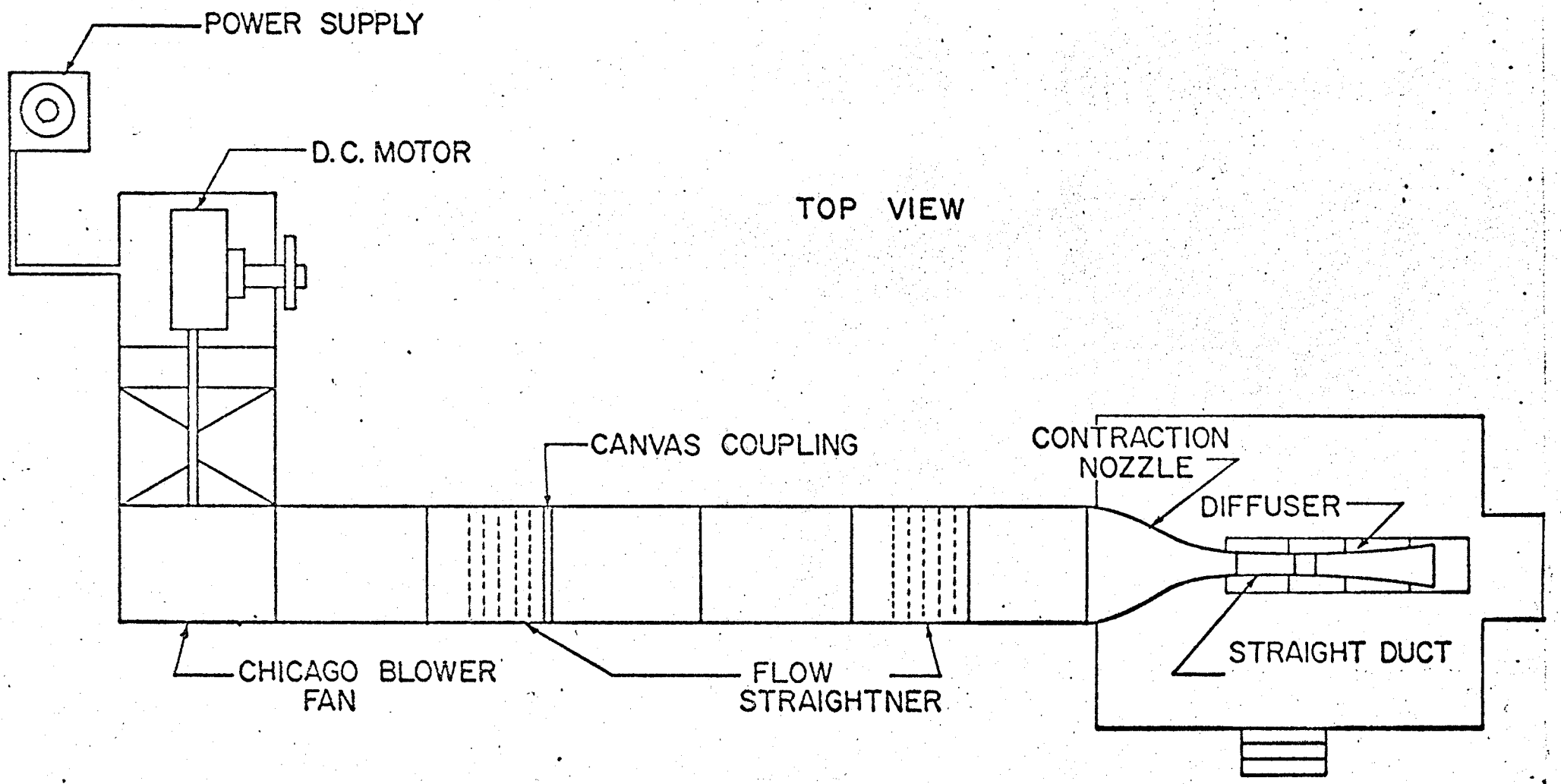

FIG. 6 A PLAN VIEW OF WIND TUNNEL FACILITIES

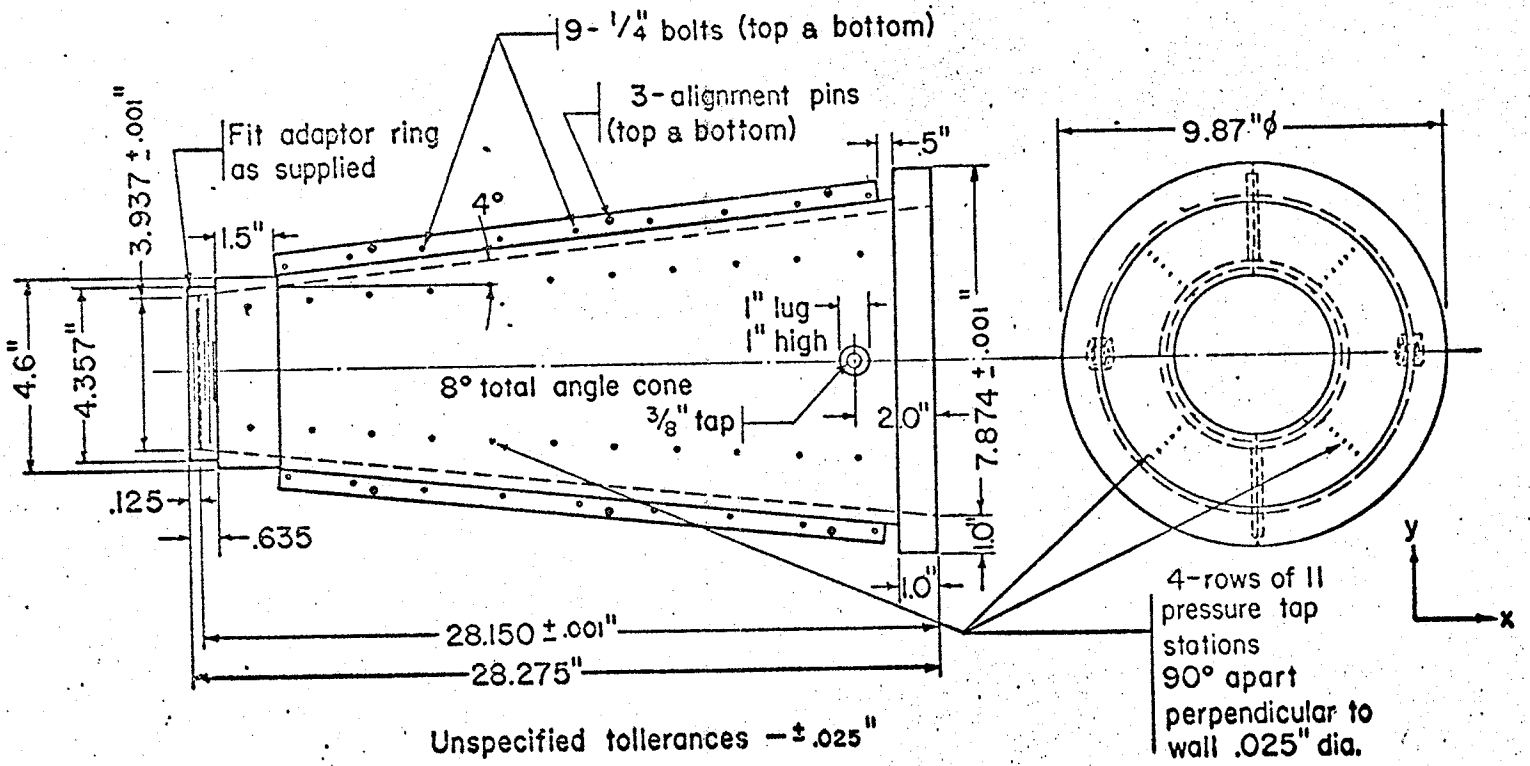

FIG. 7 CONICAL DIFFUSER DETAIL

Not To Scale

4.3 The Traversing Mechanism and Hot-Wire Probe Assembly

The traversing mechanism was designed and constructed by H. Krueger. The details are shown in Fig. 8. In the application it was used to position the hot wire probe accurately in the y direction, shown in Fig. 7. The position accuracy is better than 0.01 cm.

The hot wire probe was a modified X-probe with the mounting posts all filed down to equal lengths. A sensing wire was welded on each independent pair resulting in two parallel wires. When placed into the diffuser, the wires are at right angles to both the x and the y directions. The sense wires, 5 microns in diameter were 1 mm. long; spaced 1 mm. apart, and were made of platinum plated tungsten. Referring to Fig. 8, the hot wire probe was installed as Item VIII. Item IX was not installed. The traversing mechanism of Fig. 8 is capable of traversing the diameter of the diffuser at any cross section.

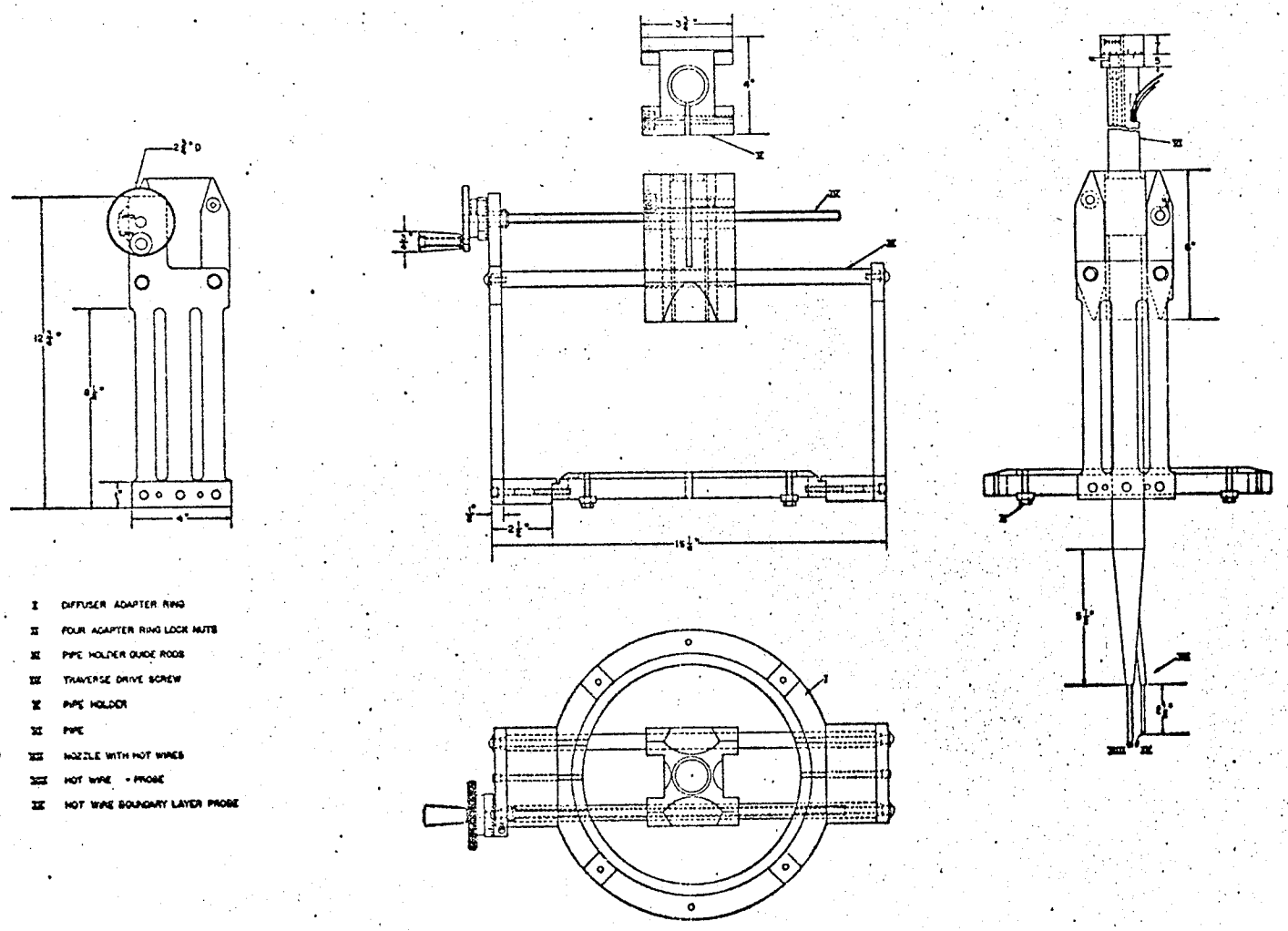

FIG. 8 DIFFUSER TRAVERSING MECHANISM

5.0 APPARATUS AND EXPERIMENTAL PROCEDURE

In this chapter the complete experimental set-up is introduced by means of an overall block diagram. The function of each instrument is briefly described. With the anemometers and linearizers suitably calibrated a procedure is outlined for recording the necessary raw data on analog tape suitable for detailed analysis at a later time.

5.1 Description of Apparatus.

The experimental set-up is shown in the block diagram, Fig. 9. Switches S1 and S5 are symbolic to facilitate explanation. Practically, this switching is done by rearranging the cables.

5.1.1 Hot Wire Anemometers and Linearizers.

The two constant temperature hot-wire anemometers were a Disa Type 55D01 fully transisterized unit, equipped with a Disa Type 55025 Auxiliary Unit; and a Disa Type 55A01 tube-type anemometer. Anemometer outputs were linearized with Disa Type 55D10 Linearizers.

Details for all units are given in their respective instruction manuals.

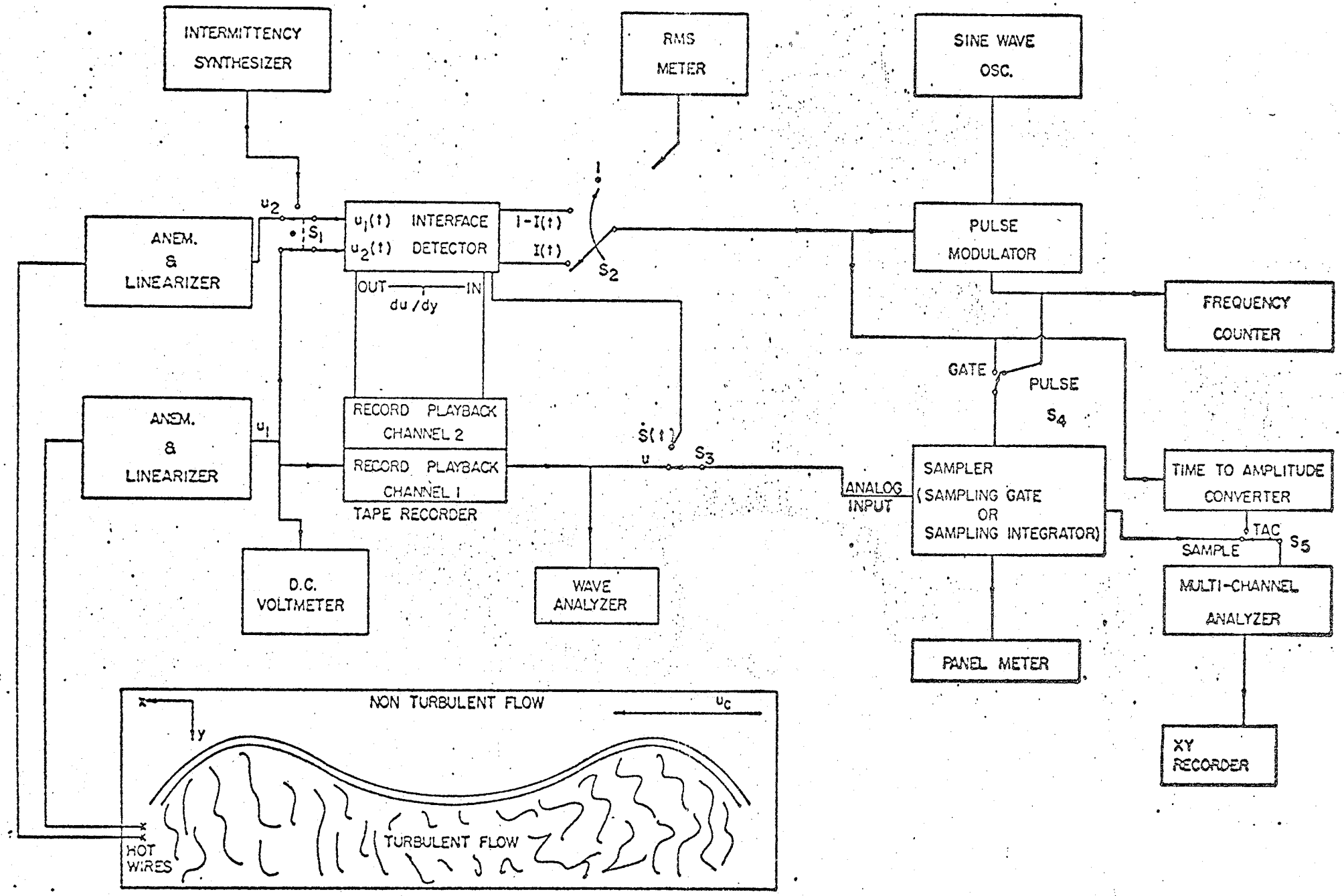

FIG.9 A BLOCK DIAGRAM OF THE EXPERIMENTAL SET-UP

5.1.2 The Intermittency Synthesizer and Sine Wave Generator.

The synthesizer was postulated by Kibens (1968), as being essential in determining the intermittency factor γ. It was therefore designed and constructed at the outset. Although this represents a substantial portion of the total effort, it has not proven to be very useful since, as is shown later, it does not adequately simulate intermittent flow in a diffuser. Although a relatively simple modification could correct this deficiency, a new technique (Chapter 6) has been developed which does not require a synthesizer. To date the unit has been used mainly as a function generator in the sense that it produces;

1) sine waves
2) triangular waves
3) square waves
4) random, white noise.

Electronic details of the complete unit are given in Appendix A1.

5.1.3 The Sampler.

The unit is described in Appendix A2.

5.1.4 The Interface Detector.

The general design philosophy for the detector is given in Chapter 3. Electronic details are found in Appendix A3.

5.1.5 The Analogue Tape Recorder.

The Lyric TR61-2 tape recorder is a seven track machine using ½" tape. The modulation technique is wide-band F.M. A novel feature of the recorder is that on playback, the outputs of the odd numbered channels can be delayed with respect to the outputs of the even numbered channels by mechanically positioning the playback heads. Thus, on playback, u can be delayed with respect to $\frac{\partial u}{\partial y}$ and compensate for the delay τ_H introduced by the detector into I(t). This feature will be found necessary when measuring zone averages (Sec. 7.4). It eliminates the need for a costly analogue delay line. Information on magnetic tape instrumentation is given by Davies (1961). Operating instructions and specifications for the recorder are given in its instruction manual.

5.1.6 The Multi-Channel Analyzer and XY Recorder.

Operation of the Victoreen TC200 Multi-channel Analyzer is outlined in Sec. 6.1. Such analyzers are discussed in detail by Chase (1961). The unit used was rented for the work reported in this thesis. The XY recorder was a HP7004A.

5.1.7 The Wave Analyzer.

The FRA-2C analyzer (borrowed by courtesy of the Red River Community College) is a constant bandwidth heterodyne-type analyzer. Three separate bandwidths are available, i.e. 2, 25 and 125 Hz. The useful frequency range extends from 5 Hz to 16 KHz Since the internal rms meter could not be suitably damped, all measurements were made with the Disa Type 55A35 RMS eter, using a 10 second integrating time constant.

5.1.8 The Pulse Modulator

A prototype was constructed as part of the interface detector unit. The modulator is a simple gate circuit with two inputs and one output. The gate input is an on-off square wave. The other input is a continuous sine wave. The circuit function is such that when the gate input is "on" each complete sinusoid produces a narrow pulse at the output. When the gate input is "off" there is no output. The complete schematic diagram is given by Hummel (1970).

5.1.9 The Frequency Counter.

The NE9010 Frequency Counter is a six decade digital counter with time presettable from 0 to 10^5-1 seconds. The maximum counting rate is 2 MHz.

5.1.10 The Time to Amplitude Converter (TAC).

A TAC produces an output pulse whose amplitude is proportional to the width of the input pulse.

Therefore -

$$V_o = K\, T_i \quad ,$$

where

V_o = amplitude of output pulse,

T_i = width of input pulse,

K = constant of proportionality.

A prototype was constructed as part of the interface detector unit. The input is the random square wave I(t) [or its complement 1-I(t)].

Considering, for example, I(t) as the input, for each burst of turbulence the TAC produces a pulse with amplitude proportional to the width of the burst. A complete circuit diagram and description are given by Hummel (1970).

5.1.11 The RMS Voltmeter.

The Disa Type 55D35 RMS Voltmeter is a true rms meter in the sense that it measures the rms value independently of wave shape. An important feature, especially useful in fluid mechanics where large fluctuations are likely to occur, is the ability to select an optimum integrating time which is variable from .1 to 30 seconds.

5.1.12 The D.C. Voltmeter.

The Disa Type 55D30 D.C. Voltmeter features digital read-out for high reading accuracy. Otherwise it is similar to conventional D.C. meters.

5.2 Calibration of Anemometers and Linearizers.

The anemometers and linearizers were calibrated following the step by step procedure outlined in the instruction manuals. A reference air stream was provided by a Disa Type 55D41/42 Calibration Unit. An overheat ratio of 1.8 was used. The resulting calibration curve, Fig. 10, shows the outputs of the two linearizers with both probes subjected to the same air velocity.

5.3 Nomenclature.

For the present work all readings were taken at an arbitrarily chosen, fixed x position. At this position, referred to as station 6, the diameter of the diffuser was 15.25 cm. All readings were taken on a single horizontal traverse in the y direction. The signal from the anemometer connected to the hot wire farthest left, as viewed from the large end of the diffuser is U_1; the other is U_2.

From a preliminary experimental investigation the flow was found to be similar on each half of the diffuser on one diameter and so only the left half, facing upstream was usually investigated. The probe position in the diffuser refers to the position of a point half way between the two hot wires. Position is given in terms of the non-dimensional number Y/D, where D is the diameter of the diffuser at the position where the measurement is taken. Position Y/D = 0 refers to the left wall.

The instantaneous value of the velocity is written -

$$U = \overline{U} + u$$

where

$\overline{U}$ is the mean value,
u is the instantaneous value of the fluctuating component.

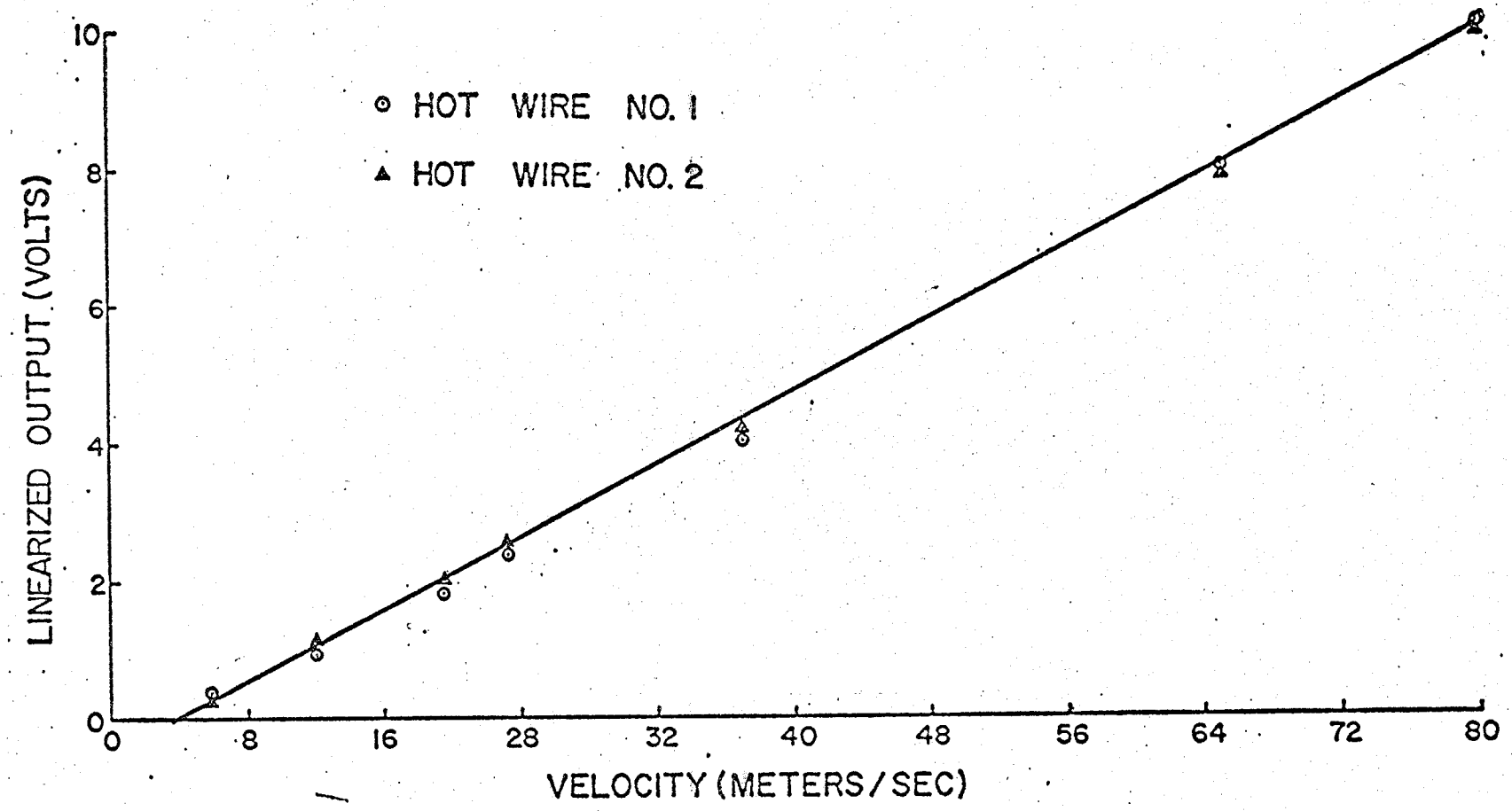

FIG.10 VELOCITY CALIBRATION CURVES

The rms value of the fluctuating component is written

$$\left(\overline{u^2}\right)^{\frac{1}{2}} = u'$$

5.4 Data Accumulation.

At each position along the traverse four quantities, u_1, $\frac{\partial u}{\partial y}$, $\overline{U}_1$ and u'_1, were recorded. The source of these signals is shown in Fig. 9.

u_1 and $\frac{\partial u}{\partial y}$ were recorded on magnetic tape for approximately two minutes at each probe position. $\overline{U}_1$ and u'_1 both have a single numerical value at a position. They were therefore measured with the d.c. and rms meter respectively, and the results tabulated. At the tape speed used, 60 ips, the recorder frequency response is essentially flat from 0 to 20 K Hz. The tunnel was allowed to "warm up" and stabilize for approximately two hours before any readings were taken.

Since the tape recorder has a finite (35 db) signal to noise ratio it is generally desirable to record all signals at as high a level as possible. Therefore, since u is generally much "smaller" the $\overline{U}$, u_1 was recorded instead of U_1.

For continuous (non intermittent) random signals the record level is easily adjusted by setting the input attenuator on the tape recorder such that the level meters on the tape recorder read as large a value as possible, but below the saturation zone indicated by a red line. This maximizes the signal to noise ratio, with no saturation, or clipping of signal peaks. However, for a strongly intermittent signal, such as $\partial u/\partial y$ (and to a lesser extent u), the above procedure fails, since the level meters

tend to read an average value. This would result in ever increasing clipping of the turbulent bursts as the intermittency factor diminished. The method adopted was to set the record level by setting the input attenuator for maximum allowable level-meter reading with the probes positioned for maximum signal $\frac{\partial u}{\partial y}$, i.e., minimum intermittency (γ=1). The channel recording u_1 is similarly adjusted. The required signals are easily observable on an oscilloscope. For the present case both maximums occurred where Y/D equals 0.16. Recordings at all stations are then taken with these attenuator settings. This technique has the added advantage that all probability density plots (see Chapter 6) will automatically have the necessary identical horizontal scales. Any decreased signal to noise ratio presents no difficulty since $\frac{\partial u}{\partial y}$, being intermitten is always large when it exists. Also, in the region of interest, i.e. when γ=0, u is generally large. It should also be stated that even a small amount of clipping of $\frac{\partial u}{\partial y}$ has a very undesirable effect since it introduces new frequences especially at the higher end of the frequency spectrum. These new frequencies will become quite large after the second time derivative is taken, i.e. $\dot{S}(t)$ is formed.

The advantages of using a tape recorder for such experimentation are several.

1) Once the experiment is recorded, the wind tunnel, anemometers and linearizers are released for other experiments.

2) Detailed experimentation can all be done using the same data. In the present case this was important since the wind tunnel has a tendency

to drift especially when first turned on. Also hot wires contaminate with use and thus require periodic cleaning and recalibration. Occasionally they also break.

3) The analogue delay line mentioned in Sec. 5.1.5 is not required.

A velocity profile ($\overline{U}_1$) and a turbulence intensity profile (u'_1) are shown in Fig. 11. Both profiles are shifted slightly to the left. The reason for this was not investigated. Due to the obstruction (item VII, Fig. 8) on the probe it was not possible to get as close to the left wall as the right wall.

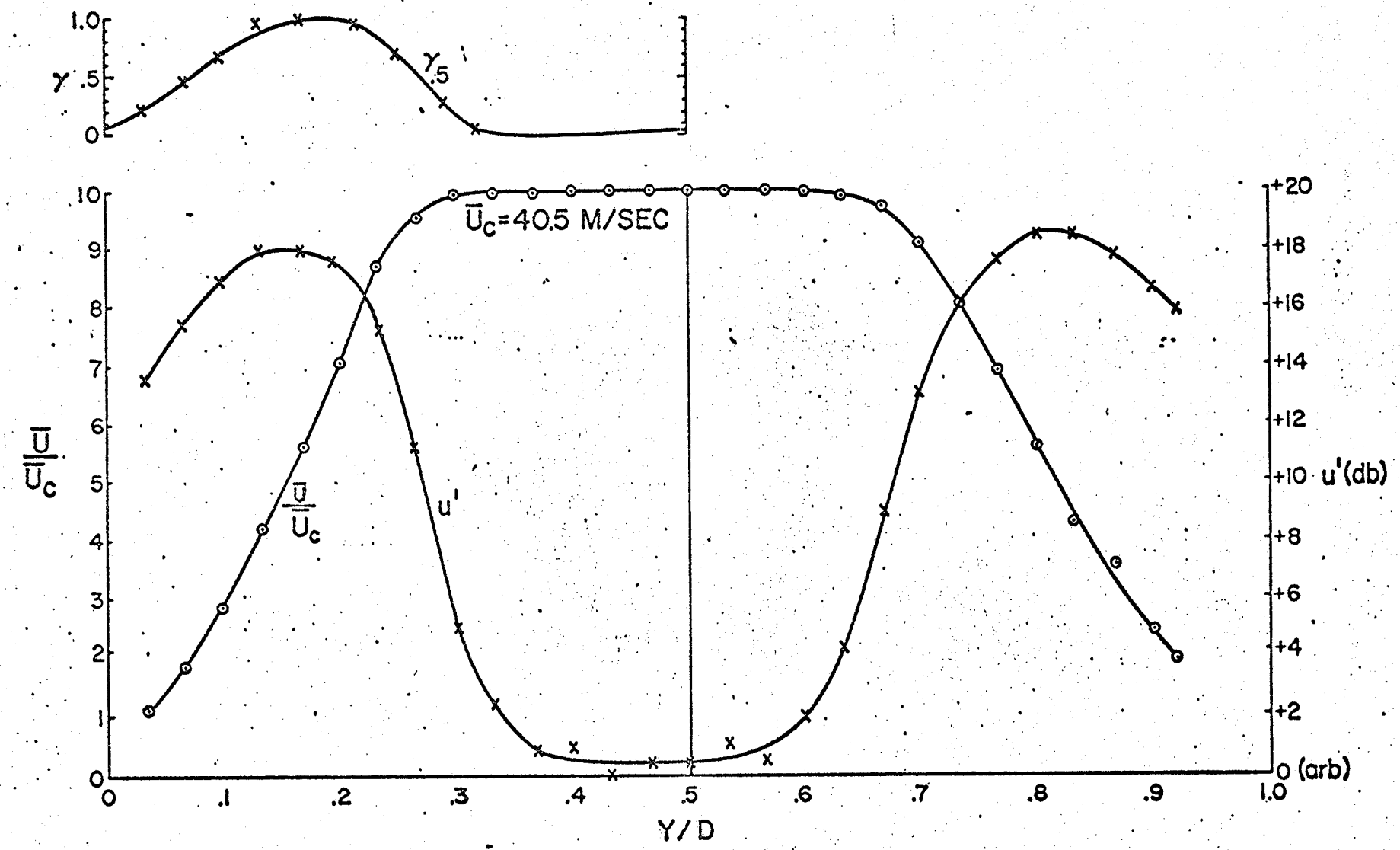

FIG.11 VELOCITY AND VELOCITY FLUCTUATION INTENSITY PROFILES AT STATION 6

6.0 A NEW METHOD OF FINDING THE INTERMITTENCY FACTOR.

As was previously mentioned the basic problem in using an interface detector lies in setting the gain or discriminator level since only a small change in setting varies the apparent intermittency over a wide range. Corrsin and Kistler (1955) attempted to solve this problem by recording the input signal (equivalent to S(t)) and the output signal I(t) on a dual-beam oscilloscope and adjusting the gain until the bursts of S(t) corresponded to 1 values of I(t). In the present investigation this method was tried but not considered successful since the results obtained were not reproducible, even by the same observer.

Kibens (1968) describes a procedure in which he uses a synthetic signal with known intermittency properties. By comparing these signals with real signals he describes a technique whereby γ may be found uniquely. It is the purpose of this chapter to introduce a new method based on probability density plots. In any case, no matter which method is used the fundamental problem is to find γ, independent of the gain setting. Thus, with γ known the gain may be easily set so that the signal I(t) has this γ.

6.1 A Technique for Making Amplitude Probability Density Plots.

A fast, accurate and economical way to make probability density plots is by using an instrument called a multi-channel analyzer (MCA). In the past these have been most often associated with experiments in nuclear physics. The high performance of these instruments can probably best be attributed to the fact that they incorporate a magnetic core memory, not unlike a digital computer.

Fig. 12 shows a sine wave oscillator, sampling gate, multi-channel analyzer, and XY recorder inter-connected to form a probability density analyzer. Assume $\dot{S}(t)$ is being analyzed. The sine wave oscillator produces the required gate signal. The sampling gate produces one pulse or sample for each complete sinusoid. The sampling rate (or number of samples produced per second) is set at 5,000., which is the maximum rate at which the multi-channel analyzer can process them. Compared with the time associated with the highest frequency component of $\dot{S}(t)$ (50 micro-seconds for 20 KHz), the width of the sample is narrow (2 micro-seconds). The amplitude of the sample is proportional to the instantaneous value of $\dot{S}(t)$ plus a suitable fixed bias, selected for convenience.

Pulses from the sampling gate are fed to the analogue to digital converter (ADC) which assigns an integer from 0 to 199 to each sample. The number assigned is proportional to the amplitude of the sample. The magnetic core memory consists of 200 words or channels each with a capacity of 10^5-1. Each number from the ADC is assigned a particular address. Thus as each sample is received it is assigned an address and the contents of the assigned address is incremented by 1. Initially all channels contain zero.

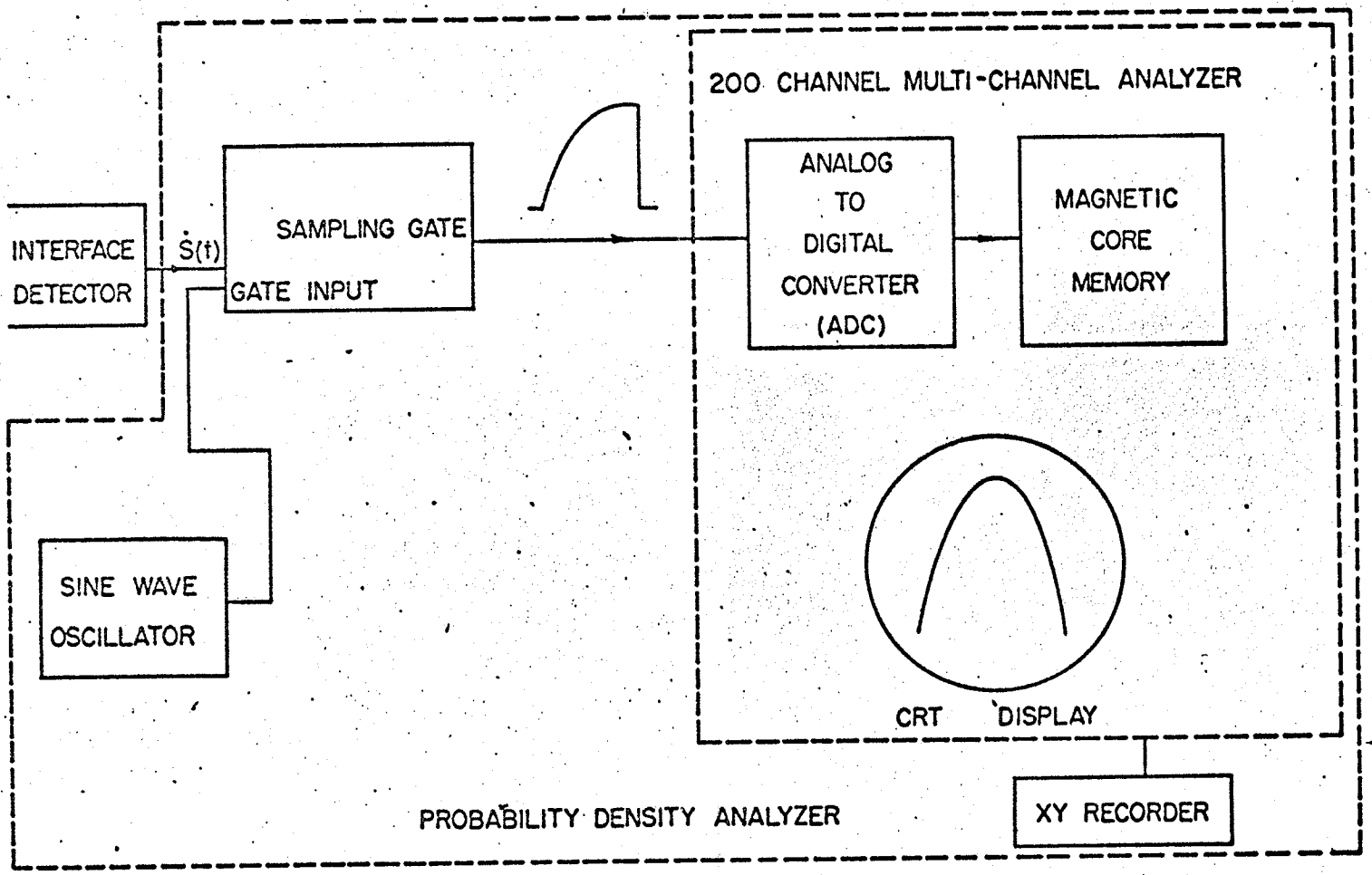

FIG.12 A BLOCK DIAGRAM OF THE PROBABILITY DENSITY ANALYZER

After many samples have accumulated, the contents of any given address (channel) is an indication of the probability of the corresponding amplitude.

Mathematically the pulse amplitudes are quantized into 200 values, $E_i; i=(o,1,2 \ldots 199)$. For each E_i an address i is assigned. From basic probability theory,

$$P(E_i) = \frac{n_1}{N} = \text{probability of amplitude } E_i,$$

where

n_i = contents of i,

N = combined contents of all channels.

A two dimensional plot with P(E) as ordinate, and E as abscissa is called a probability density plot of E (histogram). The MCA plots n_i versus i on an XY recorder. Because of the equivalence of E_i and i this is also a probability density plot if the vertical scale is divided by N. However, in this work, actual probabilities are not required, therefore N need not be calculated.

Fig. 13 shows a typical curve with the following features.

1) The horizontal scale is linear and arbitrary.

2) The vertical scale is logarithmic and arbitrary.

3) Statistical fluctuations, especially evident near the bottom of the graph where n_i is small are removed as indicated by the dotted line.

4) Even though both the horizontal and the vertical scales are arbitrary, the graph is referred to as a probability density plot.

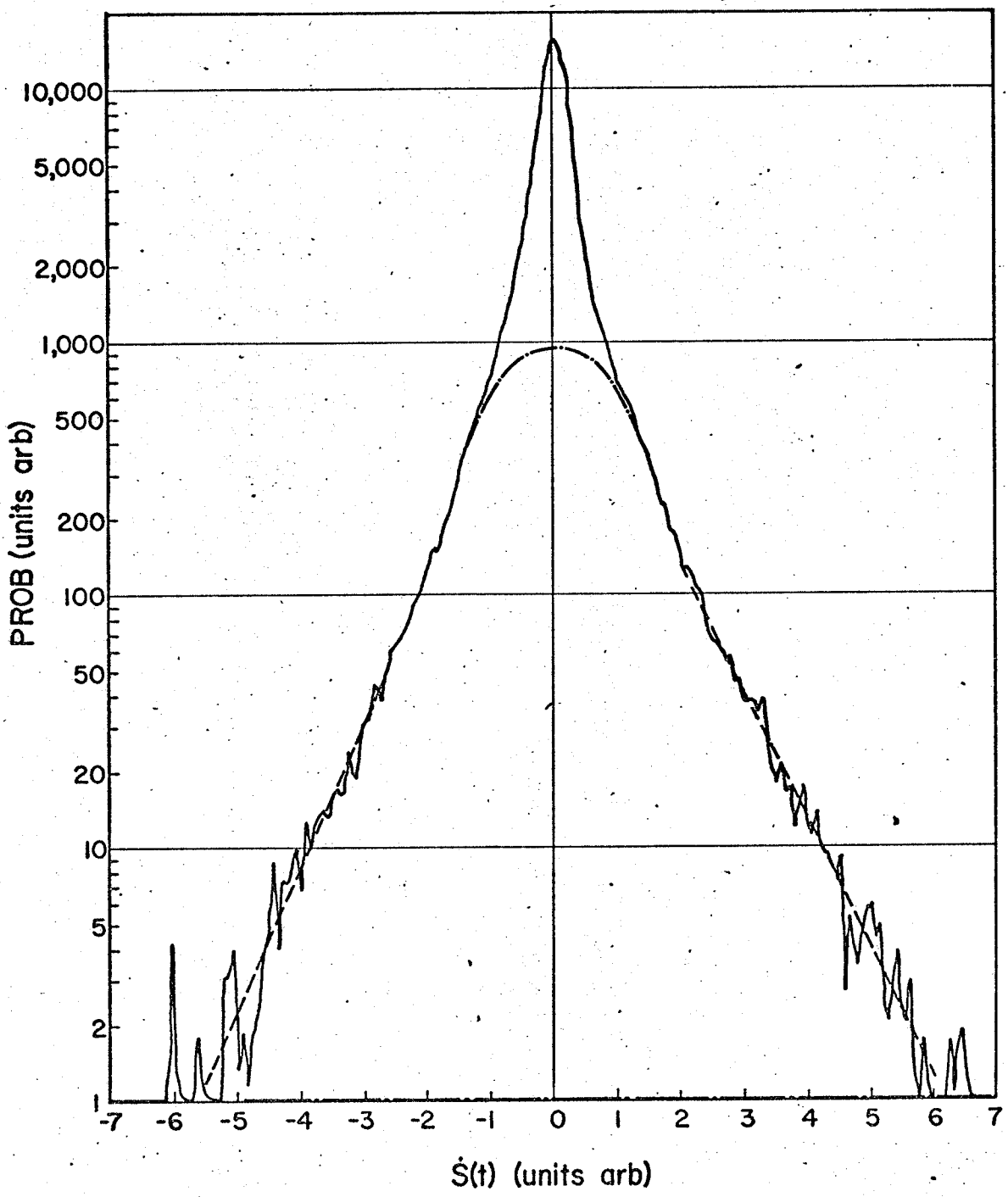

FIG.13 A PROBABILITY DENSITY PLOT OF $\dot{S}(t)$ AT Y/D=0.283

6.2 Calculation of γ From Amplitude Probability Density Plots.

Consider a synthetic signal made up as shown in Fig. 14.

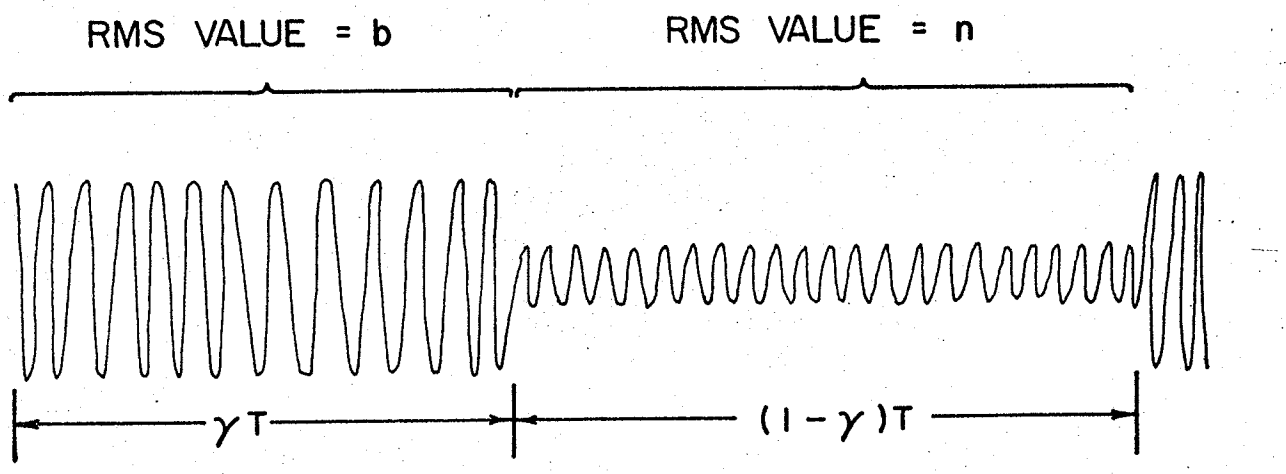

Fig. 14 The Wave Shape of a Synthetic Signal

The signal consists of alternate bursts with full time rms value b and length γT, followed by bursts with full time rms value n and length $(1-\gamma)T$. The signal is repetitive with period $\gamma T + (1-\gamma)T = T$. Clearly the intermittency factor of the signal is γ. Both signals are assumed normally distributed.

If the signal is sampled and the samples are accumulated by an amplitude probability density analyzer (See Sec. 6.1) a composite graph results, such as is shown in Fig. 15. (This graph was obtained by actually performing the experiment). Two distinct gaussian shaped peaks are evident. Assuming b larger than n, the wide peak is due to samples taken during the interval γT, the narrow peak from samples taken during the interval $(1-\gamma)T$.

Since the samples shows no preference for any time interval it

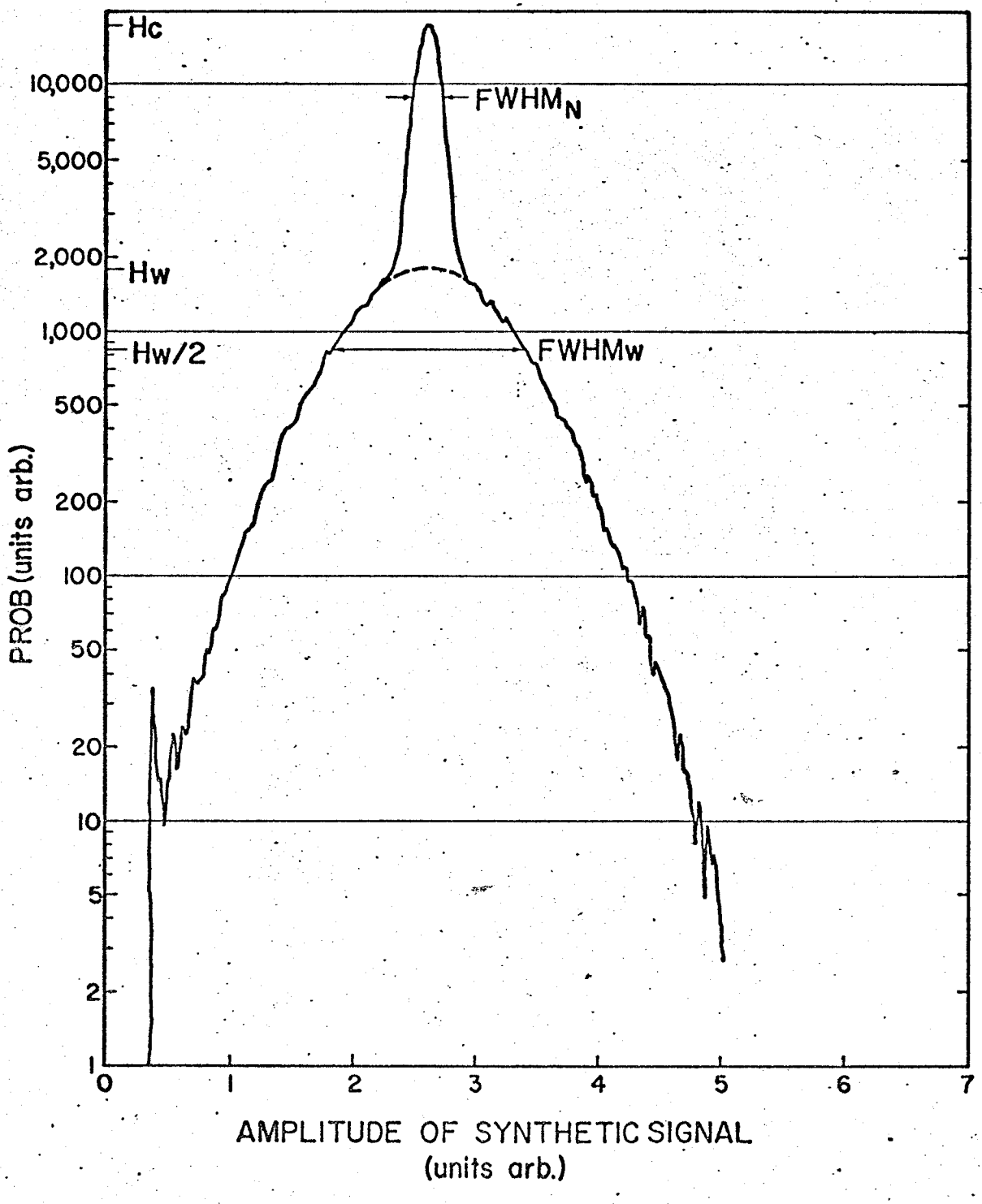

FIG.15 THE PROBABILITY DENSITY PLOT OF A SYNTHETIC SIGNAL

follows that the number of samples in any given interval is proportional to the width of that interval. Therefore

number of samples from T = KxT,

and

number of samples from $(1-\gamma)T$ = $Kx(1-\gamma)T$,

where

K is the constant of proportionality.

It follows that

$$\frac{\gamma}{1-\gamma} = \frac{\text{number of samples from } \gamma T}{\text{number of samples from } (1-\gamma)T}$$

$$= \frac{\text{area of wide peak}}{\text{area of narrow peak}}$$

$$= \frac{\text{height x width (wide peak)}}{\text{height x width (narrow peak)}} .$$

Since both peaks have the same shape (gaussian) the widths may be measured at any convenient place. It is common practice to choose the width where the height is one-half the maximum value. The width there is referred to as the full width at half maximum (FWHM). The height of the wide peak, Hw, can be measured directly after its peak is drawn in. The height of the narrow peak, Hn, equals the height of the composite peak, Hc, minus the height of the wide peak.

Substituting into the above

$$\frac{\gamma}{1-\gamma} = \frac{Hw \times (FWHM)w}{(Hc-Hw) \times (FWHM)n} ,$$

or

$$\gamma = \frac{1}{1 + \frac{Hc-Hw}{Hw} \times \frac{(FWHM)n}{(FWHM)w}}$$

Thus γ can be found accurately(within 2%) by plotting the probability density if the resulting curve can be readily decomposed into two gaussian shaped peaks.

6.3 Selecting a Suitable Field Variable for Sampling.

The field variables that could possibly be sampled to determine are the velocity u, $\frac{\partial u}{\partial y}$, S and $\dot{S}$. The criterion for the most suitable field variable is that the corresponding probability density plot should show two distinct, superimposed curves preferrably gaussian and symmetric. Plots of u and $\frac{\partial u}{\partial y}$, taken at various stations were found to be unsymmetric and in general no separate peaks were clearly defined. Probability density plots of S and $\dot{S}$ were found to be most suitable but essentially identical. Subsequently $\dot{S}$ was arbitrarily chosen.

6.4 The "Three Layer" Model.

Repeated efforts at dividing probability density plots of $\dot{S}(t)$ into two gaussian peaks as outlined in Sec. 6.2 proved unsuccessful with signals derived from diffuser flow. Comparing Figures 13 and 15 (for the natural and synthetic signals) in the former, the location of any partition, as indicated by the dash-dot line would have to be arbitrary whereas in the latter, the position of the partition line is obvious. It was therefore decided that perhaps diffuser flow could not be adequately described by

a two layer model, and the possibility of a transition layer between the turbulent and non-turbulent fluid was considered. Samples taken while the probe was in the transition zone would then produce their own characteristic gaussian peak.

Using this hypothesis let the composite peak F be approximated by

$$F = A\, G(\sigma_T) + B\, G(\sigma_I) + C\, G(\sigma_N), \qquad (5.1)$$

where A, B, and C are constants to be determined for each probe position, and where $G(\sigma_T)$, $G(\sigma_I)$ and $G(\sigma_N)$ represent gaussian peaks characteristic of turbulent, transition, and non-turbulent flow respectively. The deviations of each i.e., σ_T, σ_I, and σ_N must be found. These are independent of probe position.

The procedure is somewhat analogous to the Fourier Analysis technique. Finding the six unknowns is straight forward as outlined in the following steps.

1) Probability density plots are made at each probe position of interest as shown in Fig. 16. Since the plots turn out to be symmetric about the maximum only one side need be drawn in detail. The plots are not compared with each other in magnitude (only in shape). Therefore the maximum of all plots can be set to the same value as shown. A logarithmic vertical scale has been found desirable to facilitate the manipulations outlined in the subsequent steps. Extending the scale over four decades was found adequate. The horizontal scale is linear, arbitrary, and consistent for all plots.

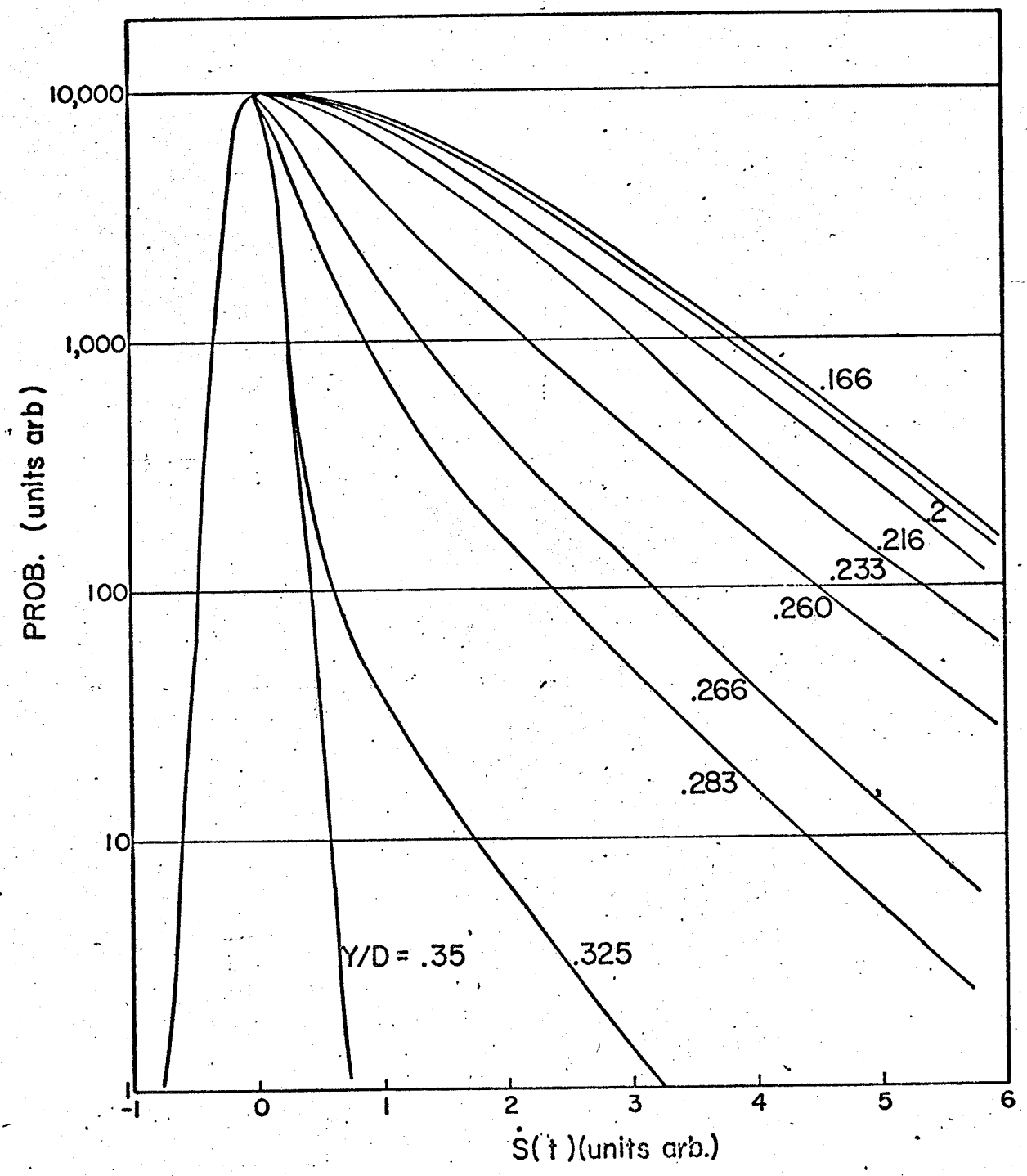

FIG.16 PROBABILITY DENSITY PLOTS OF $\dot{S}(t)$ AT VARIOUS PROBE POSITIONS

2) In particular, plots are made with the probes in the fully turbulent and fully non-turbulent flow. These plots are characterized by their mono-gaussian nature but with widely different σ values. They were found at Y/D values of .166 and .350 respectively. Thus $G(\sigma_T)$ and $G(\sigma_N)$ are obtained as shown in Fig. 17.

3) $G(\sigma_I)$ is obtained less directly. A plot is made at a position where very few bursts of turbulence occur. Since the fluid giving rise to these bursts is so close to the non-turbulent fluid it is assumed that at these points transition flow obtains. Fig. 18 shows such a plot. The outer-most flanks of the bell shaped composite curve are attributed to fully turbulent flow which is accounted for by $G(\sigma_T)$. $G(\sigma_I)$ is then drawn in of such shape as to account for the remainder of the composite curve not attributable to non-turbulent flow which is accounted for by $G(\sigma_N)$. Complete $G(\sigma_I)$ is also shown in Fig. 17. Thus the widths, or deviations of all three component peaks have been established. The widths are measured as shown in Fig. 17 and are found to be in the ratio

$$\sigma_N:\sigma_I:\sigma_T = 5.2:2.3:70 = 1:4.4:13.4$$

4) Fig. 16 shows a family of probability density curves taken at various probe positions. Assuming each curve can be approximated by Equation 5.1 it remains to find the constants A, B, and C for each curve. The results for all the non-mono-gaussian curves are given in Figures 18-24. The procedure is outlined with respect to Fig. 19 as follows.

At point M all of the composite curve must be attributed to turbulent flow. Hence $G(\sigma_T)$ is constructed of such amplitude as to merge with

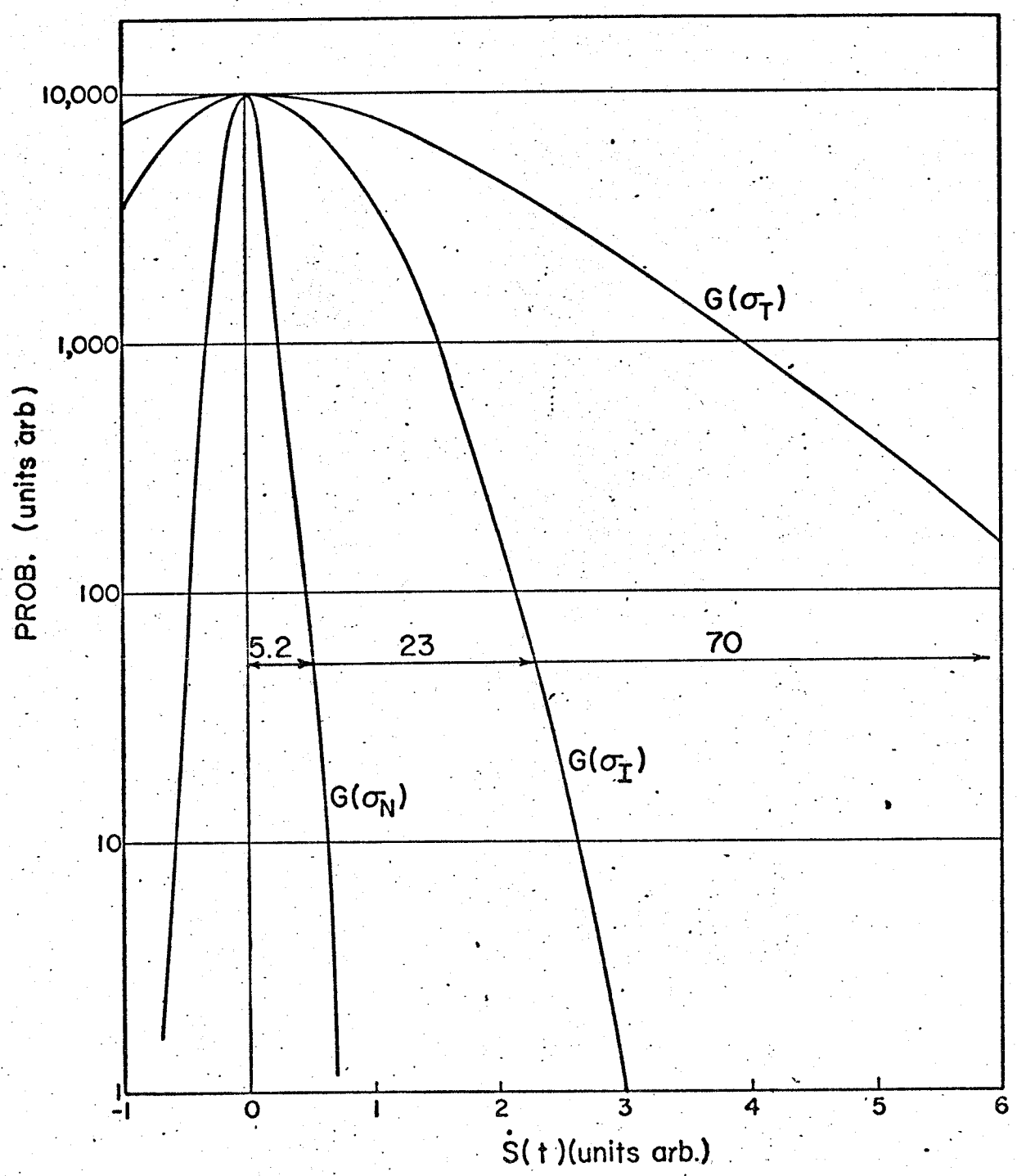

FIG.17 CHARACTERISTIC PROBABILITY DENSITY PLOTS FOR THE THREE TYPES OF FLOW

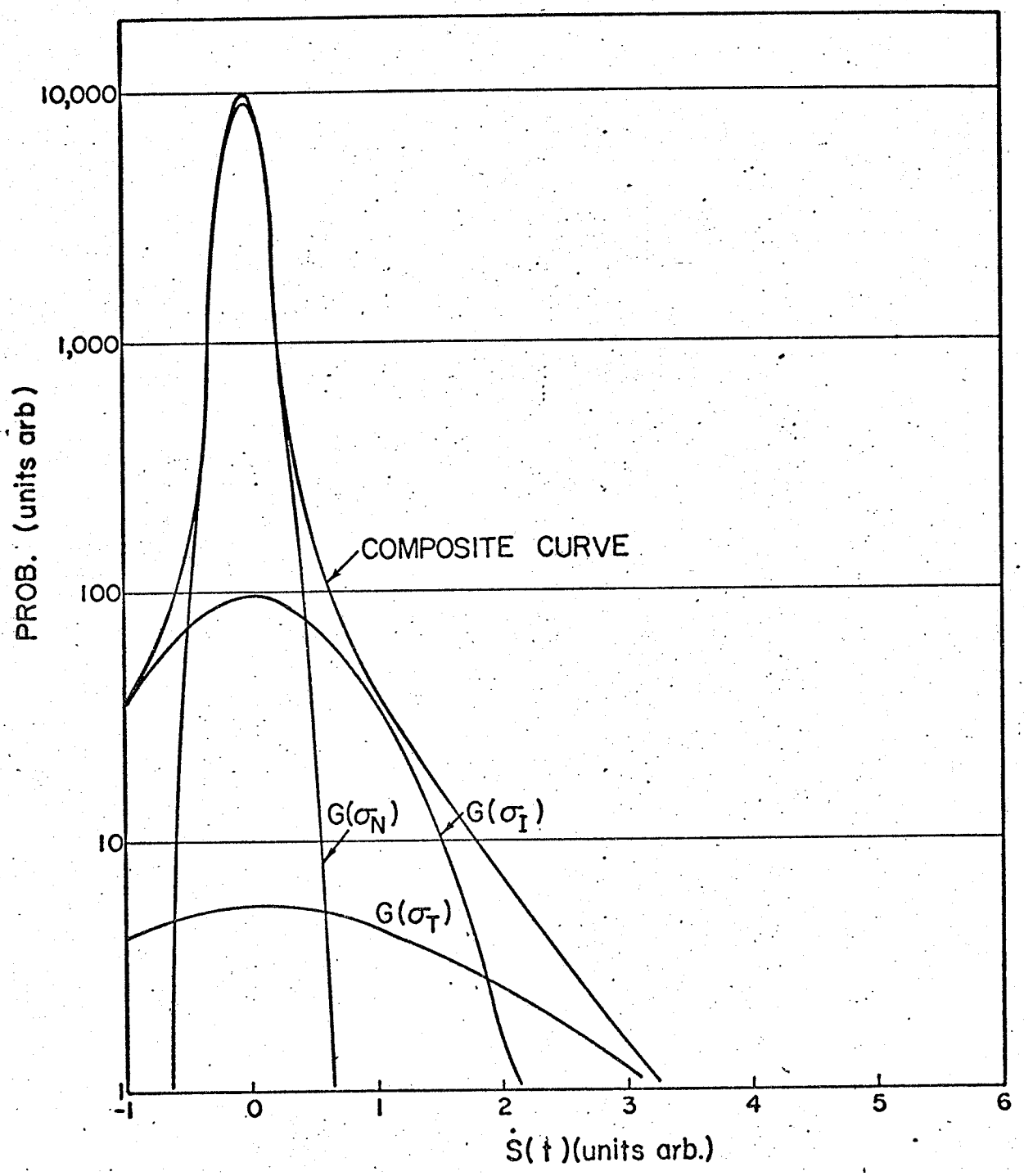

FIG. 18 PROBABILITY DENSITY PLOT OF $\dot{S}(t)$ - Y/D=0.325

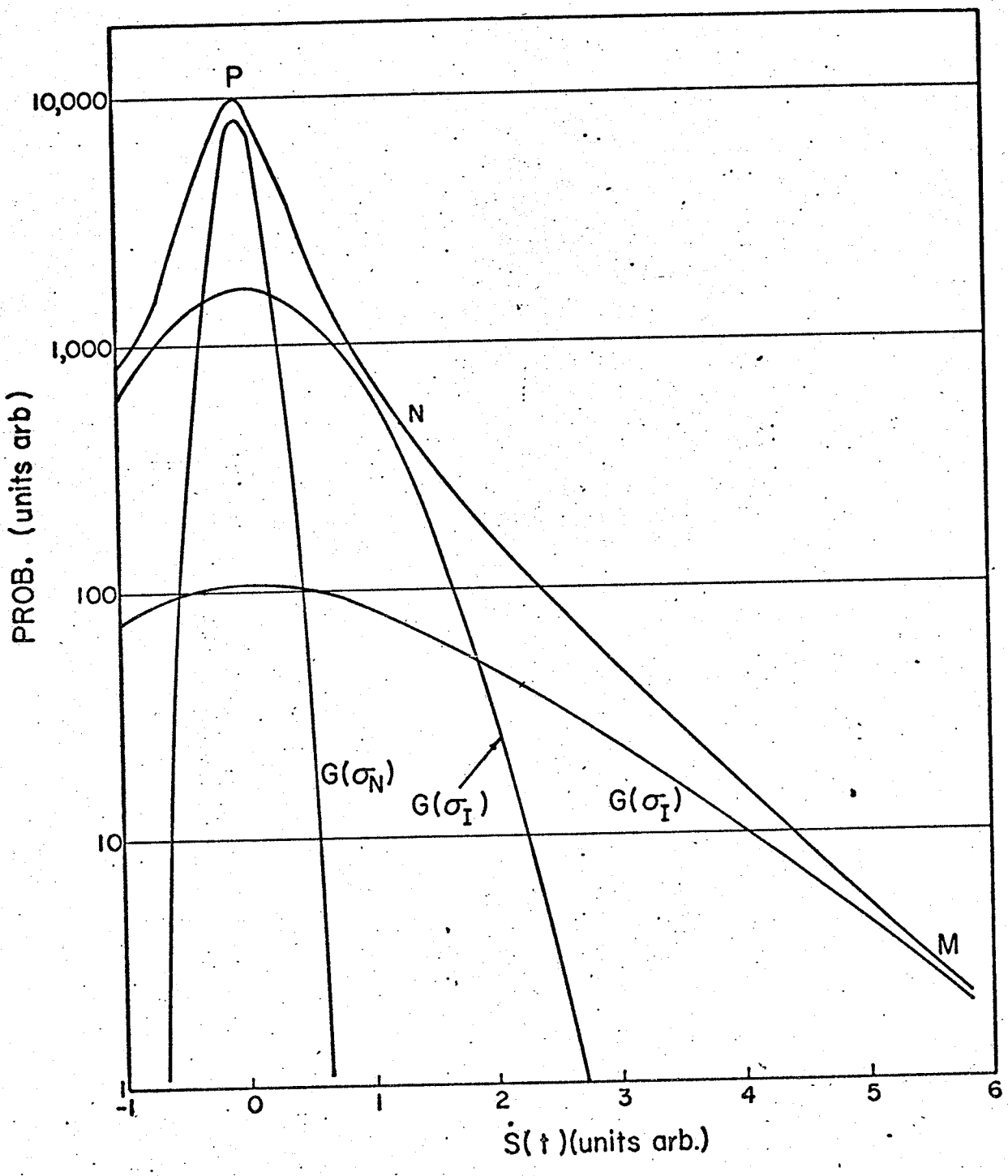

FIG.19 PROBABILITY DENSITY PLOT OF $\dot{S}(t)$ - Y/D=0.283

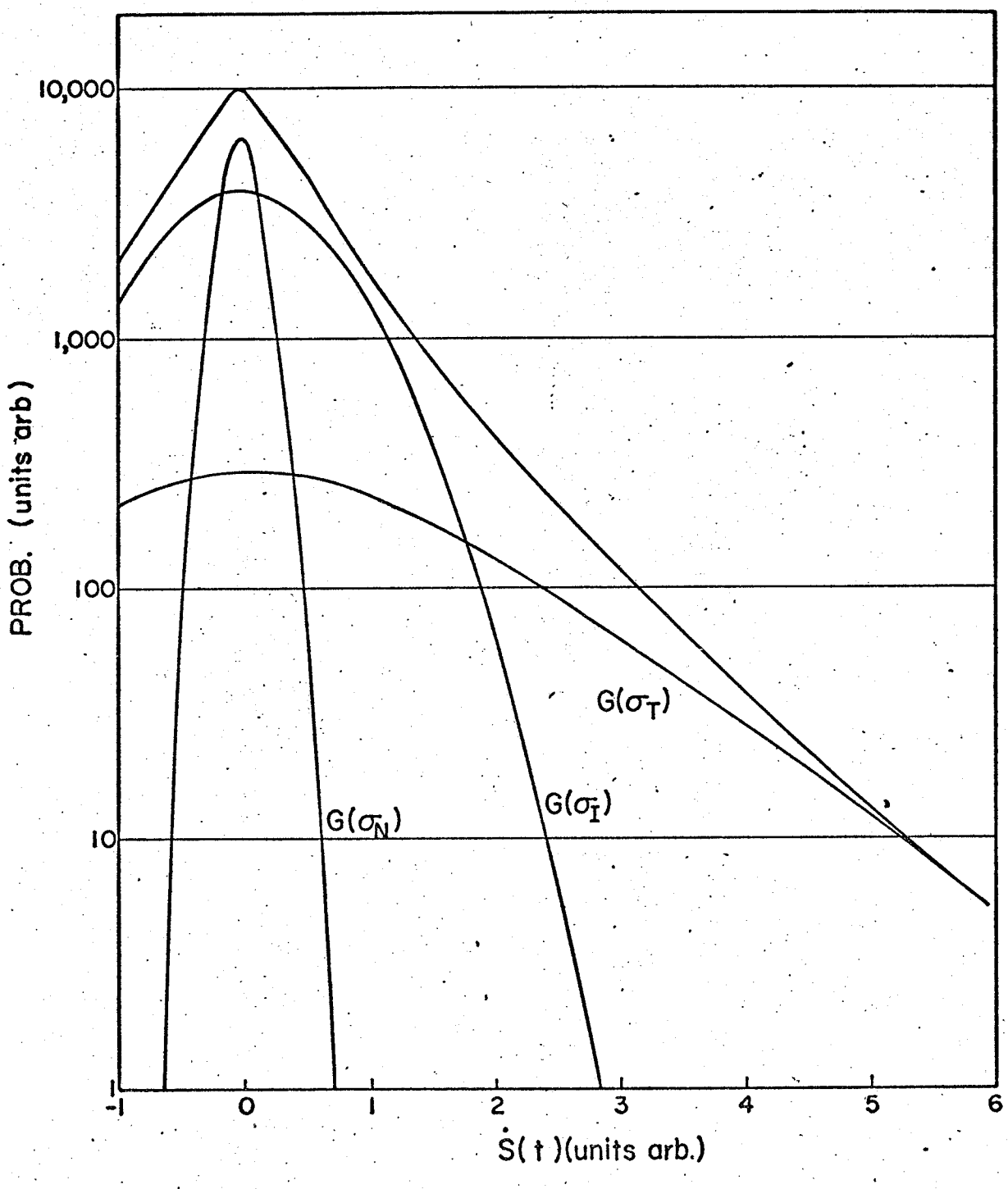

FIG.20 PROBABILITY DENSITY PLOT OF $\dot{S}(t)$ - Y/D=0.267

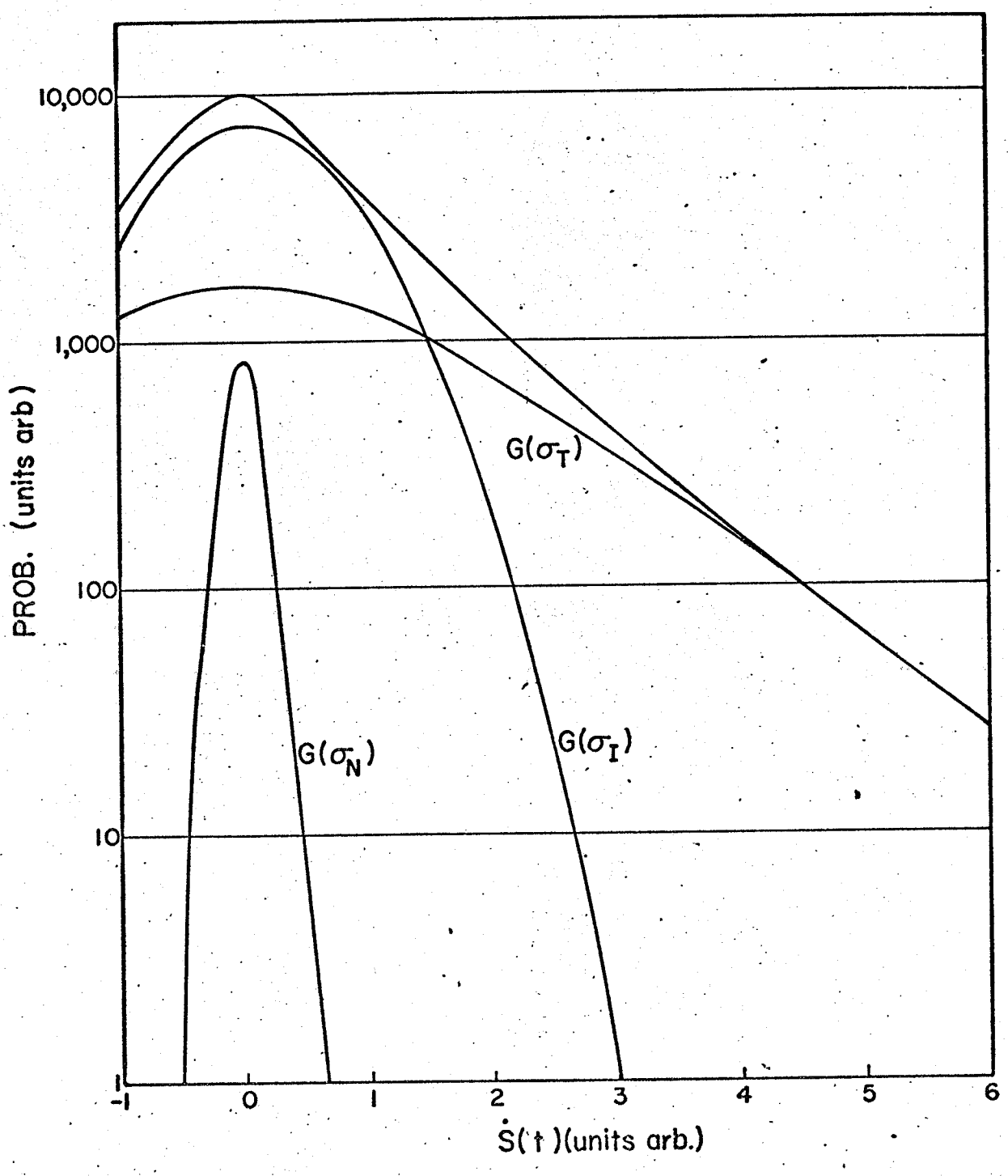

FIG. 21 PROBABILITY DENSITY PLOT OF $\dot{S}(t)$ - Y/D=0.250

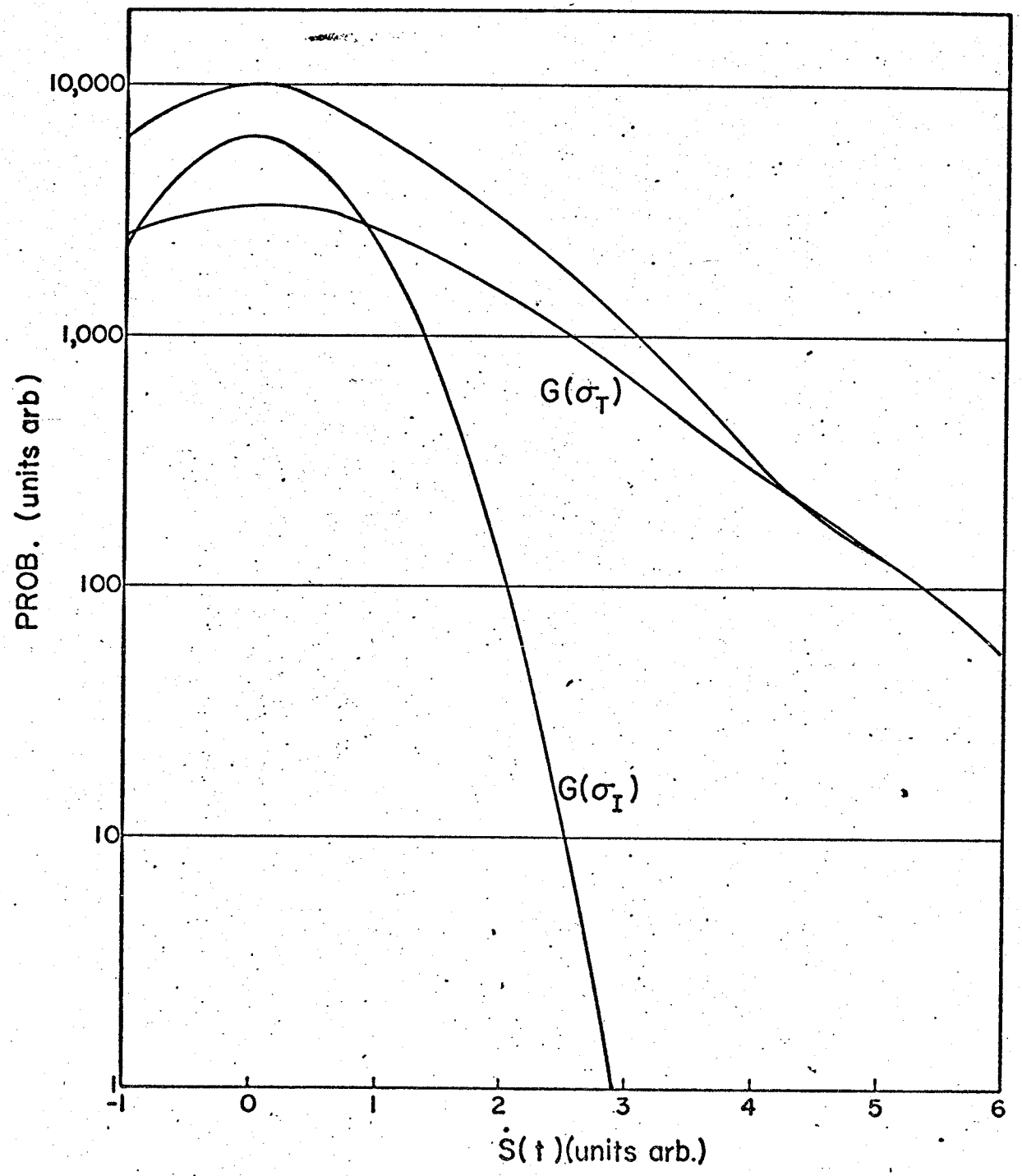

FIG.22 PROBABILITY DENSITY PLOT OF $\dot{S}(t)$ - Y/D=0.233

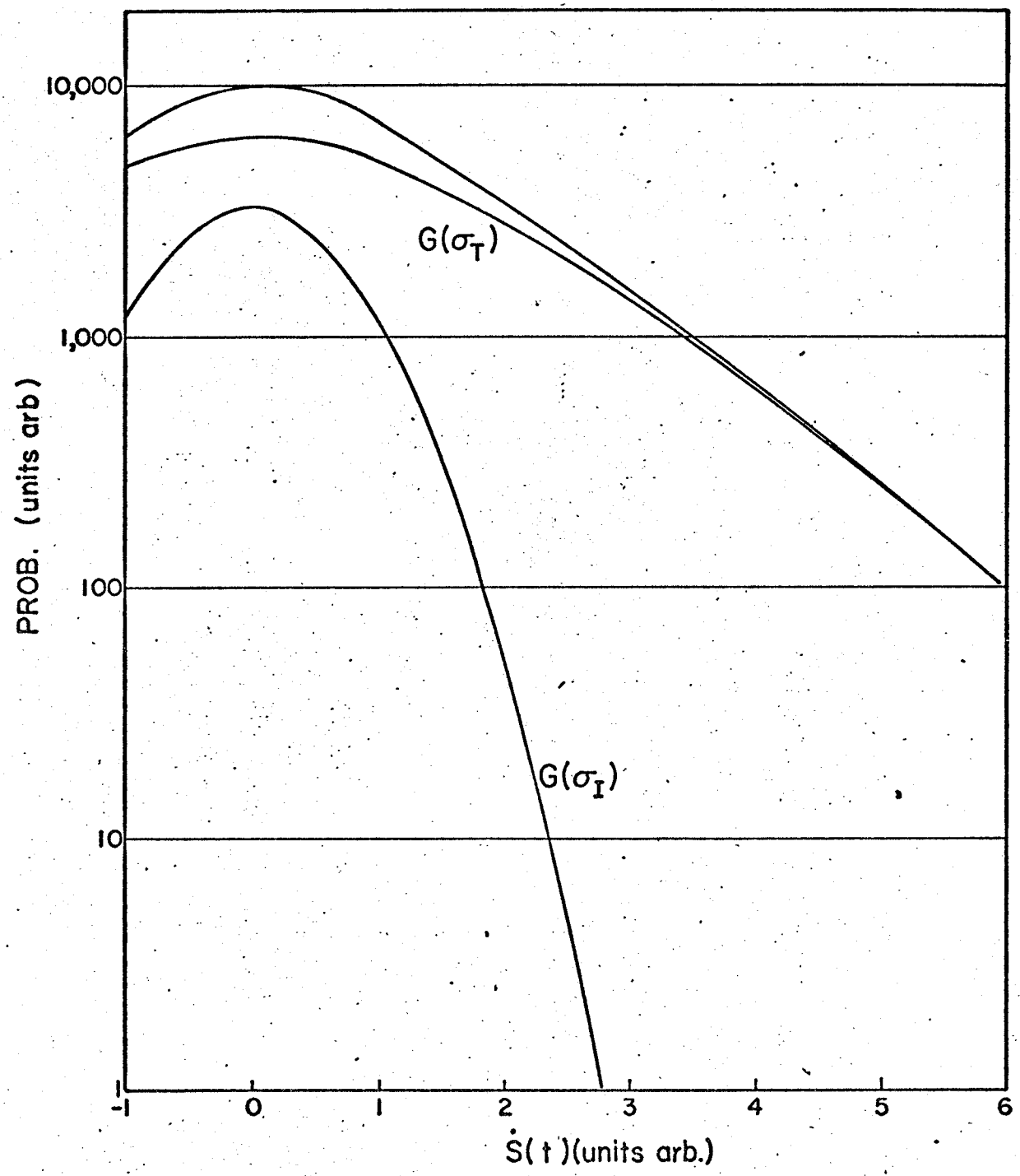

FIG.23 PROBABILITY DENSITY PLOT OF $\dot{S}(t)$ - Y/D=0.216

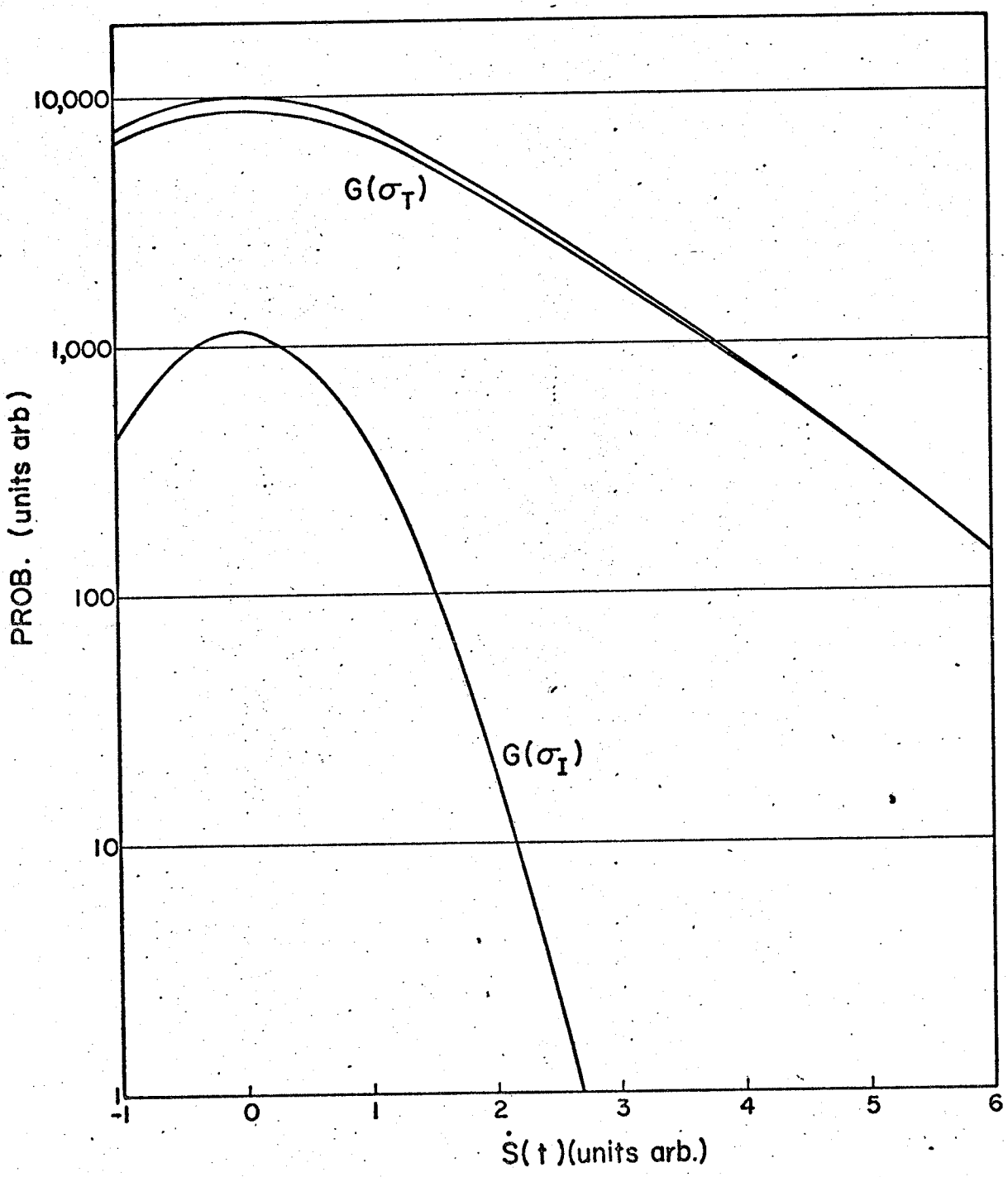

FIG.24 PROBABILITY DENSITY PLOT OF $\dot{S}(t)$ - Y/D=0.200

the composite curve at M. At point N, $G(\sigma_I)$ and $G(\sigma_T)$ must sum to the composite curve. $G(\sigma_I)$ can therefore be drawn in accordingly. Similarly at P the sum of all component peaks must equal the composite peak. Hence, $G(\sigma_N)$ can be constructed. The constants A, B and C are the maximum values of the corresponding peak. In this case

$$A = 100$$

$$B = 1700$$

$$C = 8200$$

6.5 Intermittency Calculations.

The entire concept of intermittency as presently defined by Townsend is basically of a binary nature since it implies that at any given time a probe must be in either of two distinct flow states. Present evidence indicates that there are three such states and the question is - should the transition state be considered turbulent or non-turbulent? The question of intermittency thus becomes one of giving it a more specific definition. A proposed new definition would specify the fraction of transition flow included in the turbulent flow. The fraction is designated by the symbol M, used as a subscript which varies from zero to one. Thus, γ means all transition flow is considered turbulent; $\gamma_{.5}$ means that half the transition flow is considered turbulent and γ_o means that the transition flow is considered non-turbulent etc. In general one writes γ_M, defined by:

$$\gamma_M = \frac{\text{area of turbulent peak} + M \times \text{Area of transition peak}}{\text{area of composite peak}}$$

$$= \frac{A_T + M\,A_I}{Ac} = \frac{A_T + M\,A_I}{A_T+A_I+A_N} \quad .$$

The method is illustrated by a sample calculation.

At Y/D = .283 (Fig. 19)

A_N = 8200 x 5.2 = 42,600,

A_I = 1700 x 2.3 = 39,100,

A_T = 100 x 70 = 7,000.

Therefore, for M = 0.5

$$\gamma_{.5} = \frac{7,000+.5 \times 39,100}{42,600+39,100+7,000} = \frac{26,550}{88,700} = .298$$

The results for M value of 1, 0.5 and 0 are shown in Fig.25 by the dotted graphs on the right side.

The entire experiment was repeated using completely different data. In this case measurements were extended to the wall. The results are shown by the solid line graphs in Fig. 25. It is also interesting to show the probability of the three types of flow. This is done by comparing the area of the particular flow with the total area.

Thus, for example

Probability of turbulent flow $\equiv \frac{A_T}{A_C}$

The results, using the first set of data are given in Fig. 26. $\gamma_{.5}$ is also shown.

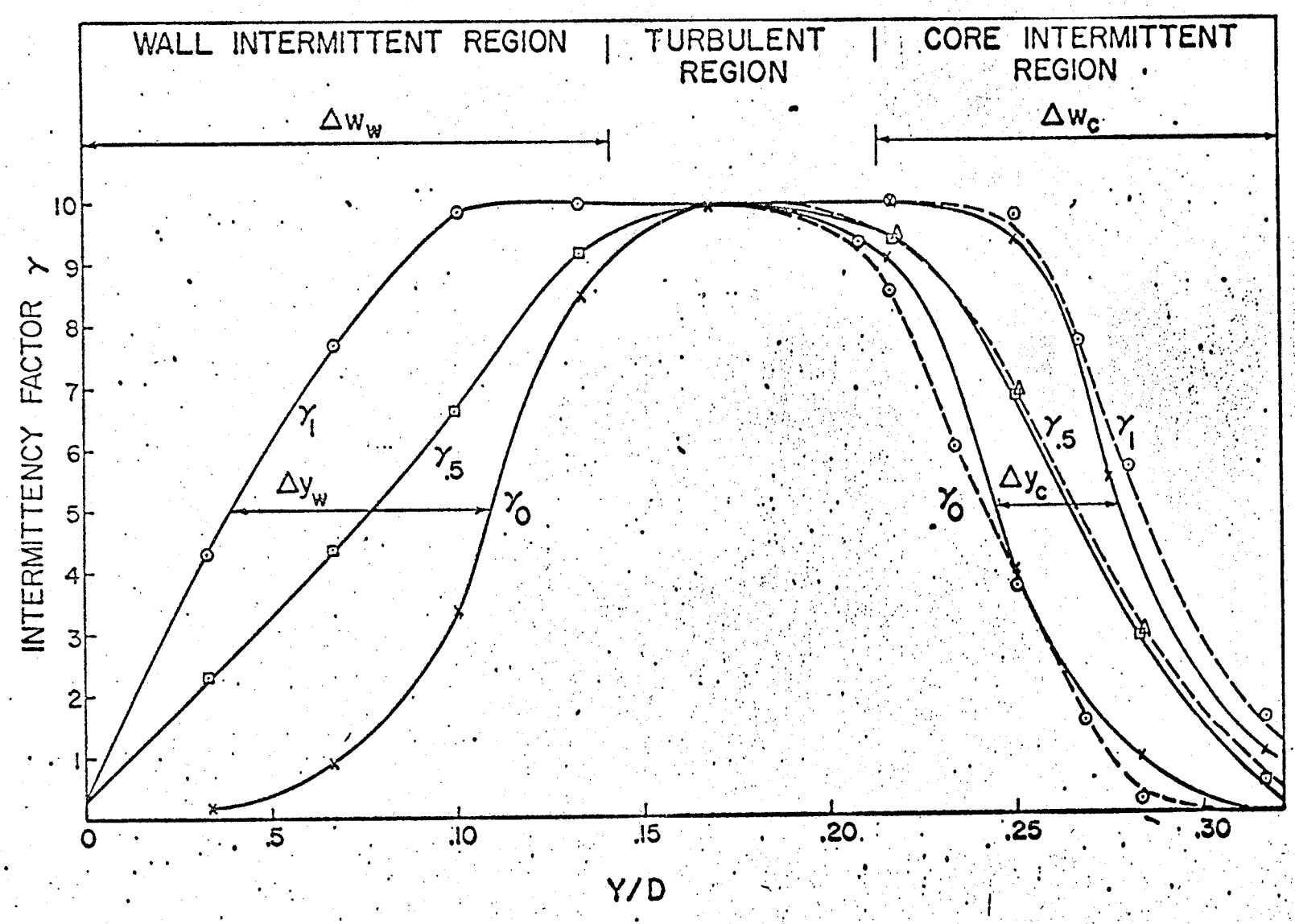

FIG. 25 INTERMITTENCY PROFILES

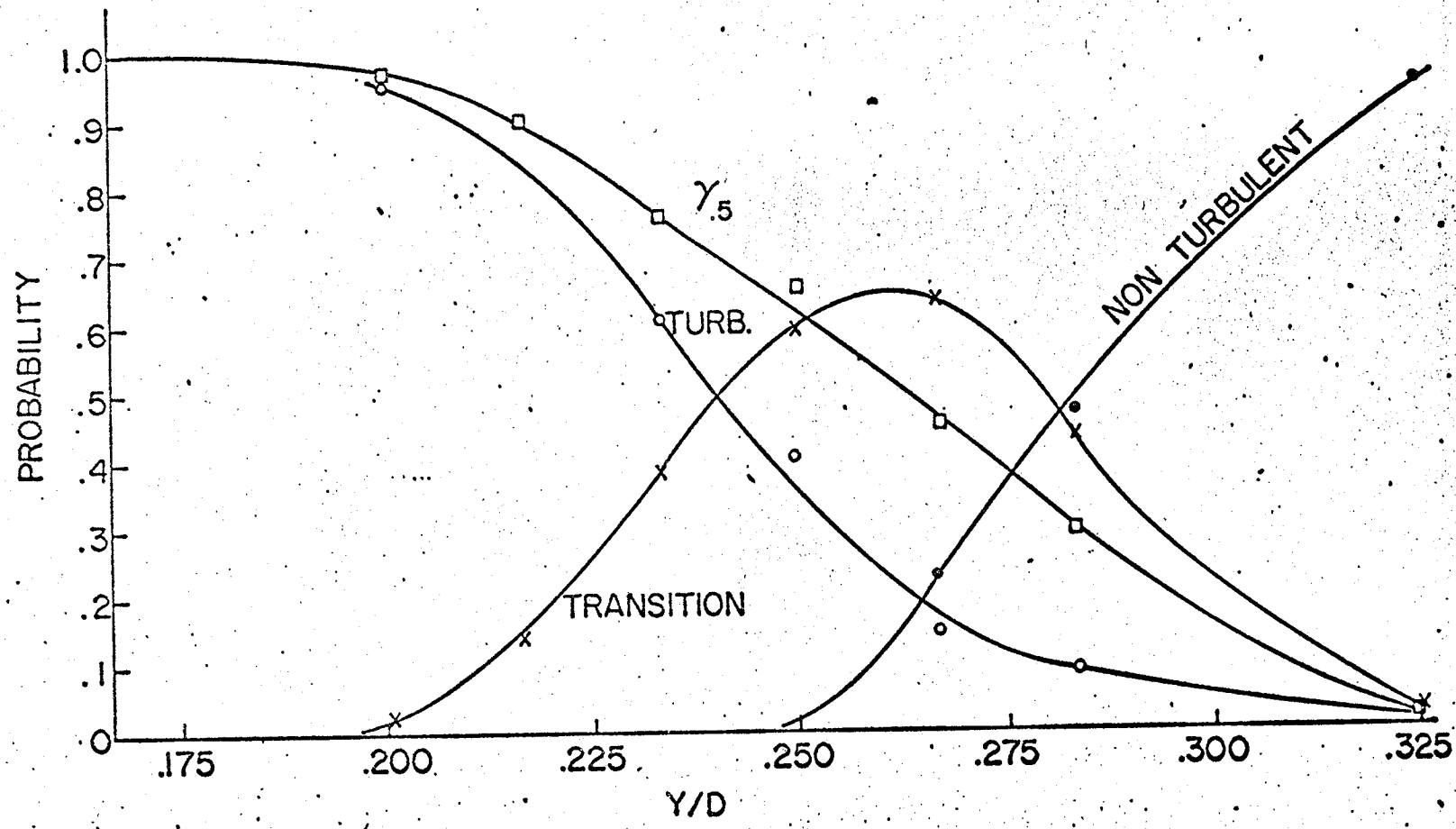

FIG. 26 THE PROBABILITY OF DIFFERENT TYPES OF FLOW

6.6 Discussion of Results.

The results show that the transition from turbulent to non-turbulent flow in a diffuser is not instantaneous. Townsend (1956,p99) has already suggested this for he says -

> "We would not then expect the boundary between the the regions of zero and appreciable vorticity fluctuations to be a sharp division between small and large velocity fluctuations, but it turns out to be a moderately distinct and in an approximate theory of motion may be treated as sharp."

An important feature of the new method is that γ can be found by a technique which is completely specified, and in this respect is somewhat similar to the flatness factor method.

The ratio of three members, σ_N, σ_I and σ_T, characterizing the three types of flow has been found. For the specified experimental conditions they were found to be in the ratio, 1: 4.4 : 13.4

On traversing from the centre of the diffuser to the wall, the intermittent zone apparently repeats itself. This tentative conclusion can only be justified in the light of more experimentation. For the present discussion, however, it is assumed to be a fact.

Referring to Fig. 25 it seems reasonable, and it is therefore proposed, that the horizontal spacing between γ_o and γ_1 be considered as an indication of the intermittency intensity, i.e. a measure of the degree to which intermittency exists. Specifically.

$\beta \equiv$ intermittency intensity factor

$$= 1 - \frac{\Delta y}{\Delta w} = \frac{\Delta w - \Delta y}{\Delta w}$$

where Δy is the horizontal distance measured from γ_o to γ_1 at γ=0.5, and Δw is the width of the intermittent zone, specified as the horizontal span of $\gamma_{.5}$ corresponding to its vertical span measured from .05 to .95.

It is assumed at this stage that Δy is always less than Δw, therefore β varies from zero to one. β values approaching one correspond to very intermittent flow, in the sense that there is very little transition flow. β values approaching zero imply no intermittent flow.

From Fig. 25

w_w = 108 (unit arb)

w_c = 81

y_w = 55

y_c = 26

Thus, for the given experimental conditions:

1) The wall intermittent region is $\frac{108}{81}$ = 1.33 times as wide as the core intermittent region.

2) The intermittency intensity factor, Δ_w, in the wall intermittent region is $\frac{108-55}{108}$ = .49.

Similarly in the core intermittent region $\beta_c = \frac{81-26}{81}$ = .62.

The intermittency in the latter region is therefore said to be 1.26 times as intense as the former.

7.0 EXPERIMENTS AND RESULTS

This chapter describes a number of experiments most of which demonstrate the type of experimentation possible with an interface detector.

7.1 Energy Spectrum Measurements of u_1.

These measurements were made at various positions on the left side of the diffuser using the FRA2C Constant Bandwidth Wave Analyzer. The bandwidth was set at 2Hz for measurements from 10 to 50 Hz and 25 Hz at higher frequencies. The results are plotted in two different ways as shown in Fig. 27 and 28. The vertical scale in both cases is given in decibels with the origin arbitrarily chosen for convenience. Thus, all the results are comparative, i.e. they can only be compared with each other. The mean velocity and intermittency factor are also shown on top of Fig. 28 for comparison.

7.1.1 Discussion of Results

From the energy spectra measurements the following can be concluded.

1) Most of the energy is in the lower frequencies, less than 500 Hz, say.

2) The amplitudes of the low frequency components increase faster than those of the high frequency components as one moves from the centre to the wall.

3) Maximum vorticity fluctuations, velocity fluctuations, and intermittency factor , all occur where the mean velocity is changing most rapidly. This occurs where Y/D is approximately 0.15.

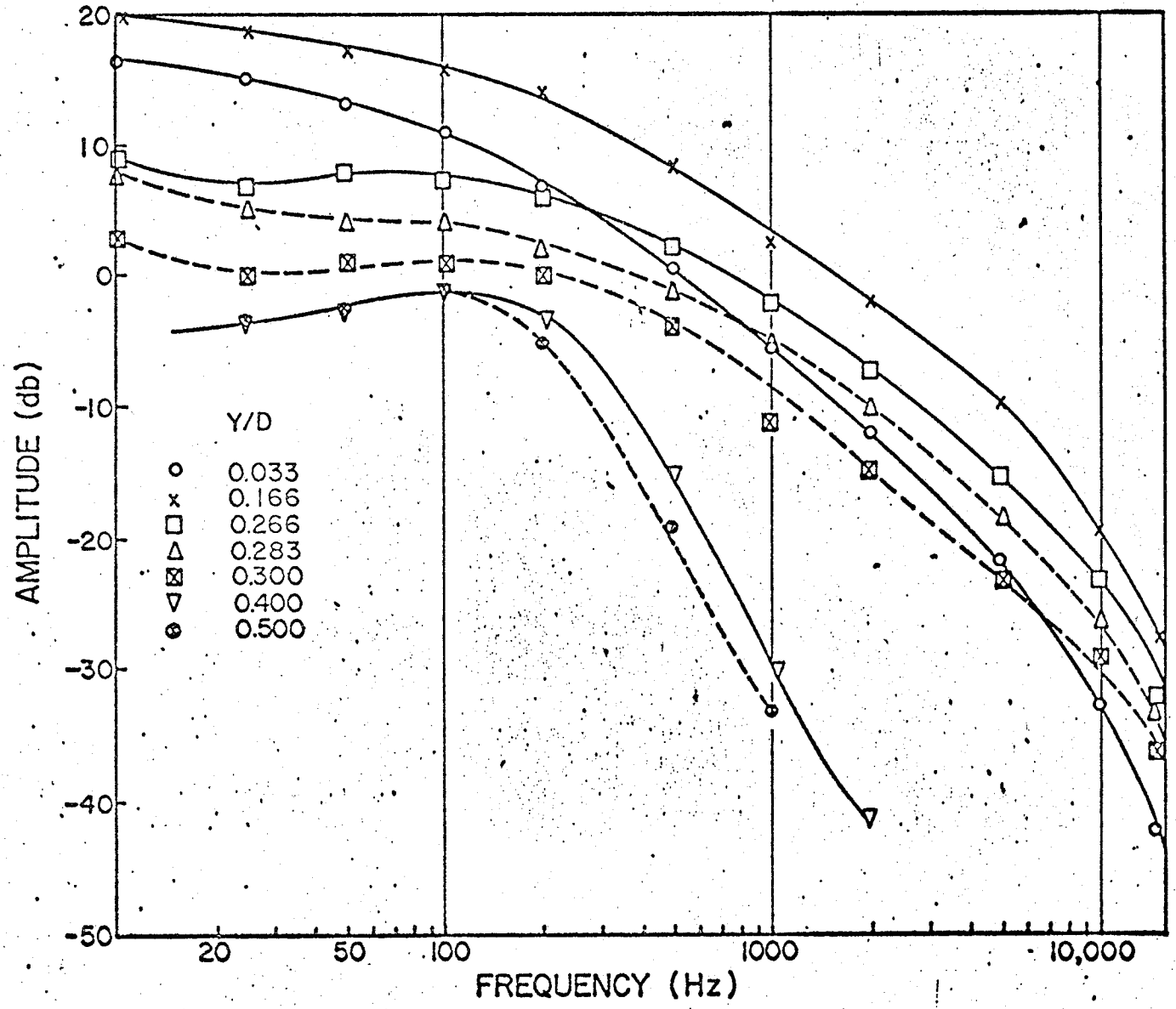

FIG. 27 THE SPECTRAL DENSITY OF THE SIGNAL u

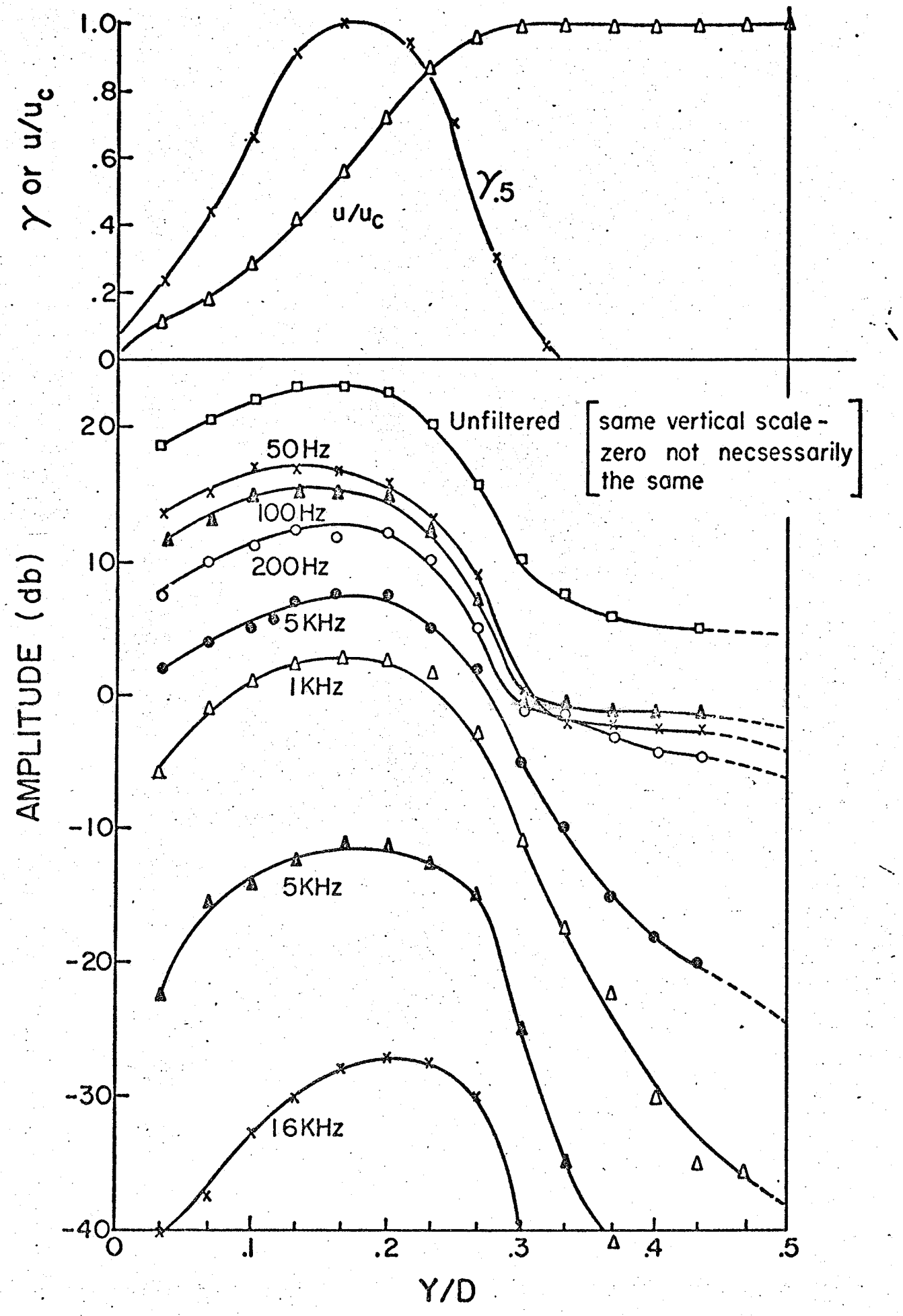

FIG. 28 THE SPECTRAL DENSITY OF THE SIGNAL u

7.2 γ Measurement Using a Digital Technique.

It was shown in Chapter 3 that an interface detector does not actually measure γ. This is done independently by the technique described in Chapter 6. The problem remaining is therefore to measure the mean value of I(t), i.e. γ, and then to adjust the gain on the interface detector such that the measured γ equals the one required.

The procedure is as follows. Refer to Fig. 9. Set the frequency of the sine wave oscillator to 100.0 KHz. Preset the frequency counter to 10 seconds. With S_2 on I(t) the frequency counter reads γ directly. Thus, if after 10 seconds the counter reads 631,215, then γ equals 0.631.

7.3 Measurement of Zone Averages and Zone Probability Density Plots.

As previously mentioned, one of the most basic advantages of using an interface detector is that it allows one to perform the operations of conditioned averaging and sampling. Thus the average of U(t) on the condition that the flow is turbulent can be found. Such an average is referred to as a "turbulent zone average" and can be formally expressed as

$$\bar{\tilde{u}} = \lim_{(T_2-T_1)\to\infty} \frac{1}{\gamma(T_2-T_1)} \int_{T1}^{T2} I(t)\, U(t)\, dt$$

A similar expression exists for the non-turbulent zone average.

The procedure for measuring zone averages is described with reference to Fig. 9. The signal u is fed to the sampling integrator, I(t) is the gate signal. Since only the fluctuating part of the velocity is recorded on

the tape recorder, the signal, equivalent to the mean velocity $\overline{U}$, is provided by an appropriate dc voltage supplied by VRI. (See Fig. 41). With the gate continuously open (S2 on 1, Fig. 9) the panel meter reads the mean velocity. With S2 switched to I(t) the panel meter reads the turbulent zone average velocity. However, the turbulent zone average is normally expressed as the difference of the above readings taken as a percentage of the mean velocity found in the centre of the diffuser. In a similar manner the non-turbulent zone average can be found by using 1-I(t) instead of I(t) for a gate signal. The results are shown in Fig. 29. A zone probability density plot of u is derived from samples taken only during those intervals when the flow is turbulent (or non-turbulent). The procedure is outlined with reference to Fig. 9. S2 is switched to "I(t)", S3 to "u", S4 to "pulse", and S5 to "sample". The sampler is used in the sampling gate mode and the frequency of the sine wave oscillator is set to 5 KHz. Thus the multichannel analyzer accumulates u on the condition that the flow is turbulent. A similar plot for non-turbulent flow is obtained with S2 on 1-I(t). An unconditional plot is obtained with S2 on 1. These three plots have been taken at three different probe positions. The results are shown in Figs. 30, 31 and 32.

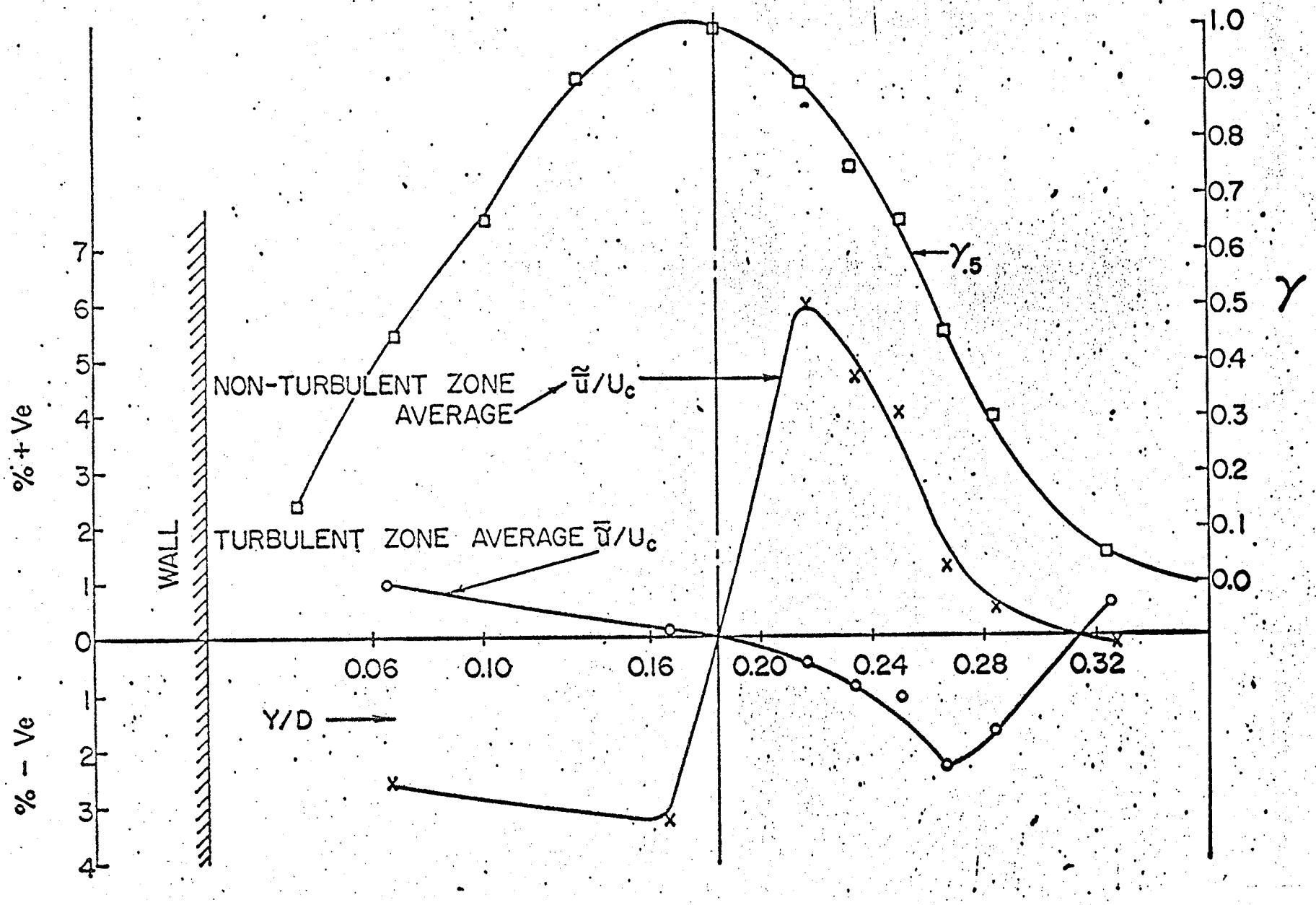

FIG. 29· TURBULENT AND NON-TURBULENT ZONE AVERAGES

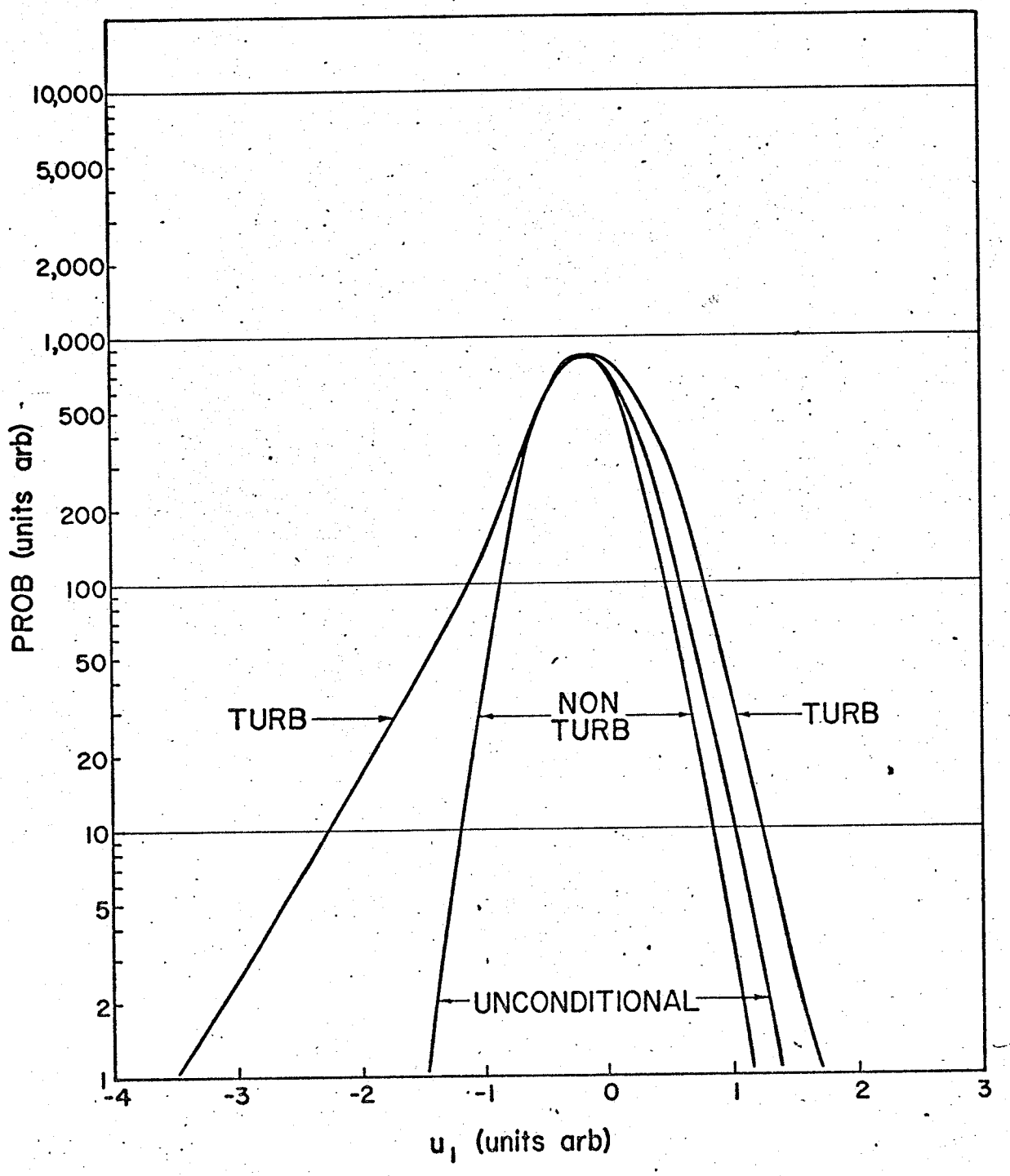

FIG. 30 ZONE PROBABILITY DENSITY PLOT OF u_1 - Y/D=0.325

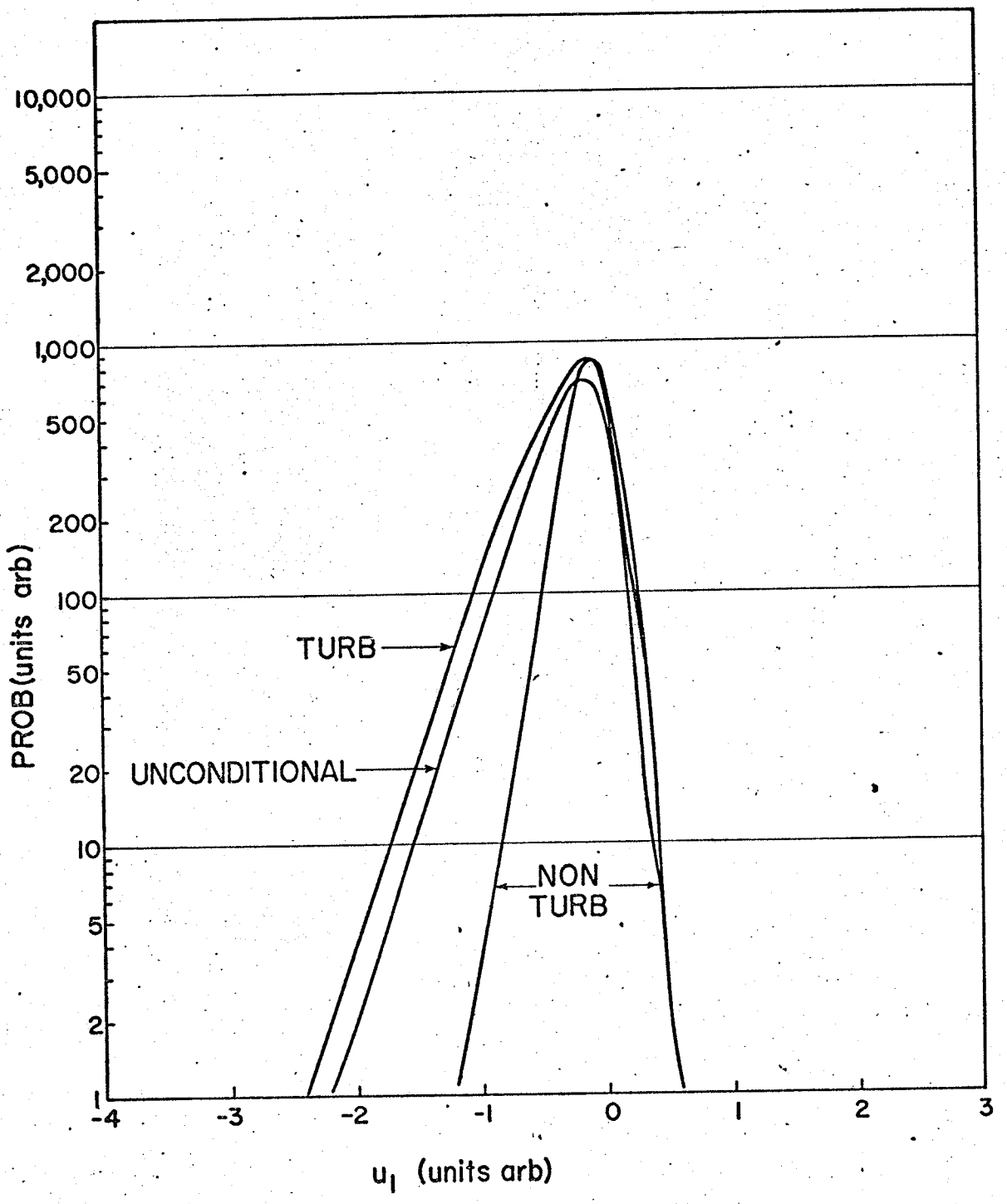

FIG.31 ZONE PROBABILITY DENSITY PLOT OF u_1 - Y/D=0.250

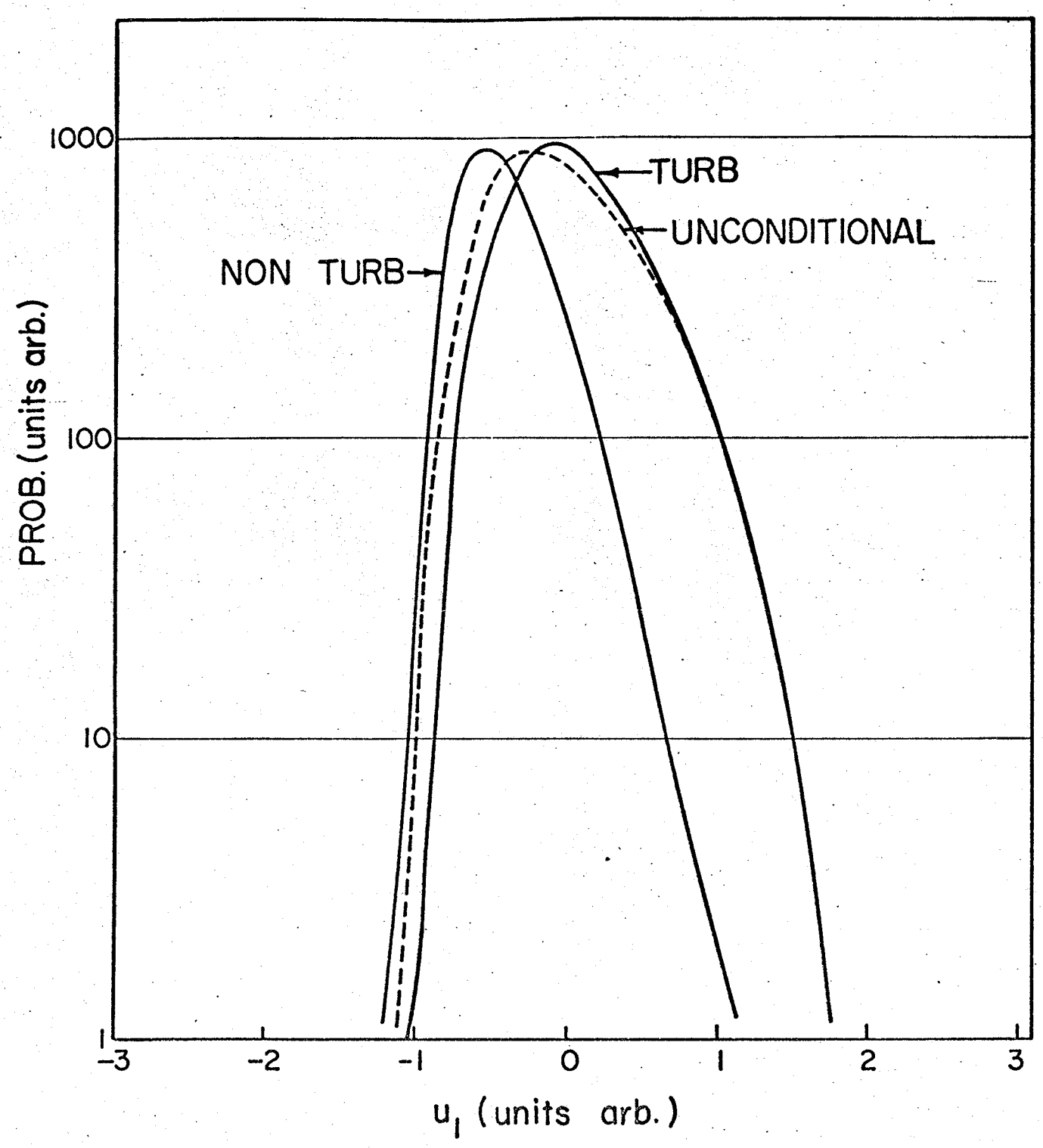

FIG. 32 ZONE PROBABILITY DENSITY PLOT OF u_1 - Y/D=0.067

7.3.1 Discussion of Results

Although interpretation of the results of these experiments from the fluid mechanics point of view is outside the scope of the present work, it seems appropriate to make a few brief comments on general curve shapes and trends.

1) For low intermittency facts, (Y/D = .325) in the core intermittent region the velocity of the turbulent fluid is larger than the mean velocity. Thus, by some process the fluid there is being accelerated. Fig. 30 shows the corresponding probability density plots. It is interesting to note that the width of the peaks for turbulent and non-turbulent flow is approximately equal and one therefore concludes that there are large fluctuations in velocity whether the fluid is turbulent or not. Comparing the turbulent peak with the unconditioned peak it is seen that for the turbulent peak the bulk of the fluid is moving faster than the mean since the peak is generally shifted to the right. However, on the left of the turbulent peak there is evidence of some "straggling" fluid as witnessed by the slowly diminishing left flank. The author, perhaps naively, visualizes the flow structure to be somewhat analogous to that of waves "breaking" on a beach. A crude approximation is shown in Fig. 33 which is similar to that given by Fiedler and Head (1966, facing page 720).

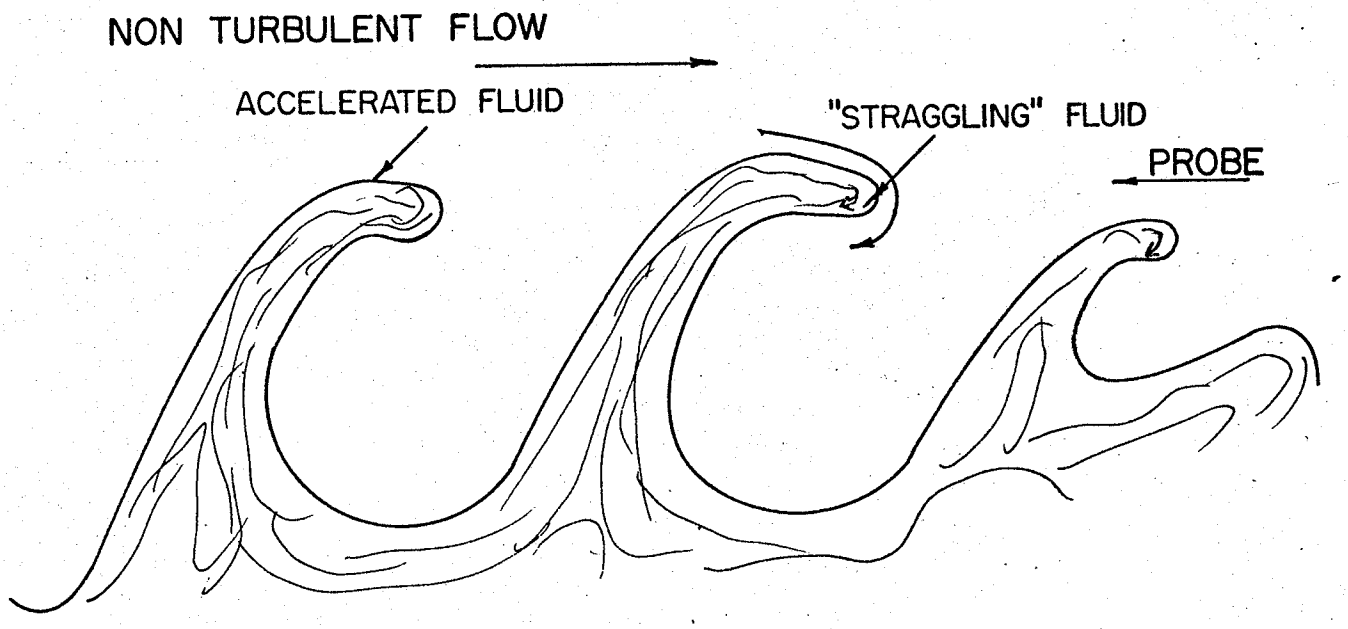

Fig. 33 - The Author's Concept of Intermittent Flow

2) As shown in Fig. 29 the zone averages change sign when going from the core to the wall intermittent regions. Referring to corresponding probability density plots Figs. 31 and 32 it is interesting to note that the skewness also reverses sign. The reasons for these are left as topics for further investigation.

7.4 Probability Density Measurements of Burst Widths.

Corrsin and Kistler (1955) have shown the usefulness of probability density plots of the widths of the bursts of turbulence (and non-turbulence). Their method was very tedious and inaccurate. It involved visual examination of long records of I(t). For the present work a method has been

devised for doing this quickly and accurately using a Time to Amplitude Converter and Multi-Channel Analyzer. Referring to Fig. 9, S2 is switched to I(t) and S5 to TAC. The MCA now accumulates the probability density of widths of turbulent bursts. A similar plot for non-turbulent bursts is obtained with S2 switched to 1-I(t). Fig. 34 shows a typical result which is similar to that obtained by Corrsin and Kistler (1955, Fig. 29).

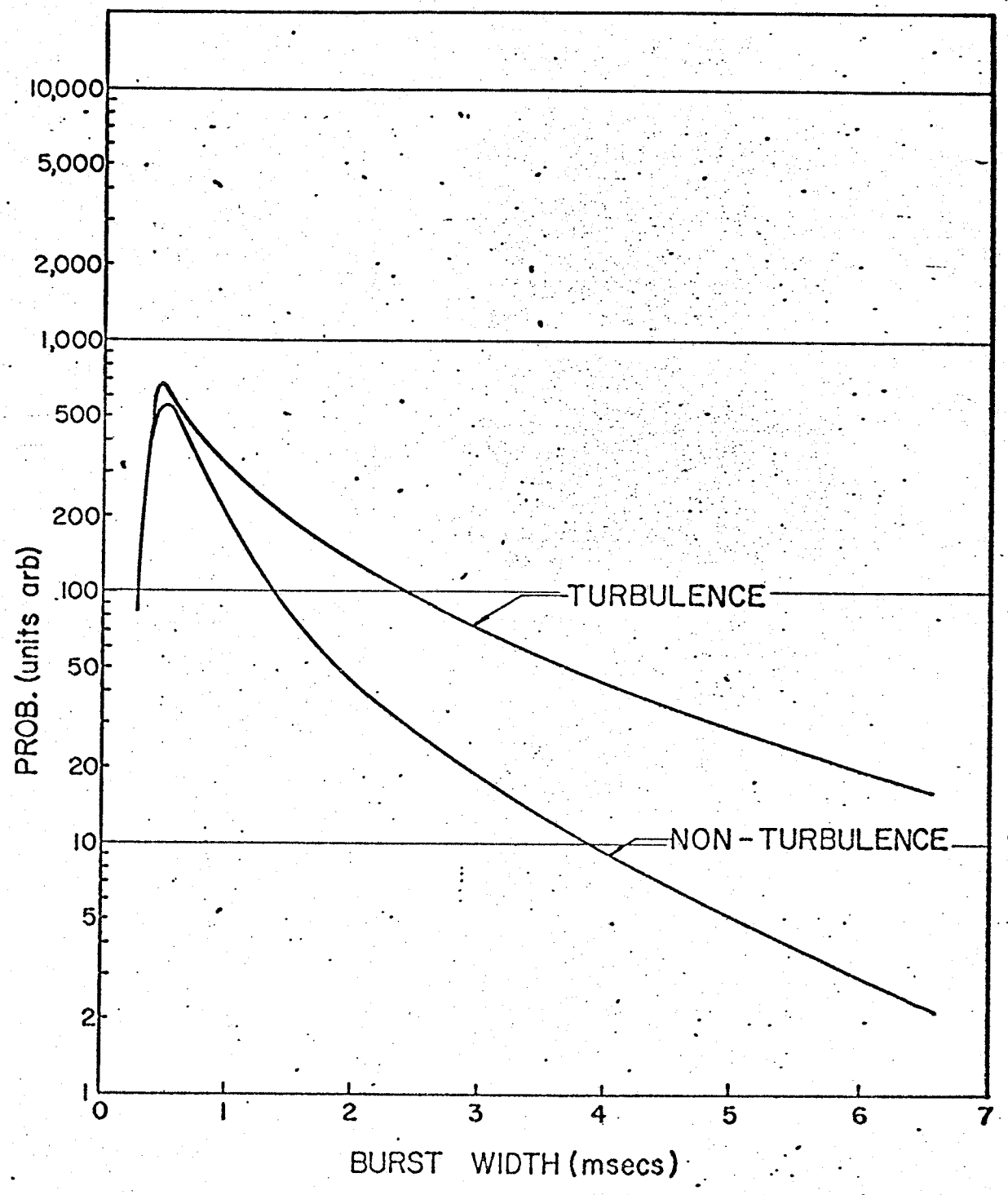

FIG.34, PROBABILITY DENSITY OF BURST WIDTHS - Y/D=0.067

8.0 A PHYSICAL MODEL OF FLOW IN A STRAIGHT CONICAL DIFFUSER.

The flow in a diffuser consists of four distinct regions, namely, (1) the core region, (2) the core intermittent region, (3) the fully turbulent region, and (4) finally the wall intermittent region. The core region is defined as the region where the mean velocity profile is relatively flat and the value of the intermittency factor is zero. The core intermittent region starts at the point of inflexion in the velocity-profile and also where the value of the intermittency factor lies between zero and one. The third, a very narrow region, the so called fully turbulent region (Townsends constant shearlayer) is the region where intense turbulent activity goes on due to maximum shear which is a product of interaction between the wall intermittent region and the core intermittent region. This region is characterized by the value of the intermittency factor being one. Lastly, the wall intermittent region is the layer of fluid next to the diffuser wall. The value of the intermittency factor in this region lies between zero, at the wall, and one at the junction with the fully turbulent region.

As the Reynolds number of the flow increases, the central core region decreases until it finally vanishes from the flow field. Consequently the flow is distributed among the remaining three regions. The fully turbulent region is still narrow in comparison to the other two intermittent zones but of course the width of the fully turbulent zone increases with Reynolds number until the entire flow is fully turbulent.

The two intermittent regions have their own typical flow structure. The core intermittent region has a fine structure of turbulence whereas the wall region has a coarse one. The above conclusion is reached by inspection

of Fig. 28 where it is seen that the lower frequencies (coarse structure) tend to be closer to the wall than the high frequencies (fine structure).

As was shown in Chapter 6, the wall intermittent region is wider but with lower intermittency intensity than the core intermittent region. The physical model is illustrated in Fig. 35.

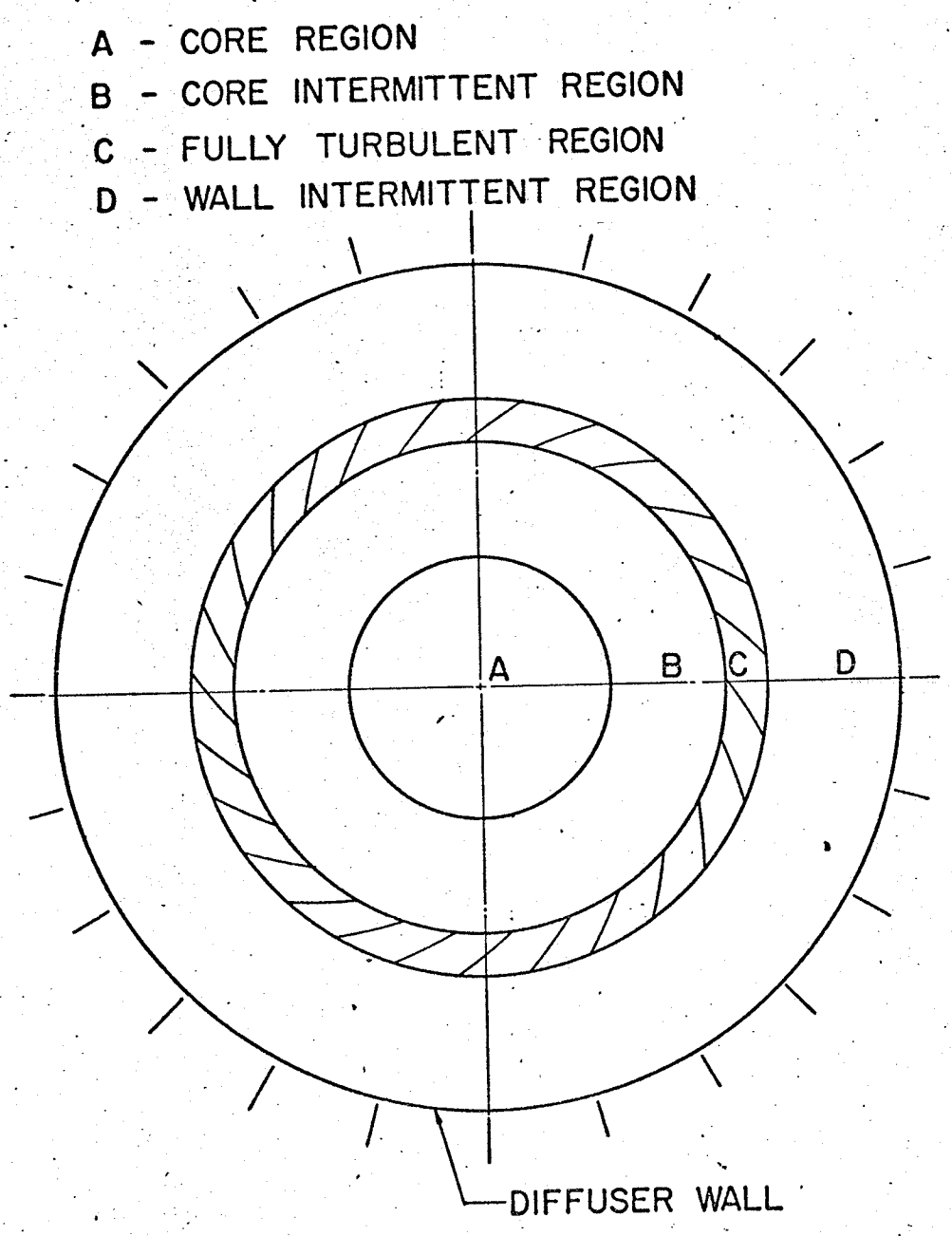

FIG.35 A MODEL FOR FLOW IN A CONICAL DIFFUSER

9.0 A PROPOSED "AUTOMATIC" INTERFACE DETECTOR.

Assuming that γ can be found using a "flatness factor" detector it would be a simple matter to devise an automatic interface detector, i.e. one with gain adjusted automatically to produce the true γ. Fig. 36 shows the proposed scheme. I(t) is averaged by the integrating circuit producing γ_1 which is compared with γ_2, the true value as determined by the "flatness factor" detector. The gain is adjusted by an analogue multiplier. If γ_1 is not approximately equal to γ_2 an error signal is produced of such phase as to adjust the gain and hence γ_1 until it is. Such a detector would combine the best features of both detectors. The major, if not insurmountable problem lies in designing a suitable "flatness factor" detector.

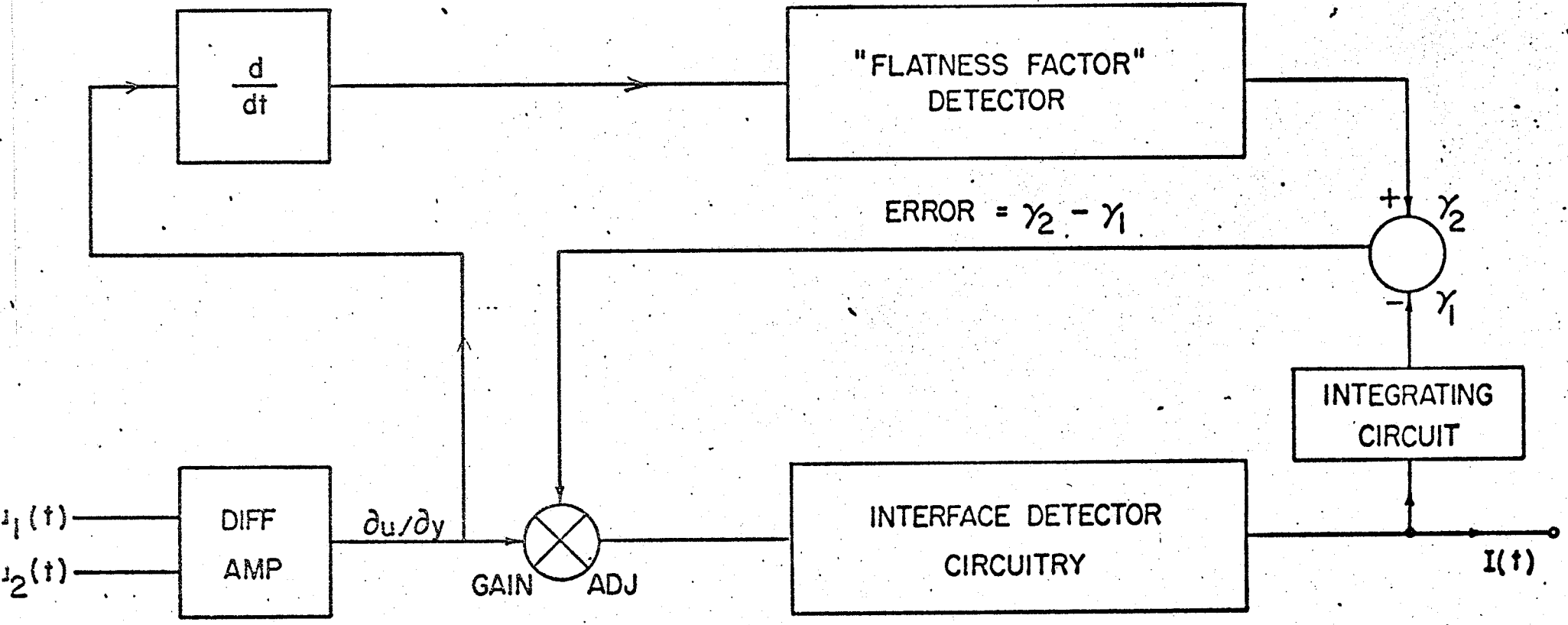

FIG.36 PROPOSED AUTOMATIC INTERFACE DETECTOR BLOCK DIAGRAM

10.0 CONCLUSIONS.

Three major pieces of apparatus were designed (as required), built, and tested for this work. They are -

1) An interface detector,

2) A sampler,

3) An intermittency synthesizer.

A number of lesser pieces of apparatus, (i.e. a low voltage power supply and a time to amplitude converter) were also designed and constructed. This apparatus was used successfully in conjunction with commercially available equipment (i.e. hot wire anemometers, etc.) and a number of experiments were performed in a conical diffuser.

Based on the limited measurements taken, the following conclusions can be drawn.

1) Probability density plots of space-time derivatives of velocity components form a convenient way of analyzing the intermittency characteristics of turbulent flow in a diffuser.

2) An interface detector is a useful tool for turbulence studies and with further development would probably enjoy wide spread use by researchers in fluid mechanics.

3) There are two distinct intermittent zones in diffuser flow, separated by a layer of intense turbulence. These have been named the wall intermittent region and the core intermittent region. The wall intermittent region was found to be wider than the core intermittent region.

4) At a fixed point in an intermittent region in diffuser flow, the transition from turbulent flow to non-turbulent flow and vice versa

is not instantaneous. To account for these gradual transitions the intermittency factor γ, was more specifically defined. The new definition specifies what fraction of transition flow is considered to be turbulent.

5) An intermittency intensity factor, β based on the fractional amount of transition flow could be defined. It is a measure of the "sharpness" of the transitions from turbulent to non-turbulent flow and varies from one to zero as the amount of transition flow increases from zero. The core intermittent region was found to be more intensely intermittent than the wall intermittent region.

APPENDIX A.1

THE INTERMITTENCY SYNTHESIZER UNIT

This unit consists of four basic curcuits,

1. The white noise generator,
2. The triangle-wave generator,
3. The noise gating circuit,
4. The sine wave generator.

Items 1, 2, and 3 above make up the intermittency synthesizer. The sine wave generator is not part of actual synthesizer but was built into the same unit for convenience. Fig. 37 shows a block diagram and a sequence of pulses designed to show the operation of the synthesizer.

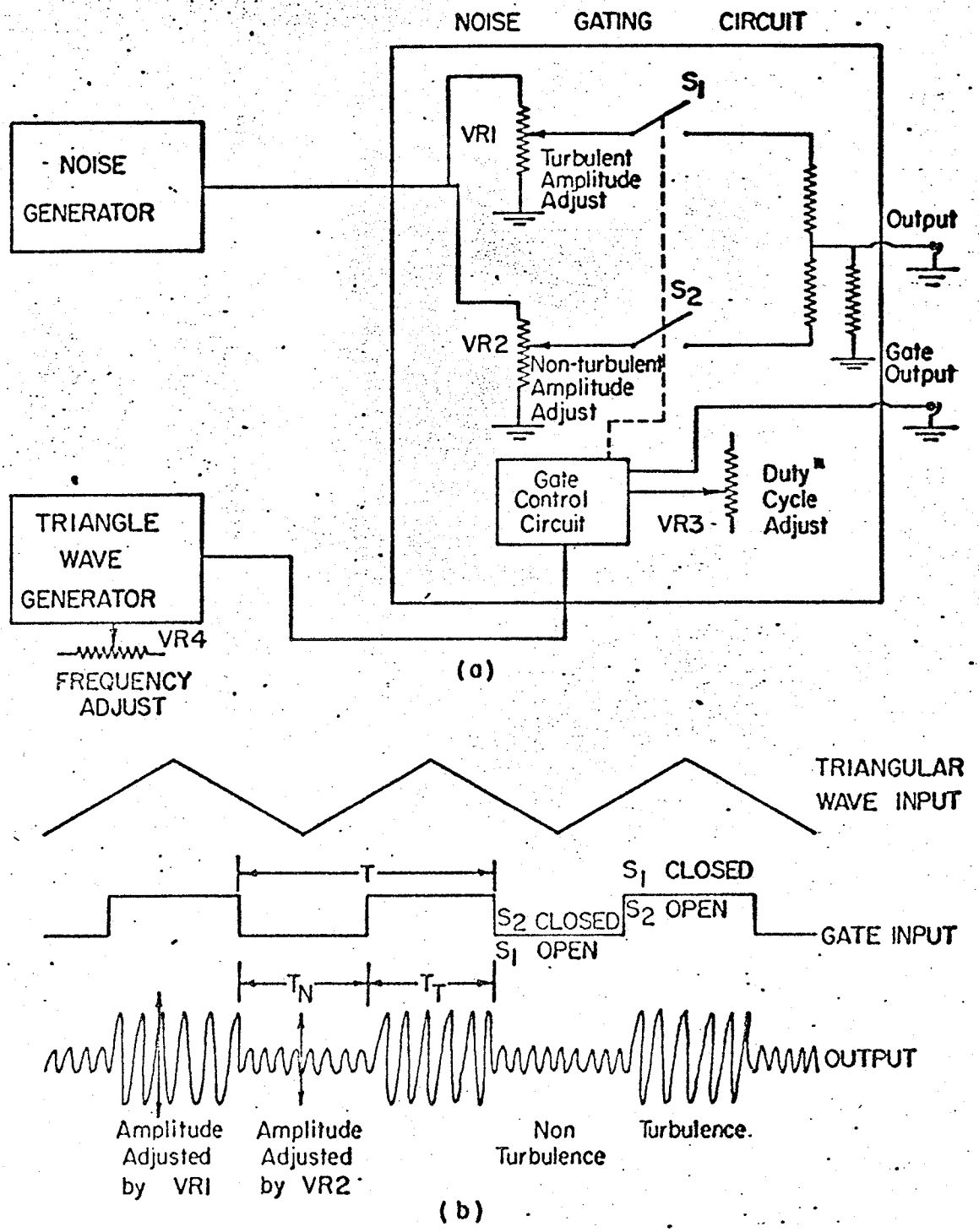

FIG. 37 - BLOCK DIAGRAM AND PULSE SEQUENCES FOR THE INTERMITTENCY SYNTHESIZER

The purpose of the synthesizer is to produce a signal simulating alternate periods of turbulence and non-turbulence as shown in Fig. 37b. The random noise generator produces the basic random signal which is fed to the two potentiometers VR1 and VR2. The output is alternately connected to VR1 and VR2 through transistorized switches S1 and S2. The triangle-wave generator operates the gate control circuit which alternately opens S1 and S2. A "GATE OUTPUT" signal is also available for monitoring.

Three parameters; duty cycle or γ, f_γ and b/n, characterize the simulated intermittent signal. Referring to Fig. 37b, the length of the turbulent bursts is T_T, and the length of the non-turbulent bursts, T_n. The sum of T_T and T_N is the length of a complete cycle T. The duty cycle (which simulates the intermittency factor and equals T_T/T) can be adjusted from zero to one by VR3, and measured using the technique of Sec. 6.2. The frequency of the triangle-wave generator, 1/T simulates the interface crossing rate f_γ. It is adjusted by VR4 and measured with the NE9010 digital counter. With the duty cycle set to one the rms value of the output is b which is adjusted with VR1 and measured with the true rms meter. Similarly n, which is set by VR2, is the rms value of the output with a duty cycle of zero. It is thus possible to adjust and measure γ, f_γ, and b/n conveniently.

A.1.1 The Noise Generator.

The ideal noise generator would have a "white" power spectrum with a normal probability distribution. However, any physically realizable generator can only produce "white" noise over a limited bandwidth which in this case is from approximately 10Hz. to 10 KHz.

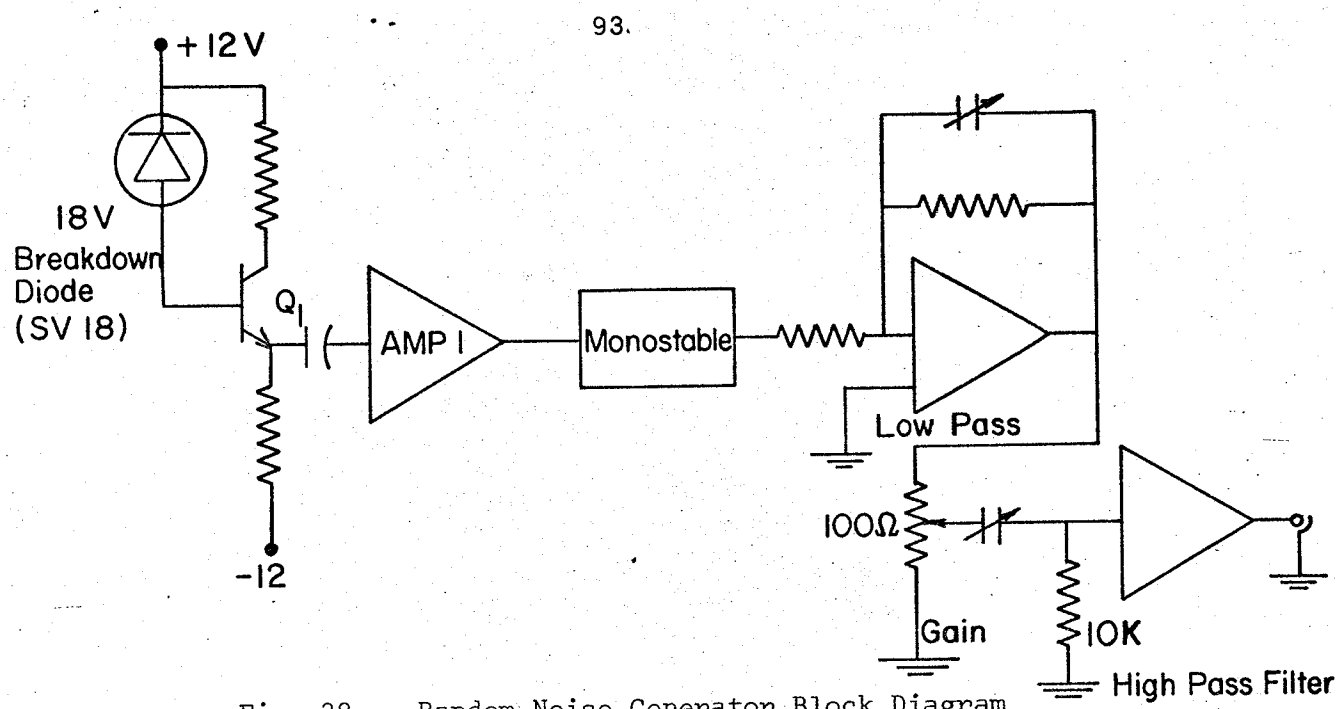

Fig. 38. - Random Noise Generator Block Diagram

A simplified schematic is shown in Fig. 38. The small d.c. current flowing in the breakdown diode biases the base of Q1. Under these conditions the diode acts as a random noise generator. This noise was found not to have the desired frequency spectrum and was therefore used to trigger a monostable at a random rate. The random pulses thus produced are passed through a low pass and a high pass filter with selectable cut-off frequencies.

Specifications for the noise generator are,

a) Whiteness

Flat within 1 db from 10Hz to 10KHz.

b) Probability distribution - gaussian.

c) Low pass filter - switch selectable at 200, 1,000, 2,000, 10,000, 14,000Hz.(3 db down).

d) High pass filter - switch selectable at 10, 20, 50, 100, 500Hz. (3 db down).

e) Output amplitude - adjustable from 0-3 volts rms with single turn potentiometer.

A.1.2 Triangle-Wave Generator.

A suitable triangle-wave generator for this non-critical application was realized following the technique outlined in Fig. 39.

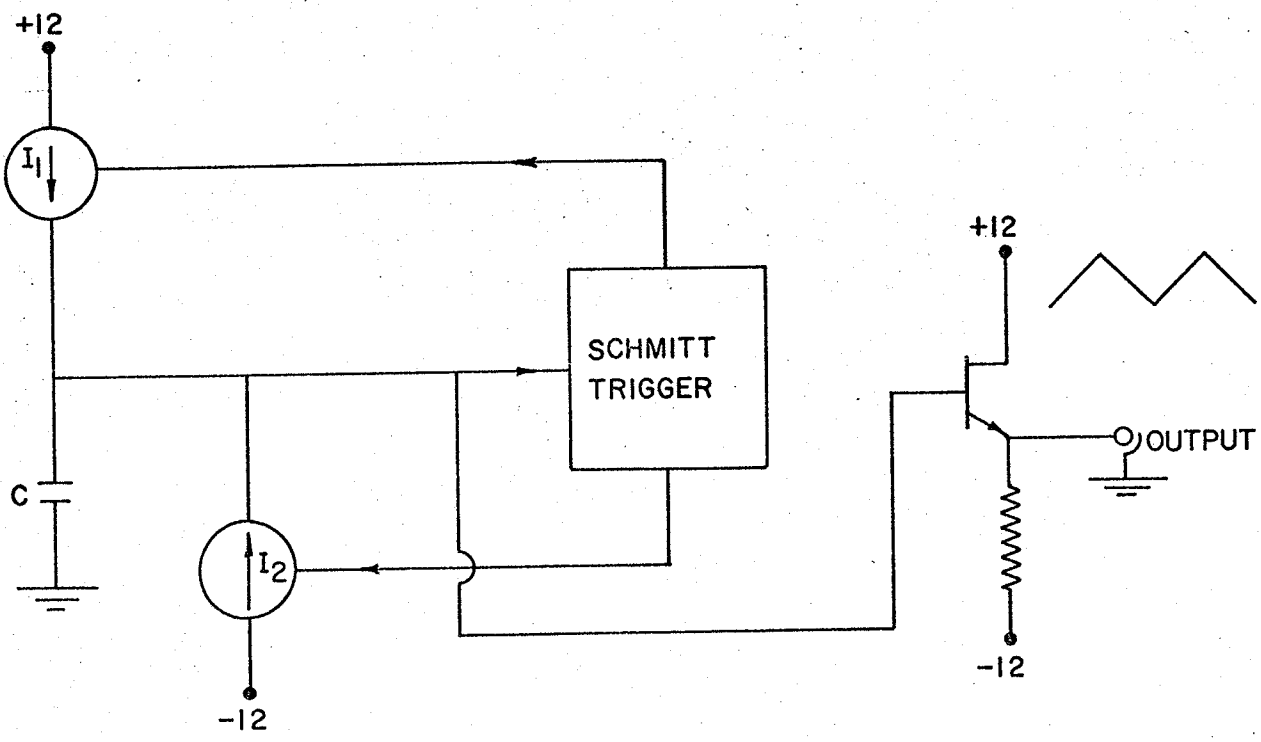

Fig. 39 Triangle-Wave Generator Block Diagram.

The circuit consists essentially of two gated constant current sources, I1 and I2, controlled by a Schmitt trigger circuit with a hysterisis of 12V centred about zero. The Schmitt trigger operates in such a manner that only one of I1 or I2 flows at any given time.

Assume I1 is flowing and I2 is off. The capacitor C is charged

up by a constant current producing a linear ramp. When the voltage on C (Vc) reaches V,the Schmitt trigger turns off I1 and turns on I2 producing a ramp of reverse slope until Vc reaches -V at which time I2 is turned off and I1 is turned on again. Thus the desired triangular waves are produced. The frequency of oscillation is varied by changing the value of capacitor C or the magnitude of I1 and I2.

Relevent specifications are:

Frequency - continuously variable from 0.7Hz to 90 KHz in 5 ranges.

Amplitude - 11 volts peak to peak, direct coupled; mean value zero volts.

A.1.3 The Noise Gating Circuit.

The circuit used is very similar to that used by Kibens (1968 p.94). The complete circuit is given by Hummel(1970).

A.1.4 The Sine-Wave Generator.

The Sine Wave Generator is basically a Wien-Bridge Oscillator, capable of producing sine waves of frequency continuously selectable from 10Hz to 700 KHz. in 5 ranges. The amplitude is continuously selectable from 0 to 10 volts peak-to-peak in 3 ranges.

APPENDIX A.2

THE SAMPLER UNIT

This unit was designed and constructed by the author to perform the following two operations.

1. Sample a continuous random signal such as u for statistical analysis. In this case the unit is said to be operated in the Sampling Gate Mode.

2. Measure the zone average of a continuous random signal. In this case the unit is said to be operated in the Sampling Integrator Mode. Such instruments are often referred to as "BOXCAR INTEGRATORS".

The Sampler cannot operate in both modes simultaneously. To simplify the discussion the two modes are discussed with the aid of separate block diagrams, Fig. 40 and Fig. 41.

A.2.1 The Sampling Gate Mode (Fig. 40)

An analogue input signal such as u is fed to the input amplifier via capacitor C1 and the potentiometer VR2 which serves as a variable input attenuator. Since all samples at the final output must be of the same polarity, the output of the input amplifier must fluctuate about a mean value so chosen that the instantaneous value never passes through zero. This is provided for by the DC RESTORE potentiometer VR1. Sampling is done by the MOSFET switch (Metal Oxide Semiconductor Field Effect Transistor). It has three terminals, s, g, and d as shown.

The sampling rate is determined by a sine wave which is fed into

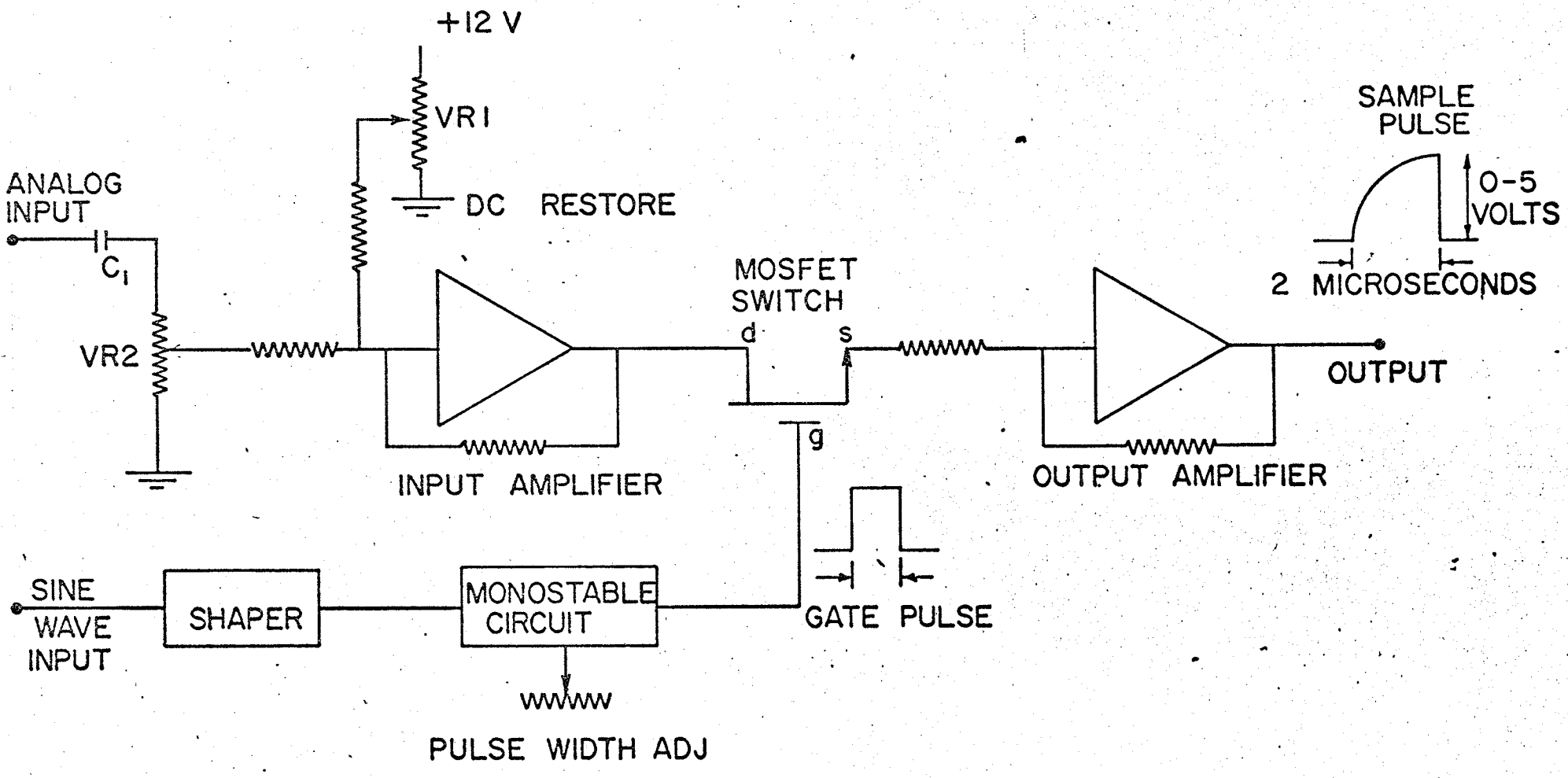

FIGURE 40- BLOCK DIAGRAM OF THE SAMPLER USED AS A SAMPLING GATE

the shaper, conterting it into a square wave. The leading edge of each square wave is converted into a positive GATE PULSE. The width of this pulse is adjusted to two microseconds by the PULSE WIDTH ADJ potentiometer. The GATE PULSE, acting on terminal g of the MOSFET switch, closes the switch for the duration of the pulse thus producing the SAMPLE PULSE at the output. The amplitude of this pulse is proportional to the instantaneous value of the analogue input signal plus the D.C. value set by VR1.

A.2.2 The Sampling Integrator Mode (Fig. 41).

In this mode the input amplifier and associated circuits are used in a manner identical to that of Sec. A.2.1. The analog input is again the velocity u; the GATE INPUT, however, is a random square wave such as I(t) which passes through the shapes essentially unchanged and is subsequently applied to the terminal g of the MOSFET switch. Whenever the GATE INPUT is "on" the MOSFET switch is closed and the INTEGRATOR has a feedback determined gain of five and a time response determined by RC, which can be varied to suit the particular experiment by changing C. Thus, whenever the switch is closed, the output will asymptotically approach the average level of the signal at "A" over the duration for which the switch is closed.

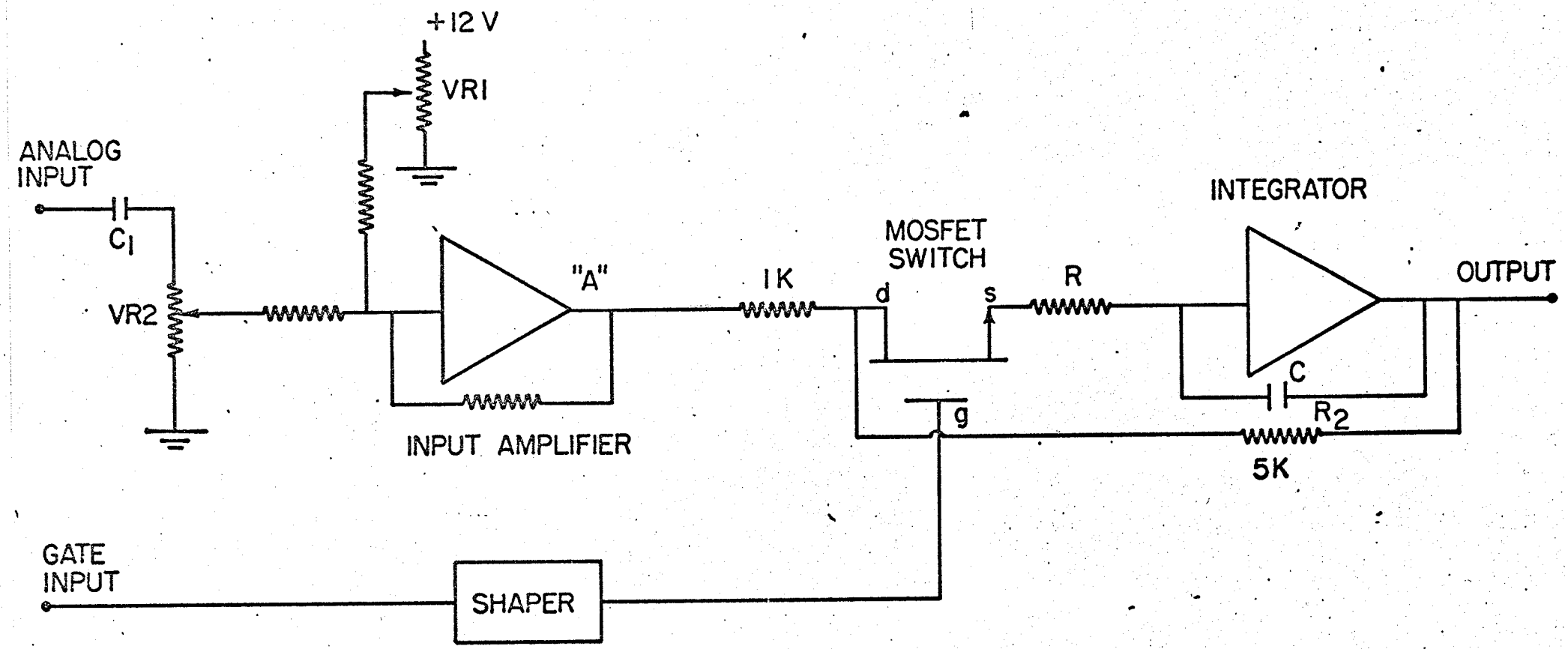

FIGURE 41 - BLOCK DIAGRAM OF THE SAMPLER USED AS A SAMPLING INTEGRATOR

A.3 The Interface Detector.

A simplified schematic diagram for the detector is shown in Fig. 42. The circuit is very similar to the one described by Kibens(1968). The exception is the manner in which the signal $\dot{S}(t)$ is derived.

The linearized outputs of the two hot-wire anemometers $u_1(t)$ and $u_2(t)$ are a.c. coupled to the emitter followers Q1 and Q2. If the Intermittency Synthesizer is used, its output replaces one of the anemometers. The other input is unused. Transistors Q3,4,5 &6 form a differential amplifier whose output represents the difference in velocity between the two hot-wires and therefore approximates the derivative $\partial u/\partial y$.

This signal is brought out to the front panel for recording purposes, and then is fed through the GAIN control VR1. The resulting signal is fed through the emitter follower,Q6a and the high pass filter C1 R1 to the amplifier Q7. C1 is adjusted such that the cut of frequency is larger than any frequency of interest, thus making C1 R1 essentially a differentiator. The circuit, R2 C2 in the collector of Q7 forms a low pass filter with cut-off frequency adjusted to be equal to that of C1 R1. This limits the overall high frequency response of the system. The resulting signal, S taken from emitter follower Q10 is thus proportional to $\frac{\partial^2 u}{\partial y \partial t}$.

The signal S(t) is also fed through $\dot{S}$ GAIN control VR2, and emitter follower Q8, to the true differentiator C3, and associated feedback amplifier Q9, Q10. The high frequency limit of the circuit is set at 20 KHz by the high frequency cut-off filter RfCf. The output signal $\dot{S}(t)$ is proportional to $\frac{\partial^3 u}{\partial y \partial t^2}$. The r.m.s. value of $\dot{S}$ is set equal to that of S by varying VR2

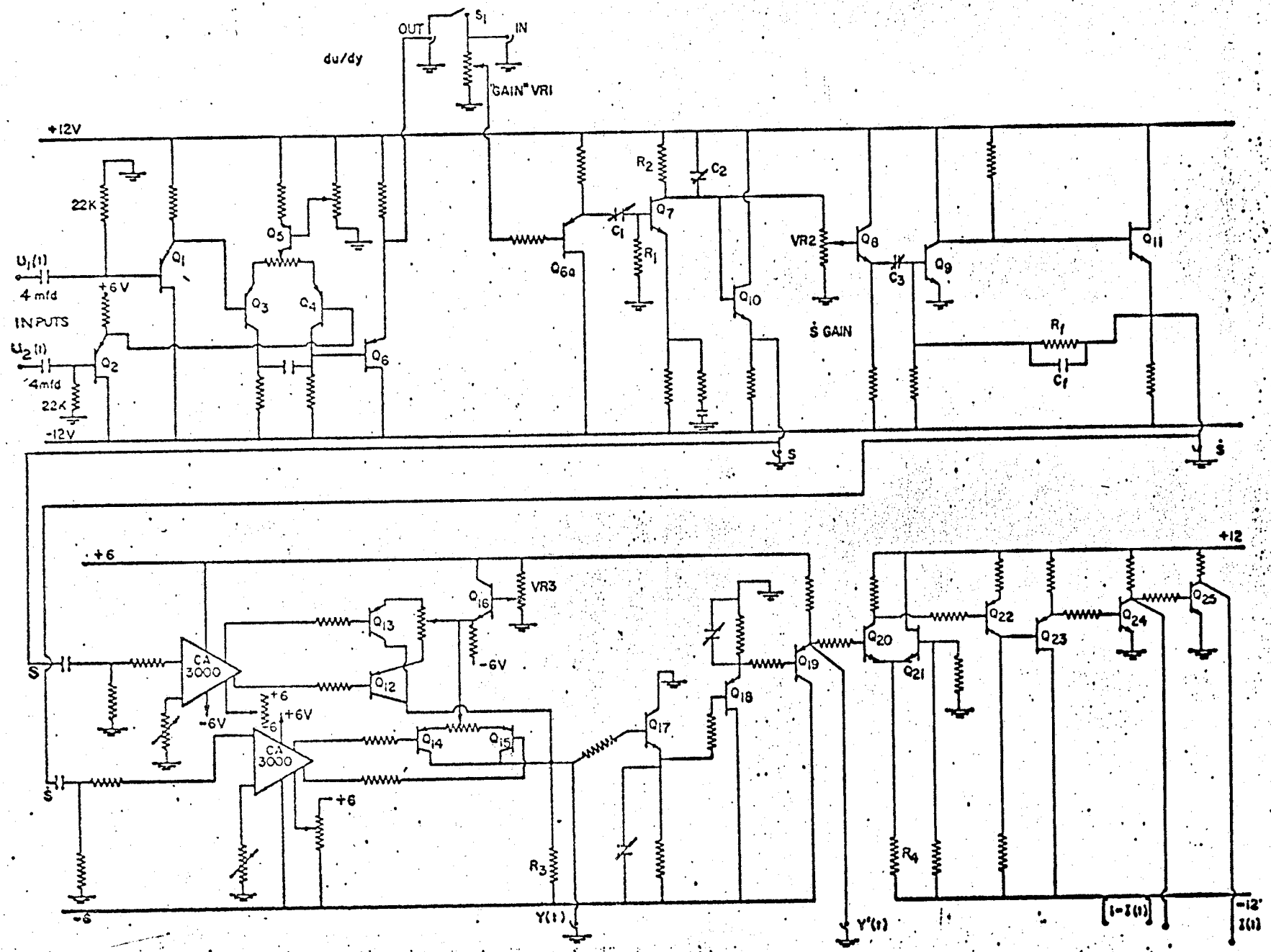

FIG.42 INTERFACE DETECTOR SCHEMATIC DIAGRAM

and C3. $S(t)$ and $\dot{S}(t)$ are brought to the front panel for monitoring.

The signals $S(t)$ and $\dot{S}(t)$ are next fed into type CA3000 integrated circuit differential amplifiers with push-pull outputs and a gain of 30. Associated balancing circuits allow all four outputs to be adjusted to the same quiescent level of plus 2.4 volts. The four outputs are fed to the bases of four rectifying transistors Q12, 13, 14 & 15, arranged so that the collectors are all connected together feeding a common resistor R3. To understand the operation of the rectifiers, or detectors as they are sometimes referred to, consider first the case where $\dot{S}(t)$ is set to zero so that no signals are applied to Q14 and Q15. The detector threshold, C, is a voltage defined as follows. If the input signal applied to the rectifiers has an instantaneous value larger than C, then the voltage on R3 is a large fixed value arbitrarily assigned a value 1. Similarly, for signals less than C, the voltage on R3 is a small fixed value assigned a value 0. But C is small compared with the maximum values of the input signal. Therefore the voltage on R3 will be 1 except for those small time intervals when the input signal is at or near zero. In summary therefore, the voltage on R3, i.e. $Y(t)$ is 1 except when $S(t)$ is small, at which time $Y(t) = 0$. These zeros in $Y(t)$ are filled in by $\dot{S}(t)$ which is 90° out of phase with $S(t)$. Since the signals are random, however, the signal $Y(t)$ shows a considerable number of lapses during the turbulent regime and also false indications of turbulence for brief noise peaks.

The "hold time" necessary to eliminate these erroneous indications is provided by Q17, 18 and associated circuitry. Each transistor has an ad-

justable parallel RC circuit in the emitter. Assume all transitions in Y(t) are instantaneous. Thus, if Y(t) goes positive the emitter of Q17 will follow quickly due to its low output impedance; a characteristic of emitter followers using NPN transistors and subjected to a positive transition. Q18 is therefore quickly cut-off and the output Y(t) increases exponentially as determined by the natural mode of the RC circuit in the emitter of Q18. Q19 is a simple emitter follower. For negative transitions of Y(t), Q17 is quickly cut-off and the output Y(t) is again an exponential but this time determined by the natural mode of the RC circuit in the emitter of Q17. This signal is then fed through Q18 and Q19. In this case the RC circuit in the emitter of Q18 has no effect due to the low output impedance of the PNP transistor (Q18) when driven negative.

Transistors Q20, 21 make up a level detector. Let C be the cross over level. It is determined by the base voltage of Q21. If Y(t) is less than C then Q21 conducts, Q20 does not conduct, and the output, taken on the collector of Q20, is said to be 0. If Y(t) is greater than C, Q20 conducts and Q21 does not; the output is now 1. This output, is fed through inverters and emitter followers, Q22, 23, 24, 25. The signal 1-I(t) appears on the collector of Q24, the signal I(t) on the collector of Q25. Both are brought to the front panel for monitoring.

REFERENCES

BATCHELOR, G. K. (1967) — Introduction to Fluid Dynamics. Cambridge University Press, 1967. p. 298.

CHASE, R. L. (1961) — Nuclear Pulse Spectrometry. McGraw Hill Book Co., New York.

CORRSIN, S. and KISTLER, A. L. (1955) — Free-Stream Boundaries of Turbulent Flows. NACA Report 1244.

DAVIES, G. L. (1961) — Magnetic Tape Instrumentation. McGraw Hill Book Co., New York.

FIEDLER, H. and HEAD, M. R. (1966) — Intermittency Measurements in the Turbulent Boundary Layer. Journal of Fluid Mechanics 25,719.

FRIESEN, G. (1970) — A Theoretical and Experimental Study of Contraction Cones. M.Sc. Thesis, University of Manitoba.

FRAENKEL, L. E. (1956) — On the Flow of Rotating Fluid Past Bodies in a Pipe. Proc. Roy. Soc. A233, 500.

HAMEL, G. (1917) — Jahresbericht der Deutchen Mathematicer-Vereignigung 25,34. English Translation, Spiral Motion in Viscous Fluids. NACA Technical Memo. 1342. Jan. 1953 44p.

HUMMEL, R. H. (1970) — Instrumentation for Measuring Intermittency in Turbulent Fluid Flow. In preparation - not for publication.

JEFFREY, G. B. (1915) — The Two Dimensional Motion of a Viscous Fluid. Phil. Mag. (6), 29, 455.

KIBENS, V. (1968) — The Intermittent Region of a Turbulent Boundary Layer. Ph. D. Thesis The Johns Hopkins University.

KOLMOGOROV, A. N. (1941) — The Local Structure of Turbulence in Incompressible Viscous Fluid for Very Large Reynolds Numbers. C. R. Acad. Sci. U.R.S.S. 30,301.

KRUEGER, H. (1970) — Turbulent Flow in Diffusers. M. Sc. Thesis, University of Manitoba.

LIPKA, R. (1968) — An Experimental Investigation of a Straight Conical Diffuser. M. Sc. Thesis, University of Manitoba.

MILLSHAPS, K. and POHLHAUSEN, K. (1953) — Thermal Distributions in Jeffrey-Hamel Flows Between Non-Parallel Walls. Journal Aero. Sci. 20, 187.

PATEL, V. C. and HEAD, M. R. (1969) — Some Observations on Skin Friction and Velocity Profiles in Fully Developed Pipe and Channel Flows. Journal of Fluid Mechanics. 38, 181.

ROSENHEAD, L. (1940) — The Steady Two-Dimensional Radial Flow of Viscous Fluid Between Two Inclined Walls. Proc. Roy. Soc. A175, 436.

SLUSAR, G. G. (1969) — Turbulence Measurements in a Straight Conical Diffuser. M. Sc. Thesis, University of Manitoba.

TOWNSEND, A. A. (1948) Local Isotrophy in the Turbulent Wake of a Cylinder.

Aust. J. Sci. Res. 1, 161.

TOWNSEND,A. A. (1949) The Fully Developed Turbulent Wake of a Circular Cylinder.

Aust. J. Sci. Res. 2, 451.

TOWNSEND, A. A. (1956) The Structure of Turbulent Shear Flow

Cambridge University Press, 1956.

VAN der SPIEGAL, P. J. A. (1969) An Experimental Investigation of the Turbulent Boundary Layer in a Straight Conical Diffuser.

M. Sc. Thesis, University of Manitoba.